Notch deficiency causes arteriovenous malformations and altered pericyte function

Natalie M. Kofler

Submitted in partial fulfillment of the requirements for the degree of

Doctor of Philosophy

under the Executive Committee of the Graduate School of Arts and Sciences

COLUMBIA UNIVERSITY

2013

ABSTRACT

Notch deficiency causes arteriovenous malformations and altered pericyte function

Natalie M. Kofler

During angiogenesis, nascent blood vessels sprout from pre-existing vasculature and recruit pericytes to induce maturation and vessel quiescence. Perictyes are associated with small vessels and capillaries where they share the basement membrane with the endothelium to provide vascular support. Pericytes are a critical component of the blood-brain barrier and regulate endothelial cell proliferation, vessel diameter, and vascular permeability. Endothelial cells express Notch1, whereas pericytes express both Notch1 and Notch3.

Here we show that Notch signaling is essential for pericyte function. Through genetic manipulation and pharmacological tools we show that Notch regulates pericyte recruitment and pericyte/endothelial cell interactions. *Notch1*$^{+/-}$*;Notch3*$^{-/-}$ mutant mice display decreased pericyte coverage and altered pericyte association with the retinal vascular plexus. Notch deficiency is associated with vascular anomalies where *Notch1*$^{+/-}$*;Notch3*$^{-/-}$ mice display retinal arteriovenous malformations (AVM) characterized by dilated vessels, vascular tangles and arteriovenous shunts that are similar to human brain AVMs. Disruption of pericyte/endothelial cell association is accompanied by an increase in vascular density, venule enlargement, and increased vascular permeability observed prior to AVM formation. In the ovary, we show that Jagged is essential for pericyte association with the endothelium where inhibition of Jagged-specific Notch activation results in luteal vessel dilation and hemorrhaging following ovarian hyperstimulation. By *in vitro* analysis of cultured pericytes we show that Notch1 and Notch3 induce plated derived growth factor receptor-β (PDGFR-β) expression to regulate cell migration. These findings expand the role for Notch in angiogenesis by demonstrating that Notch signaling in pericytes is essential for vascular development and function.

TABLE OF CONTENTS

LIST OF FIGURES

Chapter 1

Chapter 2

Chapter 3

Chapter 4

Chapter 5

Chapter 6

LIST OF TABLES

Chapter 1

Chapter 2

ACKNOWLEDGEMENTS

First, a big Thank you to my mentor Jan Kitajewksi, PhD. His support and guidance over the years has been invaluable and I am so grateful to have been shaped by such an astute and creative scientist. I also want to thank the Kitajewski lab, which has really become like a second family. I am so grateful for the wonderful friendships I have made. Thank you to Thaned Kangsamksin, my Buddah brother and wonderful baymate. I am truly grateful to know you as a friend and scientist. Your calming presence saved me on many a stressful day. I have learned so much from you! I am also so grateful to Aino Mortumäki who performed the αSMA staining analysis of Notch1/Notch3 mutant retinas and who has become one of my best friends. You have provided so much support and laughter over the years. Thank you! I am especially grateful to my first mentor in research, Carrie Shawber, PhD. Carrie, thank you for training me to be a thoughtful scientist. I so appreciate all of your advice and guidance throughout my years in lab. Thank you to Valeriya Borisenko, my lab Mom for always looking out for me. And thank you to all of the past and present members of the Kitajewski lab, Wu lab, and Shawber lab for helping me along the way. A special thank you to former lab member Hasina Outtz Reed. I first learned how to dissect out a retina from Hasina. Thank you Hasina for all of your guidance and for being one of my best buds.

I would like to thank my thesis committee Domenico Accili, MD, Darrell Yamashiro, MD/PhD, and Ramon Parsons, MD/PhD. I couldn't have asked for a better committee. Your input greatly shaped how I think as a scientist and your kindness and support has been invaluable. Thank you to Peter Canoll, MD/PhD for joining my thesis defense committee. Thank you for always giving me your time when I had questions about the brain vasculature. I am so appreciative of your enthusiasm and interest in my work.

The support and guidance that I have received from the Integrated Program in Cellular, Molecular, and Medical Biosciences over the years has been invaluable. I especially want to

thank the director of the program Ron Liem, PhD for his support. A special thank you to Zaia Sivo. We are so lucky to have you looking out for us students. You have been such an important part of my PhD process. Thank you for your wisdom, kindness, and for always being in my corner.

Thank you to Richard Kessin, PhD for you edits of Chapter 3. Thank you to Nataki Douglas, MD/PhD for your edits of Chapter 4 and for teaching me how ovaries work. Thank you to Minji Kim (soon to be PhD) for your reviews of Chapter 5, your meticulous eye and for being my buddy.

I would like to acknowledge Bruno Larivée of Anne Eichmann's lab at Yale University for his help in establishing the retinal latex perfusion assay. A special thank you to Amber Stratman, PhD and George Davis, MD/PhD of the University of Missouri for their guidance in *in vitro* pericyte culture.

I would also like to thank Teresa Swayne, PhD and Adam White, PhD of the ICRC imaging core for being two of the nicest people I know and for all of their help in image acquisition and analysis. My figures could not have been so beautiful without your help.

A huge Thank you to all of the people who have worked with me and contributed data to this thesis. Anna Cho performed beautiful immunohistochemistry on ovarian sections. Amanda Adeleye, MD performed ovarian analysis. Lilli Dash (soon to be MD) contributed greatly to the ovary chapter. She performed H&E staining, immunohistochemistry, and ovarian analysis. Thanks for being so fun to work with Lilli and thank you for your insight into the ovarian project. Another big Thank you to Elizabeth Fontana, MD who performed gene expression analysis of cultured pericytes. I am so grateful that you chose Jan's lab for your year of research, if not I may never had gained such a wonderful friend. I would also like to acknowledge that Carrie Shawber contributed Notch3 staining of the ovarian corpus luteum.

Last, but certainly not least I want to thank my family and friends who have supported me throughout this process. I could not have done this without you! I want to thank the meal, my NYC family. Bean and Butt you two are the best and I am so grateful to have you in my life. Thank you to my family who has always supported me. The years of my PhD have been great, but at times quite trying and your love has helped me every step of the way. Thank you Mom, Dad, Greg and Edda for your wisdom and undying support. I am so inspired by all of you. Thank you for being such strong and wise role models. A special thanks to Mom and Dad for you visits during the last stages of my thesis when I really needed some loving. I am so lucky! Dad, thank you for always having confidence in me and teaching me to aspire to greatness. Mom, thanks for helping me keep both feet on the ground and for being there for me no matter what. Thank you to Felice and Koko for always keeping me smiling. Thank you Dave. Brother, you always make me keep it real and I so cherish your wisdom and love.

CHAPTER 1

Introduction

Pericytes in angiogenesis

The circulatory system develops by two distinct yet intimately related processes: vasculogenesis and angiogenesis. Vasculogenesis occurs first in the developing embryo and is initiated when endothelial precursors termed hamangioblasts coalesce and differentiate to form a primitive vascular plexus of tubes lined by endothelial cells. Vascularization of some organs, primarily of endodermal origin like the lung and pancreas depends entirely on vasculogenesis[1]. However, the bulk of the circulatory system requires that the primitive vascular plexus formed by vasculogenesis be remodeled and expanded through the process of angiogenesis to produce a hierarchal vascular network composed of arteries, capillaries, and veins. Angiogenesis is the process by which blood vessels are formed from a pre-existing vascular network[2]. This process is initiated when the endothelial cells lining the established vessels are exposed to vascular endothelial growth factor-A (VEGF-A). VEGF-A activates its receptor expressed by endothelial cells, vascular endothelial growth factor receptor 2 (VEGFR-2) to induce vascular basement membrane degradation, cellular proliferation and migration towards increasing concentrations of VEGF-A. Endothelial cells of the angiogenic sprout then undergo lumenization and become stabilized through recruitment of mural cells, pericytes and vascular smooth muscle cells. This establishes a stabilized vascular network capable of delivering nutrients and oxygen throughout the body of the organism.

Pericyte recruitment parallels endothelial cell sprouting and migration during angiogenesis. Endothelial cells of angiogenic sprouts secrete platelet-derived growth factor (PDGF-B) that functions as a homodimer (PDGF-BB) to activate platelet-derived growth factor receptor-β (PDGFR-β). PDGFR-β is expressed by pericytes and its activation by PDGF-BB induces pericyte proliferation and migration to the nascent sprout[3,4]. Pericyte association with endothelial cells during angiogenesis is essential to induce vascular maturation[5]. For example, pericyte coverage induces vascular basement membrane deposition to limit endothelial

sprouting and promote vascular quiescence[6]. The PDGF-B/PDGFR-β signaling pathway is critical for pericyte recruitment whereby inhibition of PDGFR-β signaling through genetic manipulation or pharmacological inhibition prevents pericyte recruitment to most vascular beds[7,8]. In the brain, inhibition of pericyte recruitment through genetic deletion of PDGF-B or PDGFR-β causes severe vascular dysfunction characterized by increased vessel permeability, vessel dilation, and abnormal vessel morphogenesis[9]. In the ovarian corpus luteum, inhibition of luteal pericyte recruitment causes decreased vascular density and luteal hemorrhaging[10]. During developmental angiogenesis in the retina, inhibition of mural cell recruitment leads to vessel dilation, altered vessel patterning, and an abnormal capillary plexus[11]. Thus, pericytes act as an essential component of angiogenesis by regulating endothelial function to effect vessel density, vessel morphology, and to promote vascular maturation.

Defining the pericyte

To date, studying pericyte function during angiogenesis has proven difficult due to limitations in cell marker specificity and pericyte phenotype heterogeneity. Pericytes have a complex ontogeny; different vascular beds are invested by pericytes of different origins. For example, cerebral and retinal pericytes are neural crest derived, whereas pericytes of the female reproductive tract are likely of mesodermal origin[1,12,13]. Like pericytes, vascular smooth muscle cells (VSMC) also have diverse origins[2,14]. A current theory proposes that pericytes fall along a continuum of mural cell differentiation where pericytes are considered to be a highly plastic and immature mural cell as compared to the mature, contractile, and terminally differentiated vascular smooth muscle cell[3,4,15].

Bona fide pericytes are found lining capillaries as solitary cells where they share the basement membrane with the endothelium (Figure 1)[5]. Pericytes display rounded cell morphology and extend cell process that at distinct points directly attach to the abluminal

surface of the endothelium. Large arteries and veins are lined exclusively by VSMCs that form concentric rings of multiple cell layers, which are physically separated from the endothelium by the elastic lamina. These mature mural cells express contractile proteins, such as α-smooth muscle cell actin (αSMA) and smooth muscle cell myosin heavy chain to regulate vessel contraction and dilation. Intermediate-sized blood vessels, such as arterioles and venules, are lined by what appears to be an intermediate mural cell type that display features characteristic of both pericytes and VSMCs. Here we define pericytes based on their location within the vascular system (lining capillaries, as well as small arterioles and venules), the nature of their association with the endothelium (direct contact with endothelial cells through cellular processes), and expression of several validated pericyte cell markers (NG2, PDGFRβ, desmin) while excluding α-smooth muscle cell actin (αSMA) positive mural cells. The continuum of mural cell differentiation can be clearly appreciated in the mouse retina. In the mouse retina, NG2-positive, αSMA-negative pericytes line capillaries and venules, whereas more mature αSMA-positive, NG2-positive mural cells line retinal arterioles (Figure 2). Based on their location and intimate relationship with the endothelium, pericytes fulfill a role distinct from VSMCs during angiogenesis and in quiescent vasculature. Accordingly, it is important that pericytes be treated as a cell type independent of VSMCs in order to clearly understand their role in angiogenesis and the cellular mechanisms that govern their function.

The Notch signaling pathway

The Notch pathway is an evolutionarily conserved signaling mechanism that governs cell phenotype acquisition in species ranging from worms to mammals[6,16]. Notch signaling is highly context dependent where it can promote or inhibit cell proliferation, differentiation and cell death, as well as govern cell fate determination. Accordingly, Notch signaling is critical during development. Altered Notch signaling is associated with a variety of diseased states including

developmental disorders, such as Alagille Syndrome, adult-onset disorders (for example CADASIL, cerebral autosomal dominant arteriopathy with subcortical infarcts and leukoencephalopathy) and cancer[17-19].

In mammals, there are four Notch receptors (Notch1, Notch2, Notch3, and Notch4) which can interact with five Delta/Serrate/Lag-2 (DSL) ligands: Delta-like1 (Dll1), Delta-like3 (Dll3), Delta-like4 (Dll4), Jagged1, and Jagged2. The Notch receptors and their ligands are transmembrane proteins with large extracellular domains[20]. Activation of Notch signaling requires direct contact between a ligand-presenting cell and a receptor-presenting cell (Figure 1). Ligand interaction induces conformational changes of the receptor that exposes a cleavage site in the extracellular juxtamembrane region of Notch allowing for ADAM metalloprotease cleavage and release of the Notch extracellular domain (Notch-ECD). Ligand bound to Notch-ECD is then transendocytosed into the ligand-presenting cell. In the receptor-presenting cell, an additional cleavage event by Presenilin/γ-secretase releases the Notch intracellular domain (Notch-ICD) from the plasma membrane allowing it to translocate to the nucleus where it can activate transcription. During canonical Notch signaling, Notch-ICD forms a transcriptional complex with CSL (CBF-1, suppressor of Hairless, LAG-1)/RBPjκ and Mastermind-like proteins (MAML)[21]. Notch-ICD binding to CSL converts CSL from a transcriptional repressor to a transcriptional activator by displacing co-repressors and recruiting co-activators. The Notch/CSL/MAML transcriptional complex activates gene transcription through CBF1 binding motifs within the promoter of Notch target genes. Through recognition of CBF1 binding motifs, Notch-ICD can activate transcription of a variety of Notch target genes, such as PDGFR-β and αSMA[22,23]. Notch signaling can also result in indirect repression of downstream targets like VEGFR-2 through activation of the transcriptional repressors of the Hairy enhancer-of-split (HES) and Hairy/enhancer-of-split related with YRPW motif (HEY) families of basic helix-loop-

helix proteins[24,25]. In this way Notch signaling can evoke direct and indirect transcriptional outcomes to regulate cellular function.

Notch signaling in sprouting angiogenesis and mural cell differentiation

Notch signaling regulates multiple aspects of angiogenesis including endothelial cell sprouting, arterial venous specification, and vessel maturation[7,8,26]. Notch is essential for angiogenesis as evidenced by the vascular phenotypes associated with mutations in Notch receptors and ligands (Table 1). *Notch1*$^{-/-}$, *Dll1*$^{-/-}$, *Dll4*$^{-/-}$, and *Jagged1*$^{-/-}$ mice die between embryonic day 9.5 (E9.5) and 12.5 (E12.5) and display severe cardiovascular defects[27-30]. *Notch3*$^{-/-}$ mice are viable and fertile despite impaired mural cell maturation and reduced vascular tone[31,32]. Endothelial cells express Notch1, Notch4, Dll1, Dll4, and Jagged1, whereas mural cells express Notch1, Notch2, Notch3 and Jagged1[33]. At the angiogenic front, Notch functions in the endothelium to regulate endothelial cell sprouting by governing lateral inhibition events. The endothelial cell leading the angiogenic sprout called the tip cell expresses high levels of Dll4 in response to VEGFR-2 activation. Dll4 in the tip cell signals to its neighboring cell called the stalk cell through Notch1. Activation of Notch1 in the stalk cell leads to a down regulation of VEGFR-2 expression. In this way Notch signaling ensures that only the tip cell is highly responsive to VEGF-A and thereby limits excessive endothelial cell sprouting.

During vascular maturation, heterotypic Notch signaling between the endothelium and mural cells, as well as homotypic Notch signaling between mural cells induces mural cell differentiation and thus vessel maturation. Notch signaling in vascular smooth muscle cells activates expression of contractile proteins and thus promotes vascular smooth muscle cell differentiation to a mature and contractile cell phenotype[32,34,35]. During development, Jagged1 expression by endothelial cells is required to activate expression of contractile proteins in VSMCs to induce their maturation[36,37]. In adult mice, Notch3 signaling maintains mural cell

coverage in the brain, retina, and tail and Notch3 signaling is essential for proper vessel tone[34,38,39].

Alterations in Notch signaling are implicated in cerebral vascular pathologies, including CADASIL and arteriovenous malformations. Inherited mutations in Notch3 cause the lethal stroke disease CADASIL, which is characterized by Notch3-ECD cellular aggregates, loss of cerebral mural cell coverage, and deregulation of cerebral blood flow[18,40,41]. Arteriovenous malformations are also associated with abnormal Notch signaling[42]. Arteriovenous malformations (AVM) are abnormal cerebral vessels that shunt arterial blood directly into venous circulation without the normal intervening capillary plexus[43]. This direct transfer of blood results in increased hemodynamic pressure in the AVM and an increased risk of hemorrhage, and death. Endothelial activation of Notch signaling has been implicated in arteriovenous malformations in mice and in the human brain[42,44,45]. Dysplastic vessels in brain AVMs and human venous malformations also display disorganized and reduced αSMA positive mural cell coverage, suggesting that loss of proper mural cell coverage or function may contribute to vascular malformations[46-48].

Since both pericytes and the Notch signaling pathway critically regulate angiogenesis and pericytes express Notch receptors, we hypothesized that Notch functions in pericytes to regulate angiogenesis. Using the mouse retina and the ovarian corpus luteum as models of angiogenesis, we show that Notch is critical for pericyte recruitment to nascent blood vessels and that Notch signaling regulates pericyte association with the endothelium. Furthermore, we demonstrate that Notch-regulated pericyte/endothelial cell association is essential for endothelial function during angiogenesis. We show that loss of Notch signaling in pericytes alters vascular density and causes venule enlargement, increased vascular permeability, and arteriovenous malformations.

CHAPTER 1

Figures

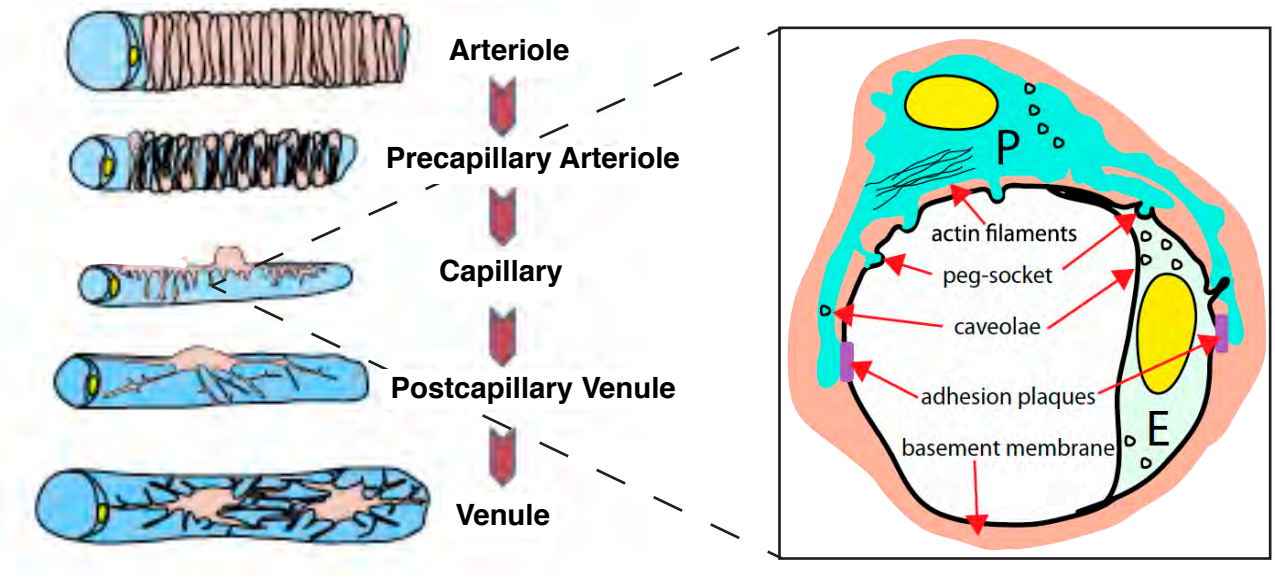

Figure 1. Diversity of mural cell phenotypes. Bona fide pericytes are found lining capillaries. Boxed region of capillary cross section shows that pericytes (P) make direct contact with endothelial cells (E) and share a basement membrane with the endothelium. Figure adapted from Armulik, A., Genové, G., & Betsholtz, C. (2011). Pericytes: developmental, physiological, and pathological perspectives, problems, and promises. *Dev Cell,* 21(2), 193–215.

.

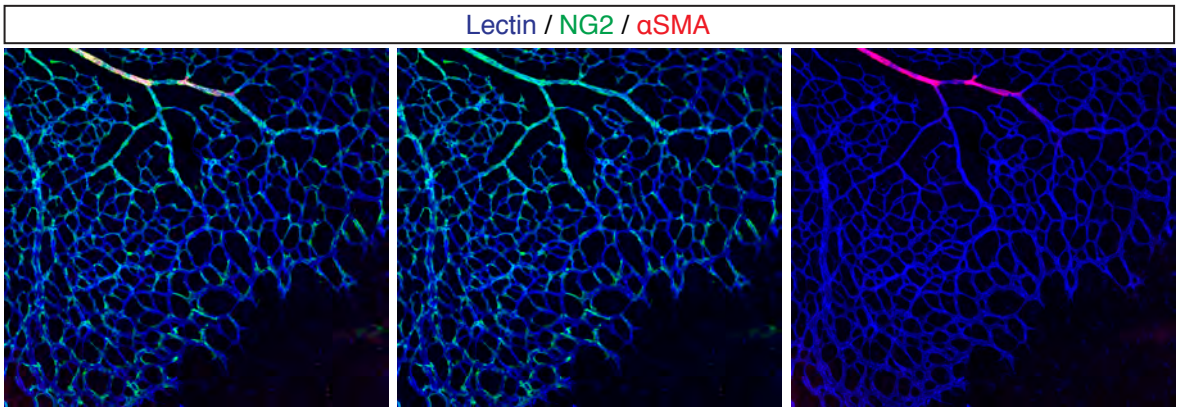

Figure 2. Mural cell marker expression in the retina. In P5 mouse retinas, only the mural cells lining the arterioles express αSMA (red). Pericytes lining the capillaries and venules express NG2 (green) and are negative for αSMA. In the retina, pericytes are also desmin positive and PDGFR-β positive (staining not shown). This staining pattern is maintained in adulthood. The endothelium is shown in blue.

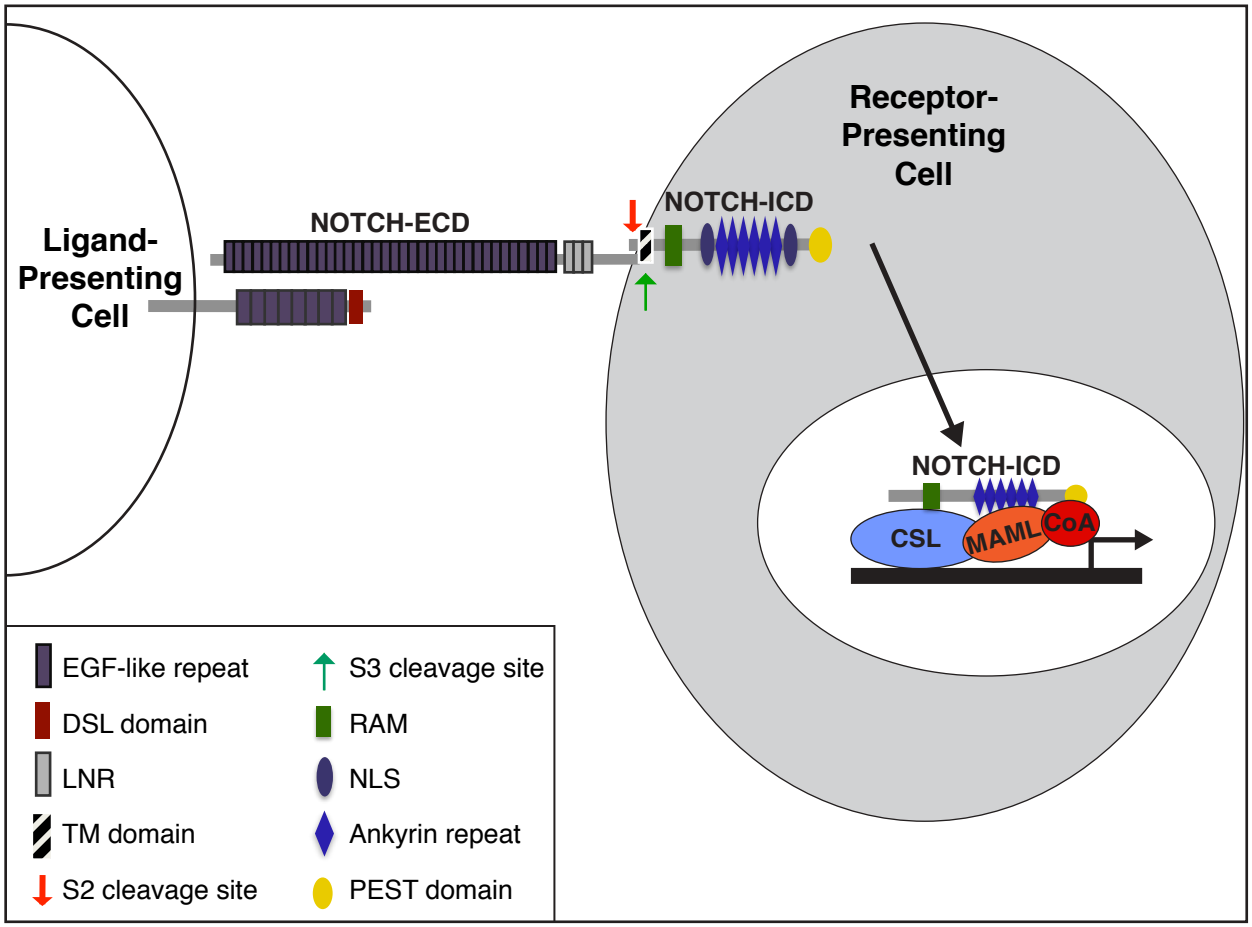

Figure 3. The Notch signaling pathway. The Notch receptor is first produced as a precursor proteint that undergoes furin cleavage at the S1 site to yield the Notch extracellular domain (ECD) and Notch intracellular domain (ICD), which contains the transmembrane (TM) domain (S1 cleavage is not shown in this diagram). At the cell surface, Notch-ECD and Notch-ICD are non-covalently linked. Ligand interaction allows for proteolytic cleavage at the S2 cleavage site by ADAM secretase followed by γ-secretase mediated cleavage at the S3 site. S3 cleavage releases Notch-ICD from the plasma membrane to enable its translocation to the cell nucleus where it activates transcription as part of the CSL/MAML/Notch-ICD transcriptional complex. EGF; epithelial growth factor, DSL; Delta/Serrate/LAG-2; LNR; Lin12-Notch repeats, RAM; RBPjκ association module, NLS; nuclear localization signal, PEST; proline/glutamic acid/serine/threonine-rich motif, CSL; CBF1/RBPjκ/Su(H)/Lag-1, MAML; mastermind like, CoA; co-activator.

CHAPTER 1

Tables

Table 1. Cardiovascular phenotypes of Notch mutant mice

Gene	Genetic Manipulation	Cardiovascular Phenotype	Reference
Notch1	Global null	Lethal prior to E11.5. Impaired angiogenesis: reduced sprouting, reduced remodeling. Collapsed aorta and cardinal vein. This angiogenic phenotype is worsened with additional loss of Notch4.	27,49,50
	Endothelial loss of function	Decreased aortic diameter. Arteriovenous malformations	51
	Global gain of function	Impaired vascular remodeling. Increased aortic diameter. Arteriovenous malformations.	51
Notch2	Global (hypomorphic) null	Lethal perinatally. Impaired kidney glomerular vascular development, myocardia hypoplasia, abnormal hyaloid vasculature.	52
	Cardiac neural crest loss of function	Reduced cardiac smooth muscle cell coverage. Narrowing of aorta and pulmonary arteries.	53
Notch3	Global null	Viable. Reduced VSMC maturation, impaired arterial VSMC specification, disrupted arterial structure. Loss of retinal VSMC coverage. Reduced vessel branching and outgrowth.	32,38,54
	R169C Notch3 mutation	Display cerebral vascular abnormalities reminiscent of CADASIL. Notch3-ECD aggregates, disrupted VSMC coverage, reduced vessel caliber and cerebral blood flow.	31
	Global null (combined with Notch2 null)	Lethal at E11.5. Decreased VSMC coverage with vessel collapse.	55
Notch4	Global null	Viable. No observed vascular defects.	27
	Endothelial gain of function	Lethal at E10. Impaired vessel branching, disorganized vascular networks, enlarged cerebral vessels.	56
Dll1	Global null	Lethal at E12. Display severe hemorrhaging. Increased venous identity with decreased arterial identity.	29
	Global heterozygote	Impaired hind limb ischemia induced angiogenesis.	57
Dll4	Global null	Lethal at E9.5. Loss of arterial endothelial identity. Defects in arterial branching and vessel remodeling.	30,58
	Global heterozygote	Viable. Increased vascular density and branching in the retina.	59
	Gain of function	Lethal prior to E10.5. Increased diameter of the dorsal aorta, decreased vascular sprouting, increased perivascular fibronectin deposition.	60
Jagged1	Global null	Lethal at E11.5-E12. Display severe hemorrhaging, defective vascular remodeling.	28
	Endothelial loss of function (Constitutive)	Lethal at E11.5-E12. Impaired VSMC maturation, cranial hemorrhaging, impaired vascular remodeling.	36
	Endothelial loss of function (Induced postnatally)	Viable. Reduced retinal vascular density with impaired VSMC coverage.	37

CHAPTER 2

Materials and Methods

The mouse retina as a model of angiogenesis

In the mouse, the retina becomes vascularized postnatally through the process of angiogenesis. *in utero*, angiogenesis produces the choroid vascular plexus, which supplies the outer layers of the retina with nutrients and the temporary hyaloid vascular network, which provides in utero support to the inner eye. Immediately following birth, retinal angiogenesis is driven by hypoxia which induces the astrocyte plane that lines the inner surface of the retina to secrete VEGF-A[61]. Endothelial cells sprout out and away from the optic nerve and along the inner surface of the retina to form a primary vascular plexus that reaches the periphery of the retina by postnatal day 8 (P8) (Figure 1). Endothelial cells then continue to sprout and migrate deeper into the retinal tissue to form a secondary and intermediary vascular plexus. Vascularization of the retina is completed by P21 in the mouse and follows tight temporal regulation. The consistent temporal regulation of retinal angiogenesis makes it an ideal model for studying various aspects of angiogenesis. Analysis of retinas isolated at P5 allows for assessment of angiogenic sprouting by measuring vascular density. Assessment of retinal vasculature at P8 can demonstrate vascular maturation events, whereas vascular function can be determined at later time points in development, such as P13.

Animals

Transgenic Notch reporter (TNR) mice harboring an enhanced GFP sequence under the control of 4 tandem copies of the CBF1 binding site consensus sequence were obtained from Jackson Laboratories[62]. *Notch1* and *Notch3* mutant mice have been previously described[49,54]. Please refer to Table 1 for genotyping primers. For ovary studies, female wildtype C57/Bl6 mice of 3 weeks of age (+/- 3 days) were obtained from Jackson Laboratories. Pregnant mare gonadotropin (Sigma) and human chorionic gonadotropin (Sigma) was used for stimulation of folliculogenesis and ovulation, respectively. All procedures were carried out according to

approved protocols and guidelines established by the Columbia University Institutional Animal Care and Use Committee.

Immunohistochemistry on Retinal Wholemounts

Following sacrifice, eyes were enucleated and fixed in 4% PFA for 2 hours at 4°C. Retinas were then dissected out and incubated in 0.5% Triton-X-100, 1% BSA, overnight at 4°C. Following washes in PBLEC (1% Triton-X-100, 1mM MgCl2, 1mM MnCl2, and 1mM CaCl2 in PBS [pH 6.8], retinas were incubated overnight in PBLEC containing biotinylated Isolectin-B4 (VectorLabs, 1:50) plus additional primary antibodies at appropriate dilutions (Table 2). On the following day, retinas were washed 3 times with PBLEC for 30 minutes each wash, and then 3 times with PBLEC diluted by half with 1XPBS (PB/2) for 30 minutes each wash. Retinas were incubated with Alexa Fluor conjugated secondary antibodies (Invitrogen) diluted at 1:500 in PB/2 overnight at 4°C or for 2 hours at room temperature while shaking. Retinas were then washed 4 times for 15 minutes each wash in PBLEC diluted by ¼ with 1xPBS (PB/4) followed by a single 10 minute wash with 1XPBS. To ensure longevity of staining retinas were post-fixed with 4% PFA for 15 minutes at room temperature. Retinas were then washed several times with 1XPBS prior to mounting on slides with mounting media containing 90% glycerol in 0.1M Tris pH 8 and 1 µg/ml of Hoechst nuclear stain (Sigma).

Latex Bead Perfusion Assay

The latex bead perfusion was performed as previously described[63]. Briefly, neonatal mouse pups were given a lethal dose of anesthesia (ketamine/xylazine). The abdominal and thoracic cavities were opened, the left and right atria were snipped, and a solution of blue latex beads (Connecticut Valley Biological Supply Company) was slowly injected into the left ventricle

of the heart. The eyes were then enucleated and processed for retinal wholemount immunostaining.

Analysis of Hyaloid Vasculature

Following sacrifice, eyes were enucleated and fixed with 4% PFA for 2 hours at 4°C and then washed with 1X PBS. Under a dissecting microscope the cornea, sclera and retina were dissected away. The hyaloid artery was cut at the optic nerve and the lens and hyaloid were kept intact and removed. The retinal wholemount immunostaining protocol was used to stain the hyaloid, aside from the mounting procedure. Instead the hyaloid and lens was kept in a 48-well the dish following post-fixing and low magnification confocal images were obtained using a Nikon A1R microscope by taking stacks through the entire lens.

Ovary Preparation and Staining

Following sacrifice, ovaries were removed and weighed after the fallopian tube was carefully removed and discarded. Ovaries were fixed with 4% PFA for 2 hours at 4°C and then dehydrated in 30% sucrose overnight at 4°C. Following sucrose dehydration ovaries were embedded in OCT for sectioning. Hematoxylin and eosin staining was performed by following an adjusted standard protocol where slides were incubated for 1 minute in hematoxylin and an acid wash was not performed. For ovary immunohistochemistry of thin sections, 7 µm ovary sections were fixed and permeabilized with acetone. Sections were then incubated for 1 hour in blocking solution containing 3% bovine serum albumin and 2% donkey serum. Ovaries were then incubated overnight at 4°C in blocking solution containing appropriate amounts of primary antibody (see Table 2). After washing in 1XPBS, ovary sections were then incubated for 1 hour at room temperature in blocking solution containing Alexa Fluor conjugated secondary

antibodies (Invitrogen) diluted at 1:1000. Vectashield® mounting medium with DAPI (Vector Laboratories) was used to visualize nuclei.

Validation of Serum Decoy Levels

For analysis of serum decoy levels prior to ovary collection blood was isolated from the tail vein. For analysis of serum decoy levels at time of ovary collection, blood was isolated by cardiac puncture. Blood was then centrifuged at maximum speed for 5 minutes to separate out the plasma. Plasma was frozen at -20°C until time of use. 2 µl of serum was run on SDS-PAGE by standard protocol. Human Fc was detecting using a HRP-conjugated antibody against human Fc (Sigma; A0170) at a dilution of 1:5000 in 2% milk, 2% BSA, 0.1% Tween in PBS.

Image Acquisition

A Nikon A1R microscope was used to acquire confocal stacked images of the stained and flat-mounted retinas. Brightfield colored tiled 5X images of latex perfused retinas were obtained using a PALM MicroBeam IV Laser Capture, Microirradiation, Histology Inverted microscope. Corresponding fluorescent 10X tiled confocal stacks were obtained using a Nikon A1R microscope. A Nikon Eclipse 200 fluorescent microscope and a Nikon A1R confocal microscope was used to obtain images of fluorescently stained images of ovary sections. Imaging of cultured cells was achieved using a Zeiss Axiovert 40 CSL inverted microscope. ImageJ and Adobe Photoshop were used for image processing.

Vessel Density and Pericyte Coverage Quantification

ImageJ was used for all quantification. For retinal vessel density quantification, 10X stacks were taken of each leaflet of each retina. The vascular area was outlined and then the

percent coverage of Isolectin-B4 staining of total vascularized area was obtained by thresholding the image. A similar procedure was performed for each leaflet stained with NG2 to analyze pericyte content per vascularized area. Pericyte coverage was calculated by dividing percent area of NG2 by percent area of Isolectin-B4. Vessel outgrowth was quantified by measuring the distance from the optic nerve to the edge of the vascular front for each leaflet. No significant difference in body weight was observed between genotypes (data not shown). For ovarian analysis, merged 10X stacks were obtained to cover the entire ovary section and account for changes in the focal plane. Each corpus luteum was outlined by hand. For each corpus luteum, thresholding was used to quantify corresponding total cell content by DAPI staining, endothelial cell content by CD31 staining, and pericyte content by NG2 staining.

Statistical Analysis

Data is presented as standard error of the mean or standard deviation, as indicated. Statistical significance was assessed using two-tailed student t-test. P-values less than 0.05 were considered significant. All data represents three independent experiments, unless otherwise noted.

Cell Culture

All cell cultures were maintained at 37°C in a mixture of 5% CO_2 and 95% humidified air. Human umbilical vein endothelial cells (HUVEC) were isolated as described and grown in EGM-2 Endothelial Cell Growth Media (CC-3162; Lonza Group)[9,64]. Human brain vascular pericytes (HBVP) (ScienCell) were maintained in 1X Low Glucose DMEM with 10% fetal bovine serum (FBS) and 1X Pen-Strep (100 U of penicillin and 100 U of streptomycin (Invitrogen). The gamma-secretase inhibitor (GSI) compound E was obtained from Korean Research Institute of Chemical Technology, an equal volume of DMSO (sigma) was used as control.

Adenovirus Infection of Cultured Cells

1.5 million cells were infected in suspension for 1 hour with adenovirus (MOI of 25). Adenovirus infection was halted by the addition of serum and cells were then plated. RNA was collected 48 hours after infection for analysis.

Production and Assessment of Stable Cell Lines

Cells with Notch activation and knockdown cell lines were made using stable lentiviral infection. Lentivirus was produced by 293T cells that were calcium phosphate transfected with viral packaging vectors with appropriate lentiviral constructs. For Notch activation 293T cells were transfected with 10 ug of pccl-GFP, pccl-RFP, pccl-Fc, pccl-N1IC, pcclN3IC, or pccl-N4/int3. For Notch knockdown experiments 293T were transected with 5 µg plko-empty vector plus 5 µg plko-scrambled shRNA, or 5 µg plko-NOTCH1 shRNA, or 5 µg plko-NOTCH3 shRNA, or plko-NOTCH1 shRNA and plko-NOTCH3 shRNA for double knockdown. To make stable cell lines, 293T supernatant containing virus was passed through a 0.45 µm filter and added to target cells (HUVEC or HBVP). All knockdown constructs were obtained from Sigma and validated by quantitative RT-PCR. Protein lysate was collected 4 days post-infection in TENT lysis buffer containing 1X HALT protease inhibitor cocktail (Thermo Fisher). The following antibodies were used for western blotting in 2% milk, 2% BSA, 0.1% Tween in 1X PBS: Rabbit anit-NG2 (1:1000) (Millipore), Rabbit anti-PDGFRβ (1:1000) (Cell Signaling), mouse anti-Vinculin (1:10 000) (Sigma). HRP-conjugated secondary antibodies were used at a dilution of 1:5000 (Sigma).

Gene Expression Analysis

RNA was collected from cultured cells using the RNeasy Mini Kit (Qiagen). Isolated RNA was treated with DNase1 for 30 minutes and then used in reverse-transcription PCR using the Verso™ Reverse Transcriptase kit with random hexamers to prime cDNA (Thermo Fisher). For quantitative RT-PCR, the reactions were done in triplicate with ABsolute Blue QPCR SYBR Green ROX Mix (Thermo Scientific) using a 7300 Real-Time PCR System (Applied Biosystems). Standard PCR to assess relative gene expression levels were performed by amplifying cDNA using specific primers and Platinum Taq Polymerase (Invitrogen). PCR amplification was performed with 35 cycles. See Table 3 for PCR primer sequences.

PDGF-BB Directed Matrigel Migration Assay

20 µl of matrigel (BD Biosciences) diluted 1:6 with serum free DMEM media was added to a BD Falcon™ cell culture insert for a 24 well plate with a pore size of 8 µm. 600 000 HBVP were seeded on matrigel in serum free DMEM containing 200 µM compound E or DMSO as control. Serum free DMEM containing 20 ng/ml of human recombinant PDGF-BB (R&D Systems) and 0.1% BSA (sigma) for stabilization was added to the lower chamber. After 48 hours the matrigel was removed and the side lining the filter was stained with toluidine blue to visualize cell content. It should be noted that due to time constraints this experiment was only performed once.

Pericyte/Endothelial Cell Co-culture Assay

The endothelial cell/pericyte co-culture assay was performed as previously described[65]. Briefly, HUVEC and HBVP at a concentration of $1x10^7$ cells/ml were embedded in 2.5 mg/ml collagen gel at a ratio of 5:1, HUVEC:HBVP. 200 ng/ml of SCF (R&D Systems), IL-3 (R&D Systems), and SDF-1α (R&D Systems) was added to the collagen gel prior to its solidification.

The collagen gel containing endothelial cells and pericytes was allowed to solidify at 37°C for 30 minutes in a half-volume 96-well plate prior to the addition of EGM-2 media to the well. Due to time constraints, this experiment was not replicated.

CHAPTER 2

Figures

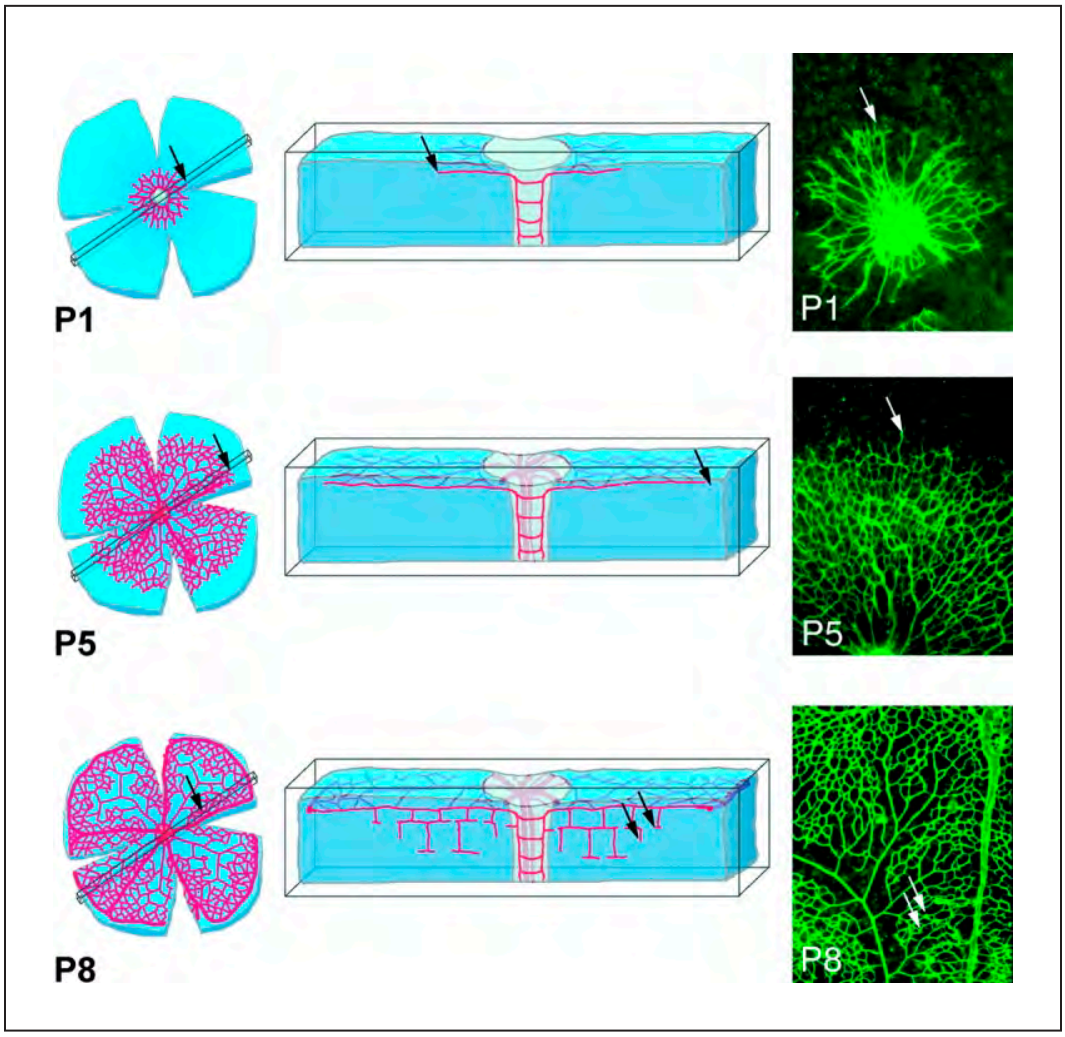

Figure 1. Developmental retinal angiogenesis in the mouse. Arrows depict endothelial tip cells. Adapted from Gerhardt, H., *et al*. (2003). VEGF guides angiogenic sprouting utilizing endothelial tip cell filopodia. *The Journal of Cell Biology*, 161(6), 1163–1177.

Chapter 2

Tables

Table 1. Genotyping primers

Primer	Sequence (5' to 3')
TNR Forward	TGCCCTTTCCTTAAAAGTGG
TNR Reverse	GCCTACTCCGACACCCAATA
Notch1 Mutant Forward	CAGGGGTTGGAGAGACATTCATTG
Notch1 Mutant Reverse	TCGCCTTCTATCGCCTTCTTG
Notch1 Wildtype Forward	TCTAAGTGCTCCGAGGAGATCA
Notch1 Wildtype Reverse	CAGGGGTTGGAGAGACATTCATTG
Notch3 Mutant Forward	TCGCCTTCTATCGCCTTCTTG
Notch3 Mutant Reverse	GGTACTGAGAACCAAACTCAG
Notch3 Wildtype Forward	CCATGAGGATGCTATCTGTGAC
Notch3 Wildtype Reverse	CACATTGGCACAAGAATGAGCC

Table 2. Antibodies for immunohistochemistry

Antibody	Host Species	Vendor	Catalog Number	Wholemount Dilution	Section Dilution
CD31	Rat	BD Biosciences	553370	1:100	1:500
NG2	Rabbit	Millipore	AB5320	1:750	1:750
NG2	Rat	R&D Systems	MAB6689	1:500	1:500
Desmin	Rabbit	Abcam	AB15200	1:500	1:500
PDGFR-β	Rabbit	Cell Signaling	3169	1:500	1:500
αSMA-Cy3	Mouse	Sigma	C6198	1:750	1:1000
GFP	Rabbit	Abcam	AB6556	1:1500	N/A
Collagen Type 4	Rabbit	Cosmo Bio	LSL-LB-0445	1:500	N/A
Laminin	Rabbit	Abcam	Ab81813	1:500	N/A
Fibronectin	Rabbit	Abcam	AB23750	1:500	N/A
Notch1	Goat	R&D Systems	AF1057	N/A	1:200
Notch3	Rabbit	Abcam	AB60087	N/A	1:100
Jagged1	Goat	R&D Systems	AF599	1:100	1:100

Table 3. Primers for mRNA expression analysis

Gene	Forward Primer (5' to 3')	Reverse Primer (5' to 3')
β-ACTIN	CGAGGCCCAGAGCAAGAGAG	CTCGTGATGGGCACAGTGTG
DLL4	CGGGTCATCTGCAGTGAAAC	AGTTGAGATCTGGTCACAAAACAG
GAPDH	GCCAAAAGGGTCATCATCTC	GTAGAGGCAGGGATGATGTTC
HES1	CCCAACGCAGTGTCACCTTC	TACAAAGGCGCAATCCATATG
HES5	TCGCCTCGTCGCCTGTTC	CCACGAGTAGCCTTCGCTGTAG
HEY1	ACGAGAATGGAAACTTGAGTTC	AACTCCGA AGTCCATAGCAAG
HEYL	CAGGATTCTTTGATGCCCGAG	GACAGGGCTGGGCACTCTTC
JAGGED1	GCTTGGATCTGTTGCTTGGTGAC	ACTTTCCAAGTCTCTGTTGTCCTG
JAGGED2	GCTATTTCGAGCTGCAGCTGAG	GCGGCAGGTAGAAGGAGTTG3
NOTCH1 (ECD)	GCAGACTATGCCTGCAGCTG	GCCACACTCGTTGACATCCTG
NOTCH1 (ICD)	CTCACCTGGTGCAGACCCAG	GCACCTGTAGCTGGTGGCTG
NOTCH2	CAGTGTGCCACAGGTTTCACTG	GCATATACAGCGGAAACCATTCAC
NOTCH3	CGCCTGAGAATGATCACTGCTTC	TCACCCTTGGCCATGTTCTTC
NOTCH4 (ECD)	ATGACCTGCTCAACGGCTTC	GAAGATCAAGGCAGCTGGCTC
PDGF-B	TGCTACCTGCGTCTGGTCAG	ACACCAGGAAGTTGGCGTTG
PDGFR-β	ATGCCTCCGACGAGATCTATG	TTGAGGAGGTGTTGACTCATTC

CHAPTER 3

Combined deficiency of Notch1 and Notch3 causes pericyte dysfunction and arteriovenous malformations

INTRODUCTION

During angiogenesis, vascular maturation requires mural cell recruitment and association with nascent blood vessels. Mural cells include contractile vascular smooth muscle cells (VSMC) and pericytes, which share the basement membrane with the endothelium. Pericytes are mural cells associated with small caliber blood vessels and capillaries that regulate endothelial cell proliferation, lumenization, and vascular basement membrane formation[6,9,66]. The platelet-derived growth factor (PDGF)-B/PDGF receptor-β (PDGFRβ) signaling pathway is critical for vascular pericyte recruitment and coverage in the central nervous system (CNS) and subsequent blood-brain barrier formation and function[9,67-70]. Lack of pericyte coverage in the CNS, including the retina, causes endothelial cell hyperplasia, vessel dilation, and increased vascular permeability[11,69,70].

The Notch signaling pathway regulates endothelial cell function and vessel maturation during angiogenesis. Specifically, Notch signaling regulates endothelial cell sprouting, arteriovenous specification, and VSMC maturation[26,71,72]. Notch signaling requires direct cell contact for receptor activation. Upon ligand binding, proteolytic cleavage events release the Notch intracellular domain from the plasma membrane allowing it to translocate to the nucleus to activate gene transcription (See Chapter 1 for detailed review). In VSMCs, Notch1 and Notch3 induce expression of genes important for mural cell function. In human aortic smooth muscle cells, Notch promotes α-smooth muscle cell actin (αSMA) expression[22]. In VSMCs isolated from human coronary arteries, Notch induces PDGFR-β expression[22,23]. Mice deficient for Notch3 and mice with endothelial-specific knockout of Jagged1 have normal pericyte recruitment, but impaired vascular smooth muscle cell coverage and maturation along larger vessels[36-38]. In these mouse models, decreased Notch signaling in the mural cell compartment was associated with vessel dilation and altered angiogenesis, suggesting that Notch signals in mural cells to regulate vessel function.

Notch signaling has also been implicated in the development of arteriovenous malformations (AVMs)[42,44,45]. Furthermore, mouse models that recapitulate human brain AVMs display vessel dilation and increased capillary density in areas of localized cerebrovascular malformations consistent with phenotypes associated with decreased CNS vascular mural cell coverage[46]. Thus, AVMs may involve both endothelial cell and mural cell dysfunction.

In the vasculature, endothelial cells and mural cells express Notch1, whereas Notch3 is restricted to the mural cell compartment. Given that Notch1 and Notch3 are expressed by pericytes, and that pericytes critically regulate angiogenesis, we sought to analyze angiogenesis in mice with combined deficiencies of Notch1 and Notch3. Specifically, we studied Notch3 mutant mice and Notch3 nulls with Notch1 haploinsufficiency. By analyzing the developing mouse retina in these mice we found that *Notch1*$^{+/-}$*;Notch3*$^{-/-}$ mice displayed increased vascular density, vessel dilation, and increased vascular permeability. *Notch1*$^{+/-}$*;Notch3*$^{-/-}$ mice also had arteriovenous malformations in the retina that were characterized by arteriovenous shunts and vascular tangles that resembled the structure of human brain AVMs.

RESULTS

Loss of Notch3 with Notch1 insufficiency results in increased vascular density and venule enlargement in the retina.

Loss of Notch1 activity results in a hypersprouted retinal vasculature, presumably due to endothelial dysfunction[59,73,74]. Notch3 mutant mice display reduced mural cell coverage and maturation[32,38]. However, both Notch1 and Notch3 are expressed by pericytes (Figure 1) and one can hypothesize that proper pericyte function may depend on the combined activity of Notch1 and Notch3. We generated viable mice null for Notch3 and heterozygous for Notch1, *Notch1*$^{+/-}$*;Notch3*$^{-/-}$ mice, to explore how these two Notch proteins may contribute to proper retinal angiogenesis. The expected genotypes of the offspring from crossing *Notch1*$^{+/-}$*;Notch3*$^{+/-}$

mice to *Notch3*$^{+/-}$ mice are wildtype, *Notch3*$^{+/-}$, *Notch1*$^{+/-}$, *Notch3*$^{-/-}$, *Notch1*$^{+/-}$*;Notch3*$^{+/-}$, and *Notch1*$^{+/-}$*;*Notch3$^{-/-}$. We analyzed these mutant mice and increased numbers for analysis by pooling multiple litters. As expected, the retinal vasculature of *Notch3*$^{+/-}$ was indistinguishable from wildtype, thus we selected *Notch3*$^{+/-}$ mice as controls.

To analyze the vasculature of mice mutant for Notch1 and Notch3 we isolated retinas at postnatal day 5 (P5) and stained them for Isolectin-B4 to visualize the vasculature and allow for analysis of vascular density (Figure 2, A-J). Here we define vascular density as the percentage of total vascularized area with endothelial cell coverage. As expected, *Notch1*$^{+/-}$ mice displayed an increase in vascular density with 45% endothelial cell coverage, as compared to 36% in *Notch3*$^{+/-}$ control mice (Figure 2K). This finding was consistent with the established role of Notch1 in the endothelium where it functions to restrict endothelial cell sprouting[59]. Interestingly, at P5 *Notch3* nullizygous mice also displayed a statistically significant increase in vascular density, as compared to control. This finding was intriguing since Notch3 expression is restricted to mural cells, thus the vascular phenotype observed in *Notch3*$^{-/-}$ mice was presumably secondary to mural cell dysfunction. Given that both *Notch1*$^{+/-}$ mice and *Notch3*$^{-/-}$ mice displayed an increase in vascular density, we hypothesized that combined loss of Notch3 with Notch1 haploinsufficiency would cause a more severe increase in vascular density. Analysis of the retinal vasculature at P5 of *Notch1*$^{+/-}$*;Notch3*$^{-/-}$ mice supported this hypothesis with *Notch1*$^{+/-}$*;Notch3*$^{-/-}$ mice displaying a significant increase in vascular density over *Notch1*$^{+/-}$ alone, 51% and 45% respectively. *Notch1*$^{+/-}$*;Notch3*$^{+/-}$ double heterozygous mice displayed an intermediate phenotype suggesting that Notch functions in a dose dependent manner to regulate vascular density. As previously described, *Notch3*$^{-/-}$ mice displayed decreased vascular outgrowth at P5. This phenotype was maintained in *Notch1*$^{+/-}$*;Notch3*$^{-/-}$ mice, despite the fact that *Notch1*$^{+/-}$ mice have normal vascular outgrowth (Figure 2L).

In addition to increased vascular density, we consistently observed abnormal vascular structures in retinas isolated from *Notch1*$^{+/-}$*;Notch3*$^{+/-}$ and *Notch1*$^{+/-}$*;Notch3*$^{-/-}$ *mice*. For example, retinal arterioles were often seen crossing over venules (a rarity in control retinas) and unusual vascular loops and tangles were also observed (data not shown). All of the mouse mutants analyzed (*Notch1*$^{+/-}$, *Notch3*$^{-/-}$, *Notch1*$^{+/-}$*;Notch3*$^{+/-}$, and *Notch1*$^{+/-}$*;Notch3*$^{-/-}$) displayed increased vascular branching from arterioles and venules, yet the overall structure and diameter of the arterioles of *Notch*$^{+/-}$*;Notch3*$^{-/-}$ mice appeared relatively normal. However, venules from *Notch*$^{+/-}$*;Notch3*$^{-/-}$ mice were severely enlarged and at points failed to fully differentiate from the neighboring capillary plexus (Figure 2,M-Q). These findings support the hypothesis that Notch1 and Notch3 are important regulators of angiogenesis since combined deficiency of Notch1 and Notch3 signaling results in increased vascular density. Furthermore, vascular analysis suggests that Notch1 and Notch3 are important regulators of venular size and vessel patterning.

Loss of Notch3 and partial loss of Notch1 causes retinal arteriovenous malformations

The enlarged veins and abnormal vascular structures observed in *Notch1*$^{+/-}$*;Notch3*$^{-/-}$ P5 retinas suggested that vascular function may be compromised in these mutant mice. By P12 the retinal vascular plexus of the mouse has sufficiently matured into arterioles, venules and intervening capillaries to allow for the segregation of oxygenated and deoxygenated blood[75,76]. Arteriovenous malformations occur when abnormal arteries and veins make direct connections through either a shunt or an abnormal intervening capillary plexus[10,77]. To assess the maturity of the vascular plexus and to analyze for the presence of AVMs in the retina, we employed a previously described latex perfusion assay[63]. Latex perfusion is assessed after blue latex beads are injected into the left ventricle of the heart of a postnatal P13 pup prior to sacrifice. In normal vasculature, the size of the latex beads excludes them from capillary networks and thus limits the latex delivery to the arterial side of circulation, which appears blue (Figure 3A). Subsequent

staining for NG2 allows for the fluorescent visualization of the retinal vasculature, including the venules devoid of latex (Figure 3 D-F). If AVMs and abnormal capillary plexuses are present the latex beads may enter venous circulation, as depicted by blue venules. Retinas from *Notch3*$^{-/-}$ P13 pups consistently presented with at least one blue venule (Figure 3B). In *Notch3*$^{-/-}$ mice, abnormal latex filled capillary connections can be seen feeding the venules (Figure 3H). This suggests that Notch3 alone is important for proper capillary structure and loss of Notch3 can cause abnormal segregation of arterial and venular blood flow. A dramatic AVM phenotype was observed in *Notch1*$^{+/-}$*;Notch3*$^{-/-}$ P13 pups as evidenced by numerous blue venules (Figure 3C). Closer examination of *Notch1*$^{+/-}$*;Notch3*$^{-/-}$ retinas following latex perfusion showed the presence of arteriovenous shunts and vascular tangles (Figure 3I). AVM structures were never observed in control retinas (n=5) (Figure3G) or Notch1$^{+/-}$ mice (data not shown). Our data demonstrates that mural cells play an important role in regulating arteriolar, capillary and venular patency since Notch3 is not expressed by the endothelium. Additional loss of Notch1 in a *Notch3*$^{-/-}$ background further compromises the retinal vascular plexus resulting in abundant and bona fide AVMs.

Loss of Notch3 and partial loss of Notch1 increases retinal vascular permeability

In the developing retinal vasculature at postnatal day 8, arterial, venous, and capillary structures can be appreciated. However, at this time point the blood vessels have yet to fully mature and become functionally segregated[78]. Vascular immaturity can be appreciated by performing latex bead perfusion assays on control P8 mice where, unlike at P13, blue latex is observed in venules and there are small micro-leaks in the capillary plexus (Figure 4A). We sought to determine if *Notch3*$^{-/-}$ and *Notch1*$^{+/-}$*;Notch3*$^{-/-}$ mutant mice displayed delayed vascular maturation at P8; a time point in retinal development that precedes the observation of functionally defined AVMs at P13. At P8, the severity of leaks and the number of latex-filled

venules was increased in *Notch3*$^{-/-}$ mice as compared to control (Figure 4B). This phenotype was worsened with the addition of Notch1 haploinsufficiency. Retinas analyzed from *Notch1*$^{+/-}$*;Notch3*$^{-/-}$ mice displayed severe vascular leakage and contained structures that were clearly vascular shunts (Figure 4C). To further characterize the vasculature at P8 we quantified vascular density at this time point. *Notch1*$^{+/-}$*;Notch3*$^{-/-}$ mice displayed increased vascular density that surpassed the severity of phenotype previously observed at P5 (Figure 5). These data suggest that Notch1 and Notch3 signaling regulates vessel permeability and maturation in the retina.

Notch1 and Notch3 regulate vascular mural cell coverage in the developing retina

Vascular leakage and endothelial hypersprouting during angiogenesis can be suggestive of impaired vessel maturation. Since mural cell coverage is critical for vessel maturation and Notch3 is restricted to the mural cell population, we hypothesized that mural cell coverage may be compromised in *Notch1*$^{+/-}$*;Notch3*$^{-/-}$ mutant mice. High magnification confocal stacks of arterioles at P8 showed that mural cell (NG2+/AMSA+) association with the endothelium was altered in *Notch1*$^{+/-}$*;Notch3*$^{-/-}$ retinas (Figure 6). In control retinas, mural cells display normal cell morphology, as evidenced by an oval-shaped cell body with processes making close association with the underlying endothelium (Figure 6A). In contrast, mural cells in *Notch1*$^{+/-}$*;Notch3*$^{-/-}$ mice do not tightly line the arterioles (Figure 6C). Mural cell processes can be seen coming off of the endothelium in *Notch1*$^{+/-}$*;Notch3*$^{-/-}$ P8 retinas. This data suggests that mural cell function may be compromised in *Notch1*$^{+/-}$*;Notch3*$^{-/-}$ mutant mice.

To determine whether abnormal mural cell coverage contributes to the vascular phenotypes observed in *Notch1*$^{+/-}$*;Notch3*$^{-/-}$ mutant mice we wanted to analyze the mural cell compartment at an earlier time point in development that precedes vessel maturation and the appearance of AVMs. We believe that analysis of mural cell coverage at P5 allows for the

assessment of mural cell dysfunction as a causal factor for the vascular phenotypes observed at P8 and P13. In the mouse retina, αSMA is a marker of a more mature and contractile VSMC that only lines the retinal arterioles (Chapter 1, Figure 2)[15]. The remaining mural cells that line the venules and capillaries of the retina are NG2-positive and negative for αSMA expression. We consider NG2-positive mural cells localized to the capillary plexus and venules to be pericytes. P5 retinas stained for NG2 to mark pericytes showed that pericytes are recruited to the vasculature in *Notch3*$^{-/-}$, *Notch1*$^{+/-}$, *Notch1*$^{+/-}$;*Notch3*$^{+/-}$ and *Notch1*$^{+/-}$;*Notch3*$^{-/-}$ mice (Figure 7, A-J). However, when NG2 staining was normalized to percent vascular area, a marked decrease in pericyte coverage was observed in *Notch3*$^{-/-}$, *Notch1*$^{+/-}$, *Notch1*$^{+/-}$;*Notch3*$^{+/-}$ and *Notch1*$^{+/-}$;*Notch3*$^{-/-}$ mice as compared to *Notch3*$^{+/-}$ control (Figure 7K). This suggests that both Notch1 and Notch3 function to regulate pericyte coverage during angiogenesis. Pericyte recruitment to nascent vasculature during angiogenesis is required for vessel maturation and is an import cue for vascular cell quiescence. The lack of adequate pericyte coverage in *Notch1*$^{+/-}$;*Notch3*$^{-/-}$ mice at P5 may contribute to the increased vascular density, increased vascular permeability and AVMs observed in mice mutant for Notch1 and Notch3.

Notch1 and Notch3 signaling contribute to VSMC maturation

Notch3 has been shown to be a critical regulator of VSMC maturation. In part, reflected by the fact that Notch induces αSMA expression in VSMCs[32,38]. AVMs in mice and humans have been shown to have decreased αSMA-positive mural cell coverage[48,79]. Since we saw a more severe AVM and vascular leakage phenotype in *Notch1*$^{+/-}$;*Notch3*$^{-/-}$ mice as compared to *Notch3*$^{-/-}$ alone, we sought to determine if Notch1 is also an important regulator of mural cell maturation, as defined by αSMA positivity. Again, we assessed mural cell maturation at P5 before AVMs appear in the retina to determine whether inhibition of VSMC maturation could contribute to their formation. As has previously been described, *Notch3*$^{-/-}$ mice displayed

decreased αSMA expression along the arteriole at P5 (Figure 8B) with normal NG2 staining (Figure 8L). *Notch1*$^{+/-}$*;Notch3*$^{-/-}$ mice displayed a greater reduction in αSMA expression, as compared to *Notch3*$^{-/-}$ alone (Figure 8E). *Notch1*$^{+/-}$ and *Notch1*$^{+/-}$*;Notch3*$^{+/-}$ mice had normal αSMA signal intensity. However, as compared to *Notch3*$^{+/-}$ control, we observed an increase in arteriole surface area that were devoid of αSMA staining in *Notch1*$^{+/-}$*;Notch3*$^{+/-}$ mice (Figure 8D).

These findings were supported by analysis of human brain vascular pericyte (HBVP) knockdown cell lines evaluated *in vitro*. Protein lysates isolated from NOTCH1 knockdown and NOTCH3 knockdown HBVP cell lines contained less αSMA, as compared to control (Figure 8P). Double knockdown of NOTCH1 and NOTCH3 showed a dramatic reduction in αSMA levels as compared to control or either NOTCH1 or NOTCH3 knockdown alone. However, NG2 protein expression remained constant in all cell lines assessed. These findings show that both Notch1 and Notch3 are involved in maintaining proper αSMA levels in mural cells, implicating both Notch receptors in mural cell maturation.

Notch1 and Notch3 are critical for pericyte association with the vasculature.

αSMA-positive VSMCs line the arterioles of the retina, yet we observed vascular phenotypes in *Notch1*$^{+/-}$*;Notch3*$^{-/-}$ mice that involved arterioles, venules and capillaries. Inadequate VSMC maturation only partially explains the vascular phenotypes observed in *Notch1*$^{+/-}$*;Notch3*$^{-/-}$ mice as NG2-postive, αSMA-negative pericytes line all of the vascular structures of the retina. Thus, we hypothesized that the retinal vascular abnormalities observed with decreased Notch1 and Notch3 signaling may be due to pericyte dysfunction. Low magnification images of P5 control retinas stained for NG2 show that pericytes completely cover the endothelium with relatively uniform staining intensity (Figure 7F). While analyzing retinas for pericyte coverage from *Notch1*$^{+/-}$*;Notch3*$^{-/-}$ and *Notch3*$^{-/-}$ mice we observed NG2-positive

pericytes with increased staining intensity lining the capillary plexus. The brightly stained pericytes appeared to have an altered morphology and they didn't line the endothelium as tightly as they do in control retinas (Figure 7F and 7H). We showed that inhibition of Notch signaling in pericytes does not alter NG2 expression *in vitro* (Chapter 5, Figure 4). Thus, we hypothesize that the aforementioned increase in NG2 staining intensity was due to an increase in cell surface area availability to antibody detection caused by pericyte dissociation from the endothelium.

To assess for changes in pericyte/endothelial cell association we took high magnification confocal stacks of P5 retinas stained for CD31 to mark endothelial cells and NG2 to visualize pericytes. High magnification images were taken at two locations where vascular phenotypes had been observed in *Notch1*$^{+/-}$*;Notch3*$^{-/-}$ mice; the capillary plexus behind the angiogenic front where we saw increased vascular density and at the first branch point of the venule were we observed venule enlargement. Since AVMs were not observed at P13 in the retinas of *Notch1*$^{+/-}$ mice we excluded this genotype in the subsequent analysis. In the retina capillary plexus and venules of the *Notch3*$^{+/-}$ control mouse the cell surface of the pericytes appears smooth, the pericytes have uniform NG2 staining intensity, and the pericytes tightly line the endothelium (Figure 9, A-D). In the *Notch3*$^{-/-}$ null retina some pericytes in the plexus displayed bright NG2 staining and had cell processes that don't make tight contact with the endothelium (Figure 9E). Pericytes lining *Notch3*$^{-/-}$ venules displayed distinctly altered cell morphology with a cell surface that appeared uneven and an increased number of cell processes (Figure 9G). Pericyte association with the endothelium was further compromised with additional loss of Notch1 in *Notch1*$^{+/-}$*;Notch3*$^{-/-}$ mice where NG2-positive pericytes can be seen coming off of the vascular plexus and at some points piling on top of one another (Figure 9M). Pericyte coverage appeared reduced along venules of *Notch1*$^{+/-}$*;Notch3*$^{-/-}$ retinas and again displayed altered cell morphology similar to that observed in *Notch3*$^{-/-}$ mice (Figure 9P). The *Notch1*$^{+/-}$*;Notch3*$^{+/-}$

double heterozygous mice showed an intermediate phenotype with pericyte dissociation that surpassed that of *Notch3*$^{-/-}$ mice, but was not as severe as the phenotype observed in *Notch1*$^{+/-}$*;Notch3*$^{-/-}$ mice (Figure 9, I-L). This data suggest that loss of Notch3 with a combined reduction of Notch1 compromises the association of pericytes with the endothelium. The observed loss of proper mural cell association with the endothelium early in retinal development may contribute to the increased vascular density, lack of vessel maturation, and appearance of AVMs observed at later developmental time points in *Notch1*$^{+/-}$*;Notch3*$^{-/-}$ mice.

Notch1$^{+/-}$*;Notch3*$^{-/-}$ mice have a disorganized vascular basement membrane

Pericytes share the vascular basement membrane with the endothelium. Vascular network formation *in vitro* with pericytes and endothelial cells demonstrate that pericyte coverage of vascular networks is required for vascular basement membrane deposition[6].

Since vascular basement membrane deposition is induced when pericytes properly associate with endothelial cells during angiogenesis, we wanted to analyze vascular basement membrane deposition in the plexus and venules where we observed pericyte dissociation in *Notch3*$^{-/-}$; *Notch1*$^{+/-}$*;Notch3*$^{+/-}$, and *Notch1*$^{+/-}$*;Notch3*$^{-/-}$ mice. In the retina, the main components of the vascular basement membrane are collagen type IV, laminin, and fibronectin. Using high magnification confocal imaging we analyzed P5 retinas stained for Isolectin-B4 to visualize the vasculature, NG2 to mark pericytes and either collagen type IV, laminin, or fibronectin to assess basement membrane organization and deposition. We observed that fibronectin is not specific to the vascular basement in the retina; it is strongly expressed by the underlying astrocyte plane. Nonetheless, deposition of fibronectin and its organization appeared normal across genotypes (data not shown). A uniform layer of collagen type IV lines the endothelium of the capillary plexus in *Notch3*$^{+/-}$ mice, as well as in *Notch3*$^{-/-}$ and *Notch1*$^{+/-}$*;Notch3*$^{+/-}$ mice despite decreased staining intensity (Figure 10, B and C). In the capillary plexus of *Notch1*$^{+/-}$*;Notch3*$^{-/-}$

mice, collagen type IV staining appears abnormal and severely disorganized, as it is not restricted to the abluminal surface of the endothelium, but instead widely dispersed across the plexus (Figure 10D). Areas of intense collagen type IV staining can be seen with severe heterogeneity in collagen type IV staining intensity across the endothelium of the plexus of *Notch1*$^{+/-}$*;Notch3*$^{-/-}$ mice (Figure 10L). Collagen type IV deposition is also severely disorganized in the grossly enlarged venules of *Notch1*$^{+/-}$*;Notch3*$^{-/-}$ mice (Figure 10X).

Localization of the vascular basement membrane component laminin was also dramatically altered in the plexus and venules of *Notch1*$^{+/-}$*;Notch3*$^{-/-}$ mice. In *Notch1*$^{+/-}$*;Notch3*$^{-/-}$ mice laminin appears disorganized in the plexus where a blush of staining can be appreciated, which is not associated with the vasculature (Figure 11D). In the venule, laminin fails to uniformly line the endothelium in *Notch1*$^{+/-}$*;Notch3*$^{-/-}$ mice (Figure 11P). Mild alterations of laminin deposition can also be observed in *Notch3*$^{-/-}$ and *Notch1*$^{+/-}$*;Notch3*$^{+/-}$ mice which display a mild blush laminin staining pattern in the plexus and venule (Figure 11, B, C, N, and O). These findings support a role for pericyte association with the endothelium in regulating basement membrane deposition. Lack of pericyte association and abnormal basement membrane deposition preceded the appearance of AVMs in *Notch1*$^{+/-}$*;Notch3*$^{-/-}$ mice. We propose that pericyte dysfunction and alterations in basement membrane resulting from combined deficiency of Notch1 and Notch3 contributes to the AVMs that appear later in retinal development.

Notch1$^{+/-}$*;Notch3*$^{-/-}$ mice display abnormal hyaloid vasculature at P5

During P5 retinal dissections, we observed that the blood vessels of the hyaloid vascular network appeared thicker and chord-like in *Notch1*$^{+/-}$*;Notch3*$^{-/-}$ mice, in contrast to the fine hyaloid vasculature observed in all other genotypes assessed. The hyaloid vascular system is a temporary vascular network that delivers oxygen and nutrients to the intraocular components of

the developing eye[61]. The hyaloid vascular network spans the vitreous space and forms a dense capillary plexus on the surface of the lens. As the retina matures and becomes vascularized, the hyaloid progressively regresses, yet at postnatal day 5 the hyaloid vascular network is still relatively intact. We isolated the hyaloid vascular network and lens from *Notch1*$^{+/-}$*;Notch3*$^{-/-}$ mice and *Notch3*$^{+/-}$ mice to serve as controls. Wholemount staining for Isolectin-B4 showed that the hyaloid vessels of *Notch1*$^{+/-}$*;Notch3*$^{-/-}$ mice were thicker and denser when compared to control (Figure 12B). The hyaloid vascular network of *Notch1*$^{+/-}$*;Notch3*$^{-/-}$ mice also appeared to be more rudimentary than controls; they lacked the normal vascular hierarchy of arterioles, venules, and capillaries. Instead the hyaloid vasculature of *Notch1*$^{+/-}$*;Notch3*$^{-/-}$ mice contained only larger vessels without an obvious capillary plexus found in controls (Figure 12B) .

Analysis of pericyte and VSMC coverage by staining for NG2 and αSMA, respectively, showed dramatic differences in mural cell coverage of the hyaloid vasculature between *Notch1*$^{+/-}$*;Notch3*$^{-/-}$ and *Notch3*$^{+/-}$ mice at P5. In the control hyaloid vascular plexus, NG2-positive pericytes line the entire vascular network and αSMA-positive VSMCs are associated with the larger hyaloid arterioles that extend from the optic nerve (Figure 12C). In *Notch1*$^{+/-}$*;Notch3*$^{-/-}$ mice NG2-positive mural cell coverage of the hyaloid is dramatically reduced (Figure 12D). Furthermore, the cell morphology of VSMCs and αSMA-negative pericytes associated with the hyaloid was dramatically altered in *Notch1*$^{+/-}$*;Notch3*$^{-/-}$ mice (Figure 12F). VSMCs in the *Notch1*$^{+/-}$*;Notch3*$^{-/-}$ mice had elongated cell bodies and made contact through cellular processes with multiple hyaloid vessels (Figure 12H). NG2-positive, αSMA-negative pericytes in the *Notch1*$^{+/-}$*;Notch3*$^{-/-}$ display similarly abnormal cellular phenotypes (Figure 12J). In the control, the hyaloid pericytes are tightly associated with the vasculature, whereas in *Notch1*$^{+/-}$*;Notch3*$^{-/-}$ mice the pericytes are dissociated from the underlying endothelium (Figure 12, I and J). Despite having reduced mural cell coverage, a greater number of macrophages were observed to be

associated with the hyaloid vasculature of *Notch1*$^{+/-}$*;Notch3*$^{-/-}$ mice (data not shown). Thus, decreased Notch1 with complete loss of Notch3 causes alterations in hyaloid and retinal vasculature by increasing vascular density and causing vessel enlargement.

DISCUSSION

Here we show that combined deficiency of Notch1 and Notch3 (*Notch1*$^{+/-}$*;Notch3*$^{-/-}$) led to increased vascular density, venule enlargement, increased vascular permeability, pericyte dissociation, and arteriovenous malformations in the developing retina. Previous work has described segregated functions for vascular Notch proteins; Notch1 functions in the endothelium and Notch3 functions in the mural cell compartment. In endothelial cells Notch1 signaling inhibits sprouting and in mural cells Notch3 functions to promote cell differentiation. However, mural cells express both Notch1 and Notch3. We showed that Notch1 and Notch3 are required for normal αSMA expression in pericytes *in vitro* and that αSMA expression is dramatically reduced in *Notch3*$^{-/-}$ mice with Notch1 haploinsufficiency. We also demonstrated that combined loss of Notch1 and Notch3 leads to mural cell dissociation from the retinal endothelium in *Notch1*$^{+/-}$*;Notch3*$^{-/-}$ mice. These studies expand upon previous findings that pericyte coverage is essential for vascular maturation and quiescence and demonstrate that Notch regulates this process[66,69,80-84]. In *Notch1*$^{+/-}$*;Notch3*$^{-/-}$ mice, pericytes failed to properly associate with the endothelium of the retinal vasculature at P5. This mural cell phenotype was associated with increased vascular density, enlarged venules, and abnormal vascular basement membrane deposition suggesting that Notch1 and Notch3 cooperate to regulate vascular maturation by promoting mural cell coverage during sprouting angiogenesis.

Notch1$^{+/-}$*;Notch3*$^{-/-}$ mice presented with numerous retinal AVMs characterized by vascular tangles, abnormal capillaries and arteriovenous shunts that recapitulated human AVMs. Retinal AVMs are rare, congenital vascular anomalies that, like brain AVMs, are

characterized by dilated, tortuous high pressure vascular tangles and arteriovenous shunts[85]. Since the vasculature of the retina-blood barrier shares many characteristics with the blood-brain barrier, the ease of vascular analysis of the retina makes retinal AVMs an attractive model for understanding the mechanisms that govern the development of cerebral vascular malformations. Previous studies implicate Notch activation in brain AVMs[42,44,45]. Notch1 is often upregulated in the endothelium and VSMCs of human brain AVMs[44]. Endothelial Notch4 activation during mouse brain development induces the formation of cerebral high-flow arteriovenous shunts[45]. Furthermore, normalization of Notch4 expression in AVMs induces regression through a decrease in vessel size and reemergence of a normal capillary plexus[86]. Our work shows that loss of Notch expression can also cause AVMs, as demonstrated by the retinal AVMs observed in *Notch1*$^{+/-}$*;Notch3*$^{-/-}$ mice. Current models for Notch in AVMs focus on Notch in the endothelium. Murphy et al. provide an elegant model that centers on arteriovenous specification and with evidence supporting a model that activated Notch causes venule arterialization. In addition, they show that when Notch expression is normalized, endothelial cells regain their venular identity and AVM regression ensues[86]. In our mouse model, Notch expression is lost in both endothelial cells and mural cells, thereby expanding the functional role of Notch in vascular abnormalities. Thus, we conclude that loss of Notch in both cell types contributes to AVM formation.

In *Notch1*$^{+/-}$*;Notch3*$^{-/-}$ mice, pericyte dissociation from the endothelium was observed prior to the emergence of retinal AVMs. We suspect that the dramatic loss of pericyte association with the endothelium in *Notch1*$^{+/-}$*;Notch3*$^{-/-}$ mice contributes to the vascular abnormalities observed in these mutant mice. The mechanism underlying pericyte dissociation in *Notch1*$^{+/-}$*;Notch3*$^{-/-}$ mice remains to be determined. Pericytes share a basement membrane with the endothelium, and their recruitment to nascent blood vessels has been shown to be critical for proper vascular basement membrane deposition[6,15]. The vascular basement

membrane has also been shown to limit endothelial cell sprouting through regulation of endothelial Notch signaling[87,88]. We observed that *Notch1*$^{+/-}$*;Notch3*$^{-/-}$ mice had an altered vascular basement membrane characterized by reduced laminin expression and enhanced fibronectin expression. Furthermore, *Notch1*$^{+/-}$*;Notch3*$^{-/-}$ mice displayed severe disorganization of both collagen type IV and laminin in the capillary plexus and venules. Our model posits that the retinal vasculature of *Notch1*$^{+/-}$*;Notch3*$^{-/-}$ mice fails to become quiescent due to loss of proper pericyte coverage and altered basement membrane deposition. Lack of vessel quiescence in *Notch1*$^{+/-}$*;Notch3*$^{-/-}$ mice presents as increased vascular density, venule enlargement and contributes to the observed AVMs in *Notch1*$^{+/-}$*;Notch3*$^{-/-}$ mice. It is also possible that pericytes in *Notch1*$^{+/-}$*;Notch3*$^{-/-}$ mice could have an impaired ability to interact with the basement membrane. Integrins bind the basement membrane and are critical regulators of angiogenesis[89]. Notch signaling in retinal αSMA-positive VSMCs regulates integrin αvβ3 expression allowing for adhesion of VSMCs to von willebrand factor (VWF) in the basement membrane[90]. Vascular integrin expression may be altered in *Notch1*$^{+/-}$*;Notch3*$^{-/-}$ mice, which requires further investigation.

Notch1$^{+/-}$*;Notch3*$^{-/-}$ mice also displayed abnormal hyaloid vasculature. This phenotype included increased vessel content, vessel thickening and abnormal mural cell coverage at postnatal day 5. These observations support a role for Notch1 and Notch3 in pericyte function in multiple vascular beds. However, whether Notch functions in hyaloid mural cells to regulate the development or regression of the hyaloid vascular plexus remains to be determined.

The severity of the vascular phenotypes displayed by *Notch1*$^{+/-}$*;Notch3*$^{-/-}$ mice highlights an important role for Notch in pericyte function by regulating their association with the endothelium. We demonstrate that Notch regulated pericyte association is critical for proper vascular function and that pericyte dysfunction can result in arteriovenous malformations.

CHAPTER 3

Figures

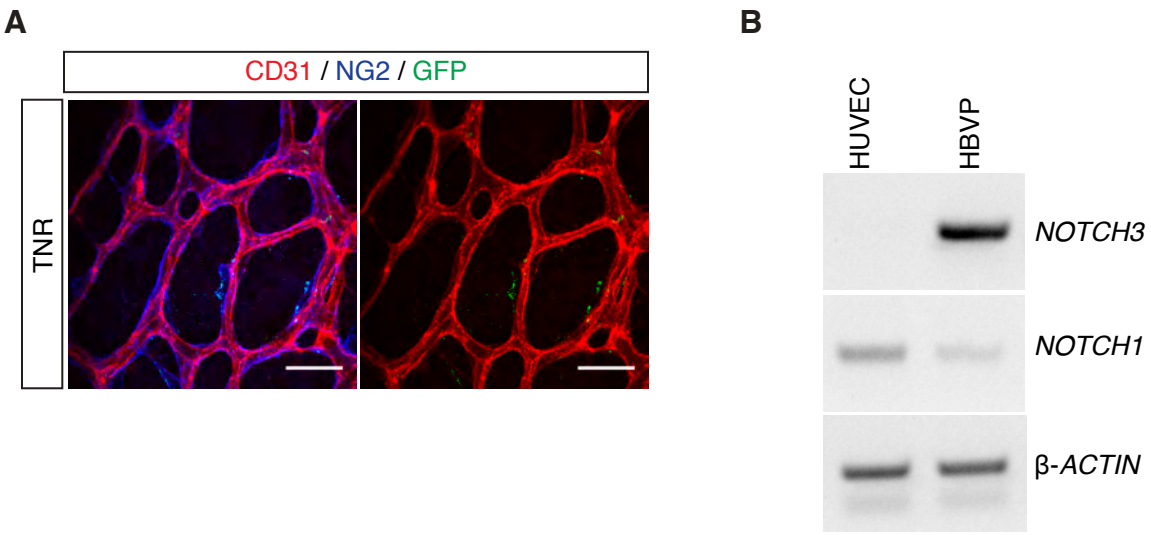

Figure 1. Notch1 and Notch3 are expressed by pericytes. The vascular plexus of P5 retinas isolated from Transgenic Notch Reporter (TNR) mice stained for GFP (green) to visualize Notch activation in endothelial cells (red) and pericytes (blue) (A). PCR amplification using primers specific for *NOTCH1* and *NOTCH3* of cDNA isolated from HUVEC or HBVP. *β-ACTIN* used as control (B). Scale bars; 25 µm.

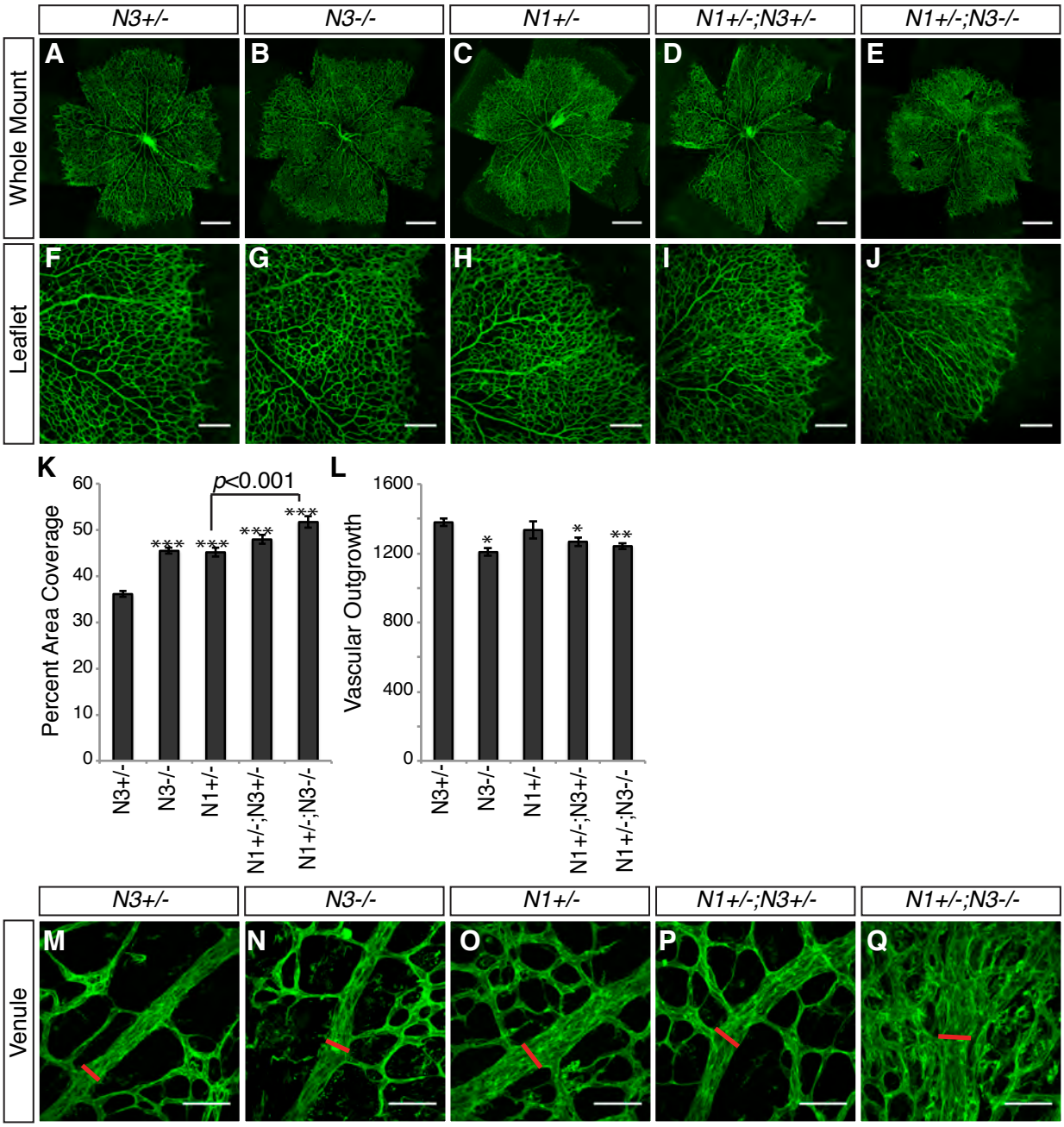

Figure 2. Notch1 and Notch3 limit vessel density in the retina at P5. Wholemount retinas isolated from P5 mice stained for Isolectin-B4 to visualize the vasculature (A-J, M-Q). Tiled confocal stacks show the entire primary plexus and vascular outgrowth (A-E). Confocal stacks of individual retinal leaflets allow for greater detail (F-J). Quantification of vessel density as measured by percent of IsolectinB4 staining within the total vascularized area (K). Quantification of vascular outgrowth as measured by the average distance (μm) between the optic nerve and furthest vascular point of each leaflet (L). Confocal stacks of venules taken at the first branch point from the optic nerve show enlargement of *Notch1*$^{+/-}$*;Notch3*$^{-/-}$ venules, as compared to control (M-Q). Red lines mark venule diameter. Scale bars; 500 μm (A-E), 200 μm (F-J), 50 μm (M-Q). Error bars represent SD of the mean. n≥3, with 8 leaflets/mouse,*p<0.01, **p<.001, *** p<1x10^{-10}. *N1=Notch1*, *N3=Notch3.*

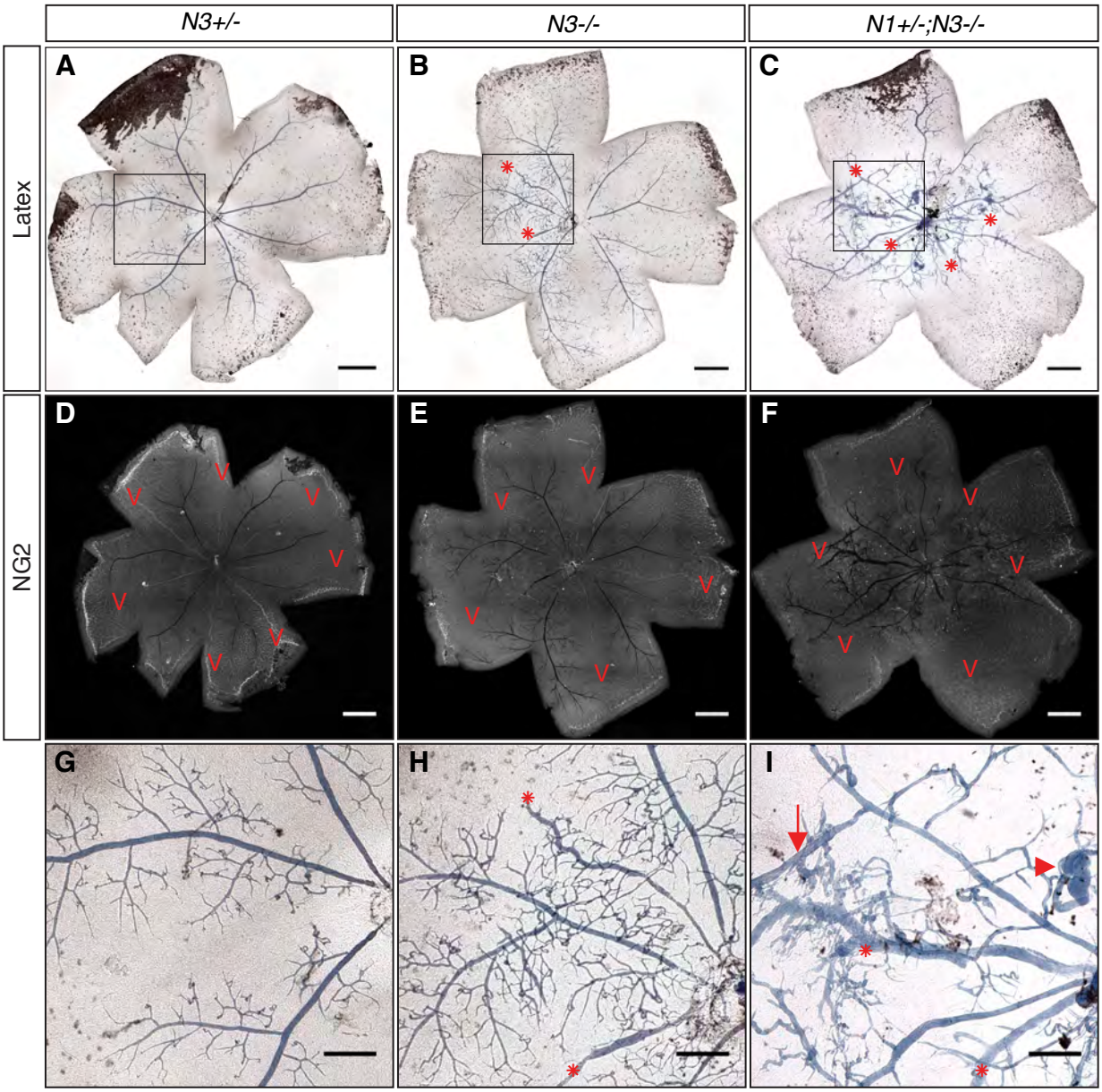

Figure 3. Latex bead perfusion shows arteriovenous malformations in *Notch1*$^{+/-}$;*Notch3*$^{-/-}$ mouse retinas. Bright field images of wholemount retinas isolated from P13 mice following blue latex bead perfusion (A-C). Corresponding fluorescent images of the same whole mount retinas stained for NG2 to visualize the vasculature (D-F), venules marked by “V”. Higher magnification images (G-H) show blue venules (asterisks), arteriovenous shunts (arrow) and vascular tangles (arrowhead). Scale bars; 500 µm (A-F), 200 µm (G-I).

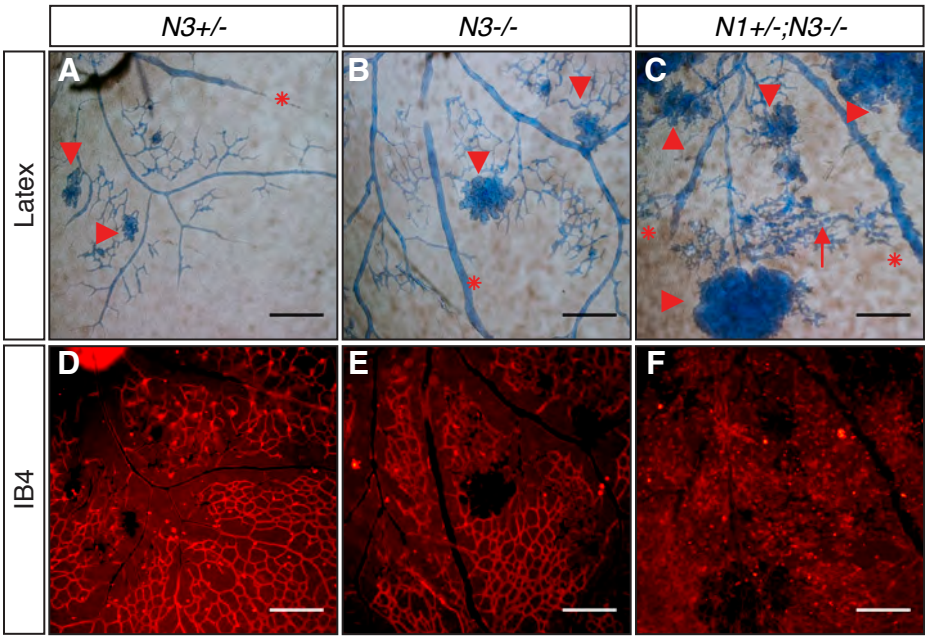

Figure 4. *Notch1*$^{+/-}$*;Notch3*$^{-/-}$ mice display decreased retinal vascular maturity at P8. Bright field images (A-C) and corresponding fluorescent Isolectin-B4 staining (D-F) of retinal leaflets of P8 mice following blue latex bead perfusion. Bright field images show blue venules (asterisks), latex leaks (red arrowheads), and developing arteriovenous shunts (arrow). Scale bars; 200 µm.

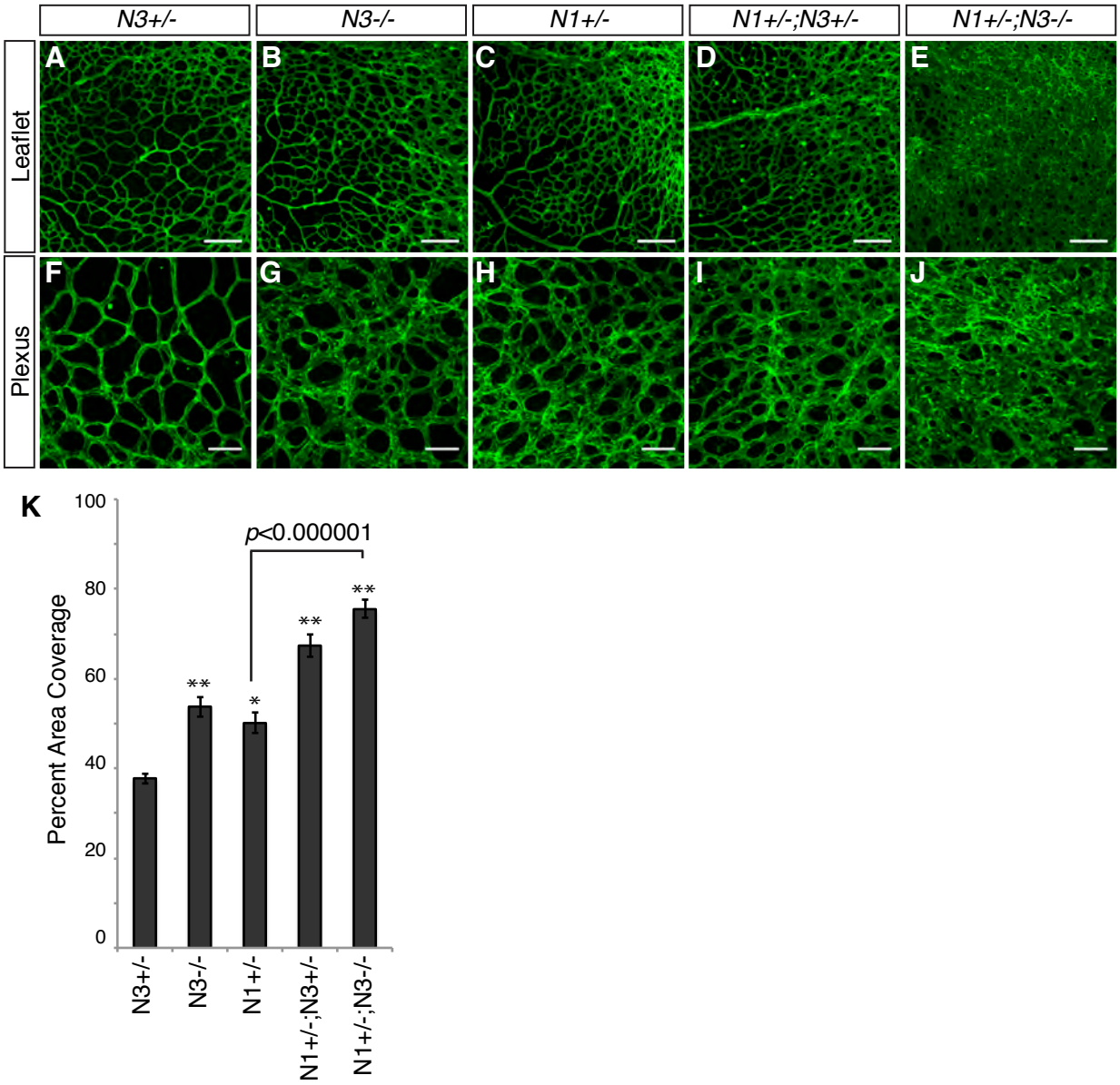

Figure 5. Notch1 and Notch3 limit vessel density in the retina at P8. Wholemount retinas isolated from P8 Notch1/Notch3 mutant mice stained for Isolectin-B4 to visualize the vasculature (A-J). Low magnification images show a severe increase in vessel density in the vascular plexus of *Notch1*$^{+/-}$*;Notch3*$^{-/-}$ mice (A-E). High magnification images were used to quantify vascular density (F-J). Quantification of percent area coverage quantified from high magnification confocal stacks taken at the vascular plexus behind the arteriovenous vascular front (K). n≥3, 4 images taken per retina. **p< $5x10^{-4}$, ***p<$5x10^{-5}$. Error bars represent SD of the mean.

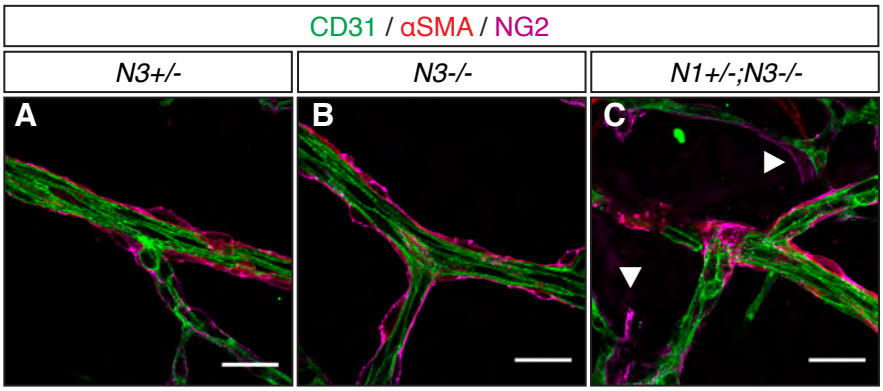

Figure 6. *Notch1*$^{+/-}$*;Notch3*$^{-/-}$ P8 mice display loss of arteriolar mural cell association
Mural cell association is assessed from high magnification confocal stacks taken through the center of the arteriole at the first branch point from the optic nerve. Endothelial cells are stained with CD31 (green) and mural cells are stained for αSMA (red) and NG2 (magenta). Dissociated mural cells are marked with white arrowheads. Scale bars; 25 μm.

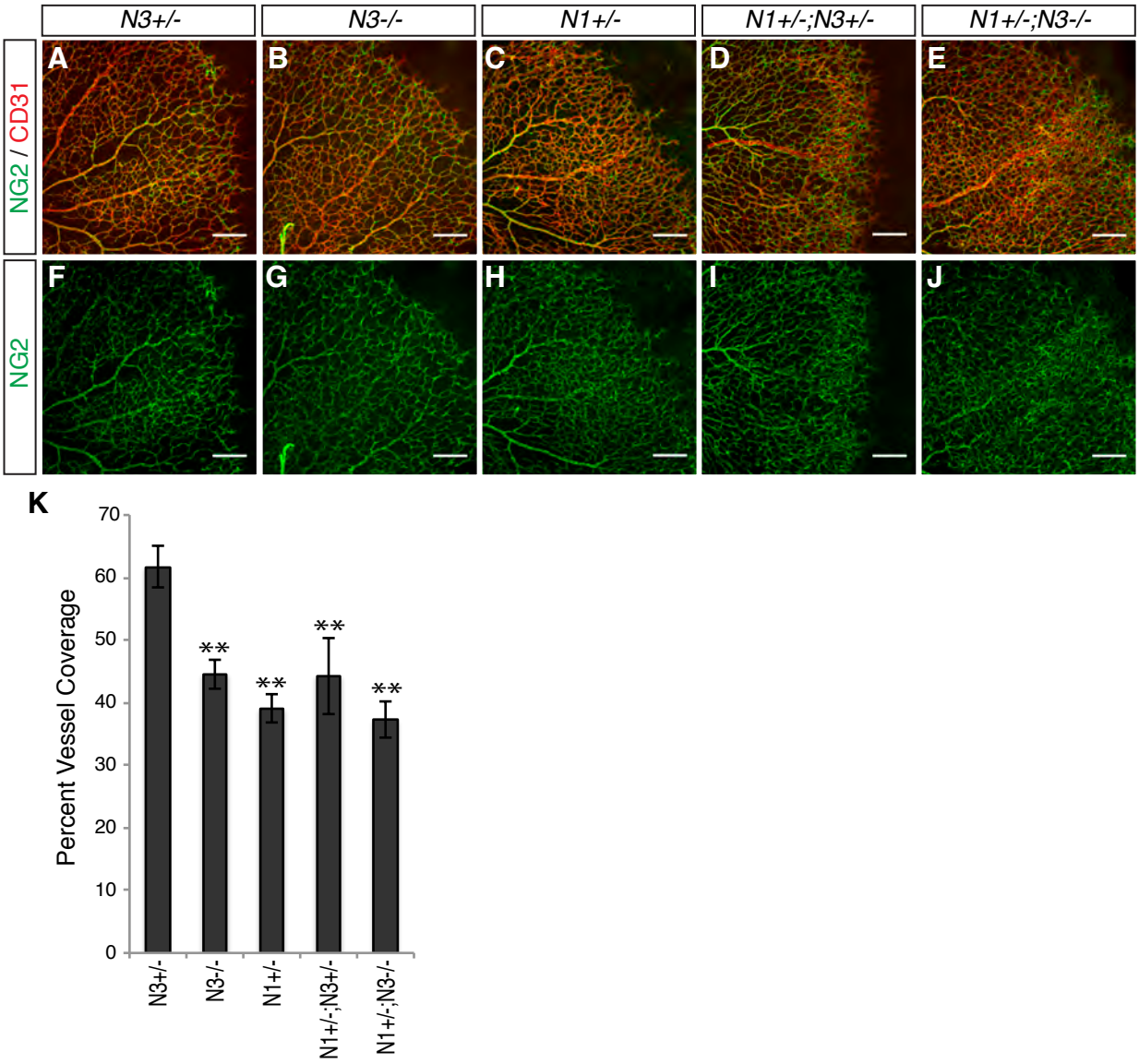

Figure 7. *Notch1*$^{+/-}$*;Notch3*$^{-/-}$ P5 mice display reduced pericyte coverage. Confocal stacks of leaflets of P5 retinal wholemounts stained for CD31 (red) and NG2 (green) (A-J). NG2 alone shows that pericytes recruitment occurs in all mutant mice analyzed. Quantification of NG2 staining normalized to vascular area shows that *Notch3*$^{-/-}$, *Notch1*$^{+/-}$, *Notch1*$^{+/-}$*;Notch3*$^{+/-}$ and *Notch1*$^{+/-}$*;Notch3*$^{-/-}$ mice have decrease vascular pericyte coverage as compared to *Notch3*$^{+/-}$ control (K). n≥3, 8 leaflets/mouse, **p<0.001. Error bars represent SD of the mean. Scale bars; 200 µm.

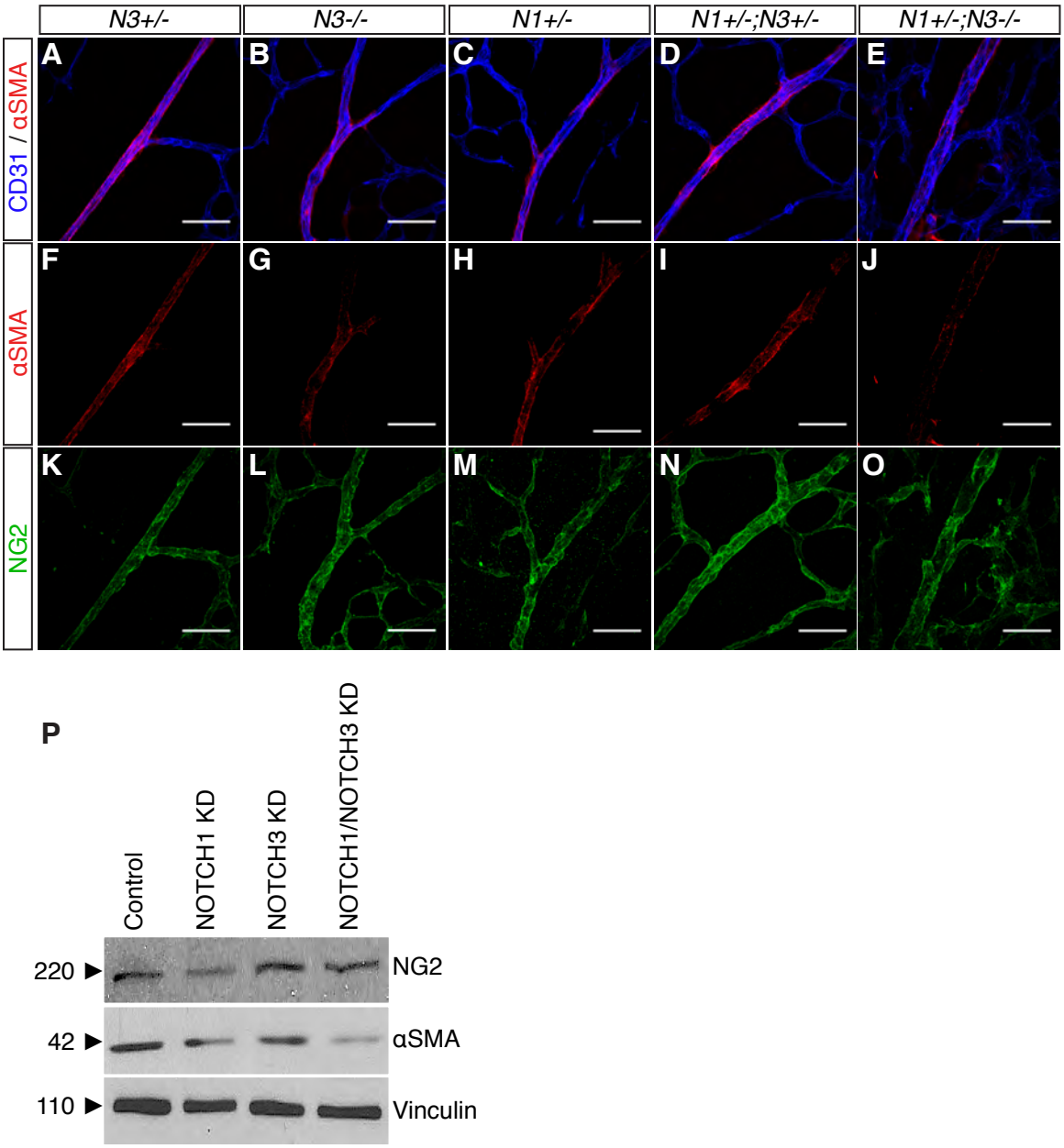

Figure 8. Notch1 and Notch3 are required for mural cell αSMA expression. High magnification confocal stacks taken of arterioles at the first branch point distal to the optic nerve. Wholemount retinas were stained for CD31 (blue) to visualize the endothelium, NG2 (green), and αSMA (red) to visualize more mature VSMCs (A-O). *Notch1*$^{+/-}$*;Notch3*$^{-/-}$ mice show a significant reduction in αSMA expression. Western blot on protein lysates isolated from HBVP cell lines expressing scrambled shRNA (control), *NOTCH1*-shRNA, *NOTCH3*-shRNA, or both *NOTCH1*- and *NOTCH3*-shRNA (P). The blot was probed for NG2, αSMA, and vinculin as a loading control. Scale bars; 50 μm.

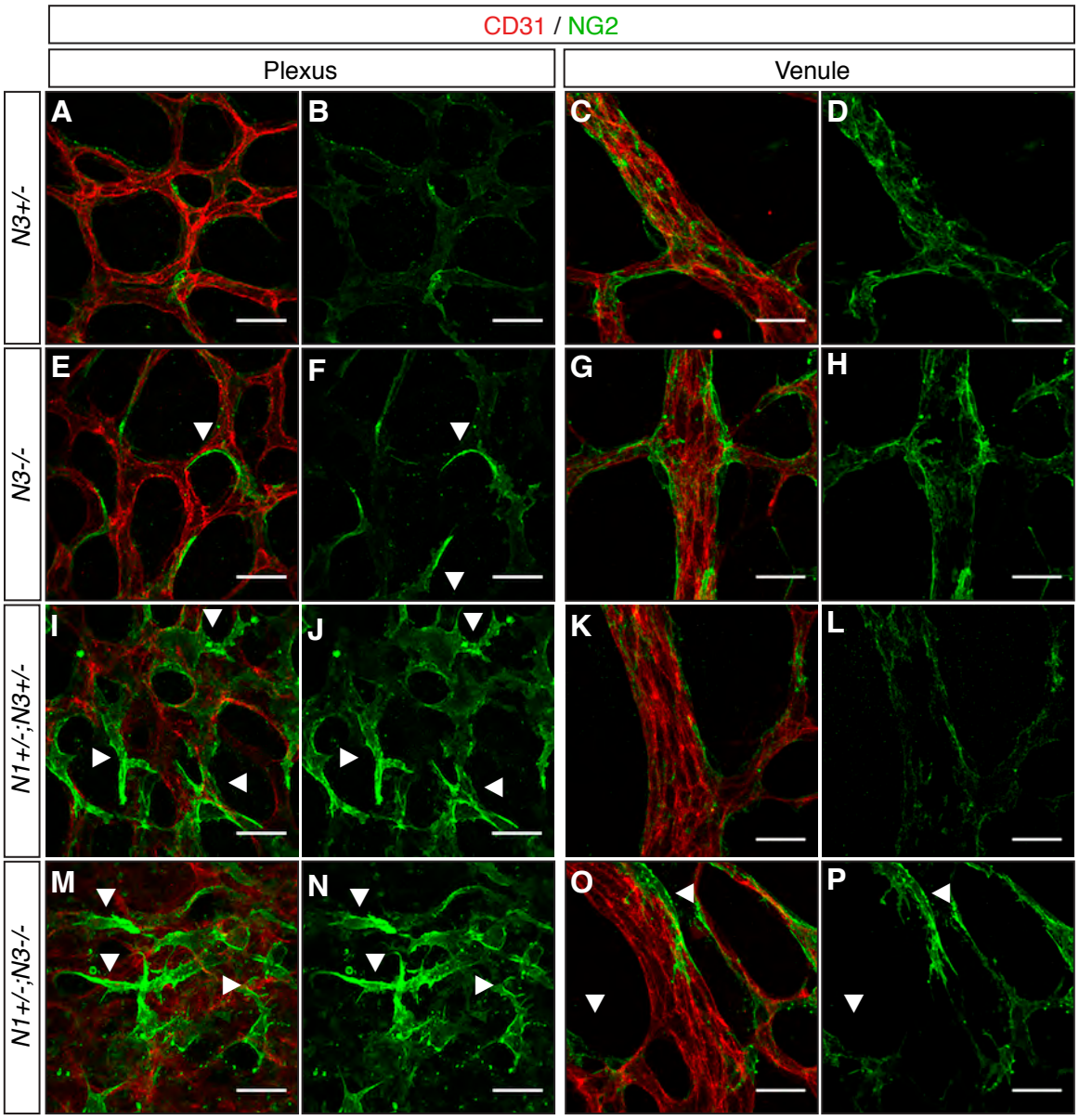

Figure 9. Pericyte association with the endothelium is compromised in the retina of *Notch1*$^{+/-}$*;Notch3*$^{-/-}$ P5 mice. High magnification confocal stacks taken at the vascular plexus behind the arterial/venous vascular front (A-B, E-F, I-J, M-N) and of the venule at the first branch point form the optic nerve (C-D, G-H, K-L, O-P). Images were taken of wholemount retinas fluorescently stained fro CD31 (red) to visualize the endothelium and NG2 (green) to mark pericytes. Scale bars; 25 µm.

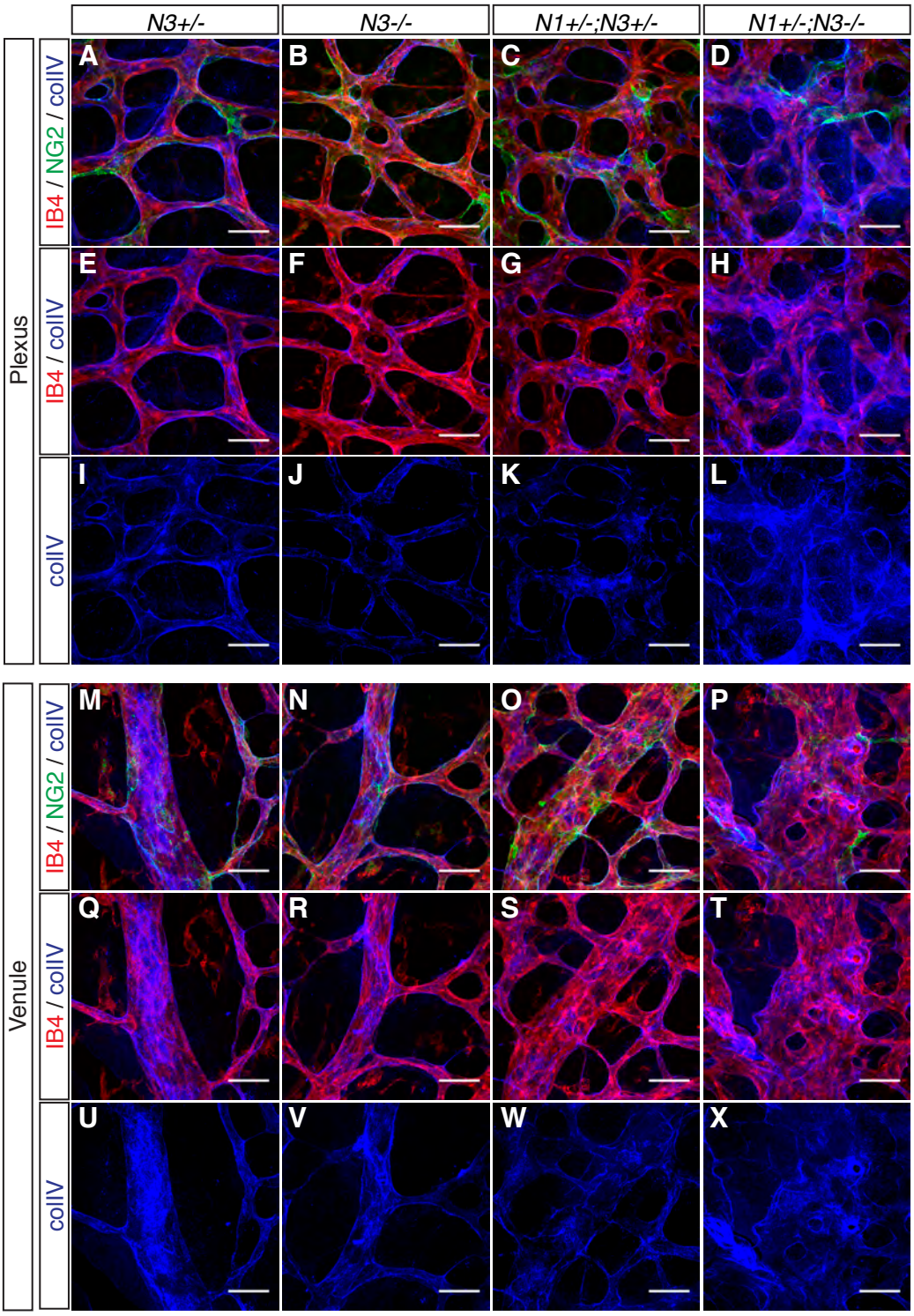

Figure 10. *Notch1*$^{+/-}$*;Notch3*$^{-/-}$ mice display altered collagen type IV deposition. High magnification confocal stacks of P5 retinas stained for isolectin-B4 (red), NG2 (green), and collagen type IV (colIV) (blue). Images were taken at the capillary plexus (A-L) and of the venule at the first branch point from the optic nerve (M-X). Scale bars; 25 µm.

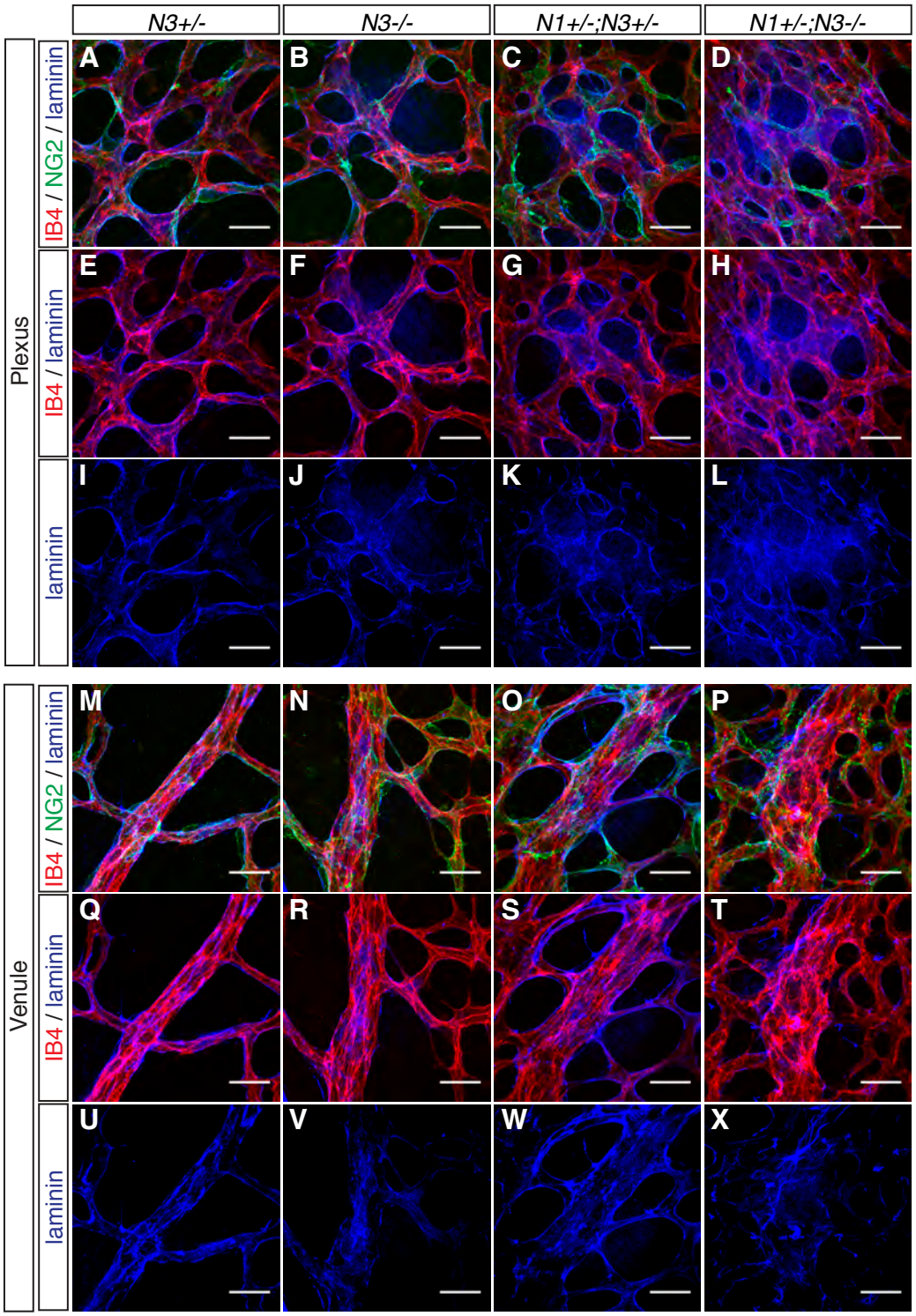

Figure 11. *Notch1*$^{+/-}$*;Notch3*$^{-/-}$ mice display altered laminin deposition. High magnification confocal stacks of P5 retinas stained for isolectin-B4 (red), NG2 (green), and laminin (blue). Images were taken at the capillary plexus (A-L) and of the venule at the first branch point from the optic nerve (M-X). Scale bars; 25 µm.

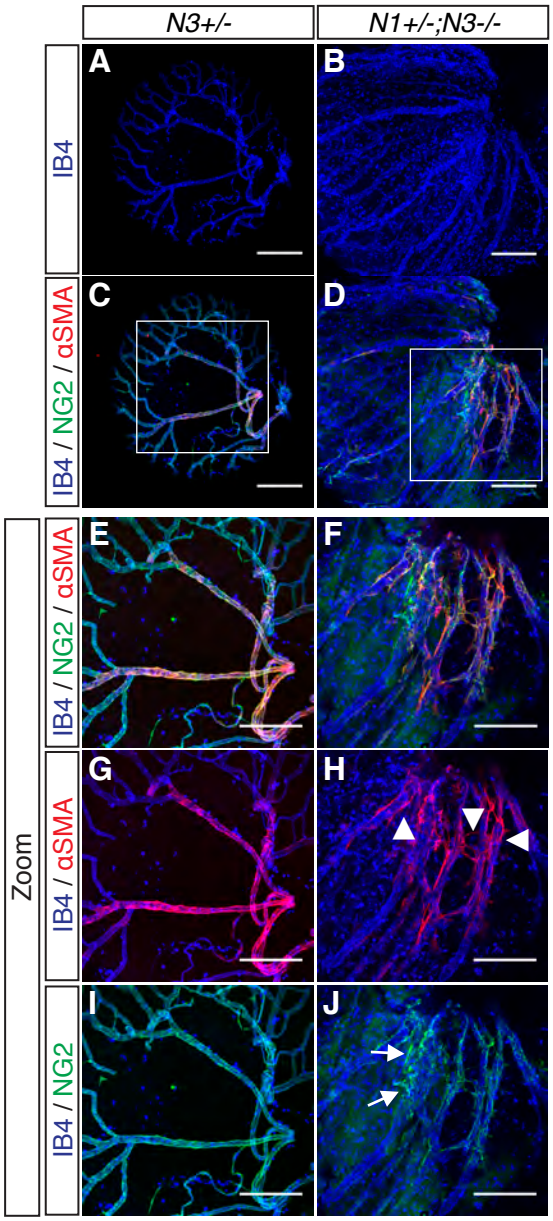

Figure 12. Assessment of the hyaloid vasculature of *Notch1*$^{+/-}$*;Notch3*$^{-/-}$ mice at P5. The hyaloid vasculature and lens was wholemount stained for isolectin-B4 (blue), NG2 (green) and αSMA (red). Low magnification confocal stacks show an altered hyaloid vascular plexus in *Notch1*$^{+/-}$*;Notch3*$^{-/-}$ mice (A-D). Zoomed area of white boxes allows for analysis of mural cell coverage and association with the hyaloid endothelium (E-J). Scale bars; 200 µm.

CHAPTER 4

Inhibition of Jagged-specific Notch activation causes luteal pericyte dysfunction and luteal hemorrhaging

INTRODUCTION

Physiological angiogenesis is essential during development to establish the circulatory system. In adulthood, angiogenesis is mainly restricted to diseased states characterized by inflammation, such as wound healing and tumor vascularization. In adult mammals, the female reproductive tract is a unique site of physiological angiogenesis. Angiogenesis in the ovary and uterus are required for maintenance of the non-pregnant estrous/menstrual cycle and for establishment and maintenance of pregnancy. The ovary supports the reproductive lifespan of an organism through cyclic production of follicles, follicular maturation, ovulation of oocytes, development of the corpus luteum (CL) and luteal regression, in the non-pregnant state (Figure 1). After ovulation of an oocyte from the dominant follicle, the CL develops. Ovulation induces follicular granulosa cells to proliferate and then terminally differentiate into hormone producing luteal cells[91]. Steroid hormone production, such as estradiol and progesterone by luteal cells is critical for pregnancy maintenance and requires a functional capillary plexus for hormonal delivery to distant sites. Thus, angiogenesis in the corpus luteum must occur efficiently and effectively to ensure its function as an endocrine organ.

Initiation of luteal angiogenesis occurs immediately following ovulation when the basement membrane surrounding the ovulated follicle is degraded allowing for theca vessels to invade the avascular granulosum[92,93]. Proliferation and migration of the theca endothelial cells is dependent on VEGF-A, which is primarily secreted by the follicular granulosa cells[94,95]. VEGF-A has been shown to be required for luteal angiogenesis, as VEGF blockade inhibits angiogenesis in the corpus luteum and impairs luteal function[96-98]. VEGFR-2 has been shown to be an essential receptor for VEGF-A in endothelial cells during luteal angiogenesis[99,100].

In addition to the VEGF pathway, pericytes have also been shown to regulate luteal angiogenesis. Unlike developmental angiogenesis, where pericyte recruitment is typically secondary to that of endothelial cell recruitment, in some animal models pericytes are the first

vascular cells to invade the ovulated follicle[101]. Analysis of sheep ovaries suggested that luteal pericytes promote vascular recruitment to the CL through secretion of VEGF-A[101]. Thus, it has been proposed that pericytes may function as vascular guides within the developing corpus luteum[92]. Pericytes also fulfill their traditional vascular role in the CL by providing maturation cues and support to nascent capillary vessels[102]. The importance of vascular pericytes in luteal angiogenesis has been shown previously by inhibiting their recruitment to the CL in mice[10]. Blockade of pericyte recruitment through expression of soluble PDGFRβ ectodomain caused severe luteal hemorrhaging, as well as decreased luteal vascularization. This work demonstrates that pericytes have a dual function in luteal angiogenesis by promoting both endothelial recruitment and vessel stability.

The Notch pathway is a critical regulator of both endothelial function and pericyte/endothelial interactions during angiogenesis. Previous work by our group demonstrated that Notch1 and Notch4 are expressed by luteal and theca endothelial cells, whereas Notch3 is expressed by theca mural cells[103]. In addition, luteal endothelial cells and mural cells express the Notch ligand, Jagged1. Analysis of mouse models mutant for Jagged1 showed that endothelial Jagged1 activates Notch signaling in mural cells to promote mural cell maturation and coverage of the vasculature[36,37,90]. In the developing retina, specific deletion of endothelial Jagged1 caused decreased vascular density and decreased αSMA expression by the mural cell compartment[37]. Unpublished data from our group showed that therapeutic inhibition of Jagged-specific Notch activation resulted in decreased tumor vessel density and loss of pericyte/endothelial cell association in the tumor vasculature (Kangsamaksin T., *et al*., unpublished data). Thus, we hypothesized that inhibition of Jagged-specific Notch signaling would inhibit luteal angiogenesis by altering pericyte function. Using tools to specifically inhibit Notch activation by Jagged we demonstrate that Jagged-specific Notch signaling is required for pericyte recruitment to the CL following controlled hormonal stimulation of ovulation in the

mouse. We also show that Jagged/Notch signaling is critical for luteal vessel stability under more intense angiogenic conditions induced by ovarian hyperstimulation. Inhibition of Jagged-specific activation of Notch caused luteal hemorrhaging and loss of vascular pericyte association following ovarian hyperstimulation.

RESULTS

Characterization of the mural cell population in the corpus luteum

To analyze angiogenesis in the corpus luteum, we employed a model of hormonal induction of ovulation. Ovulation was induced in sexually immature female C57/Bl6 mice by intraperitoneal injections of 5 i.u. of pregnant mare serum gonadotropin (PMSG) to induce folliculogenesis, followed by 5 i.u. of human chorionic gonadotropin (hCG) two days later, to induce ovulation and luteinization. Ovaries were collected two days after hCG injection (day 4) and used to assess luteal angiogenesis.

We defined the mural cell population of the ovary following hormonal induction of ovulation through assessment of mural cell marker expression (NG2, PDGFRβ, desmin, and αSMA) in ovaries isolated from sexually immature females induced to ovulate with PMSG and hCG. In the mouse retina, the pericytes that line the capillaries are positive for NG2, desmin, and PDGFRβ, but do not express the more mature VSMC marker, αSMA (Chapter 1, Figure 2). We observed a similar pattern of expression in the ovary where the mural cells lining the luteal capillaries are positive for NG2, desmin, and PDGFRβ, and negative for αSMA. Interestingly, we also observed specific staining patterns for NG2, desmin, and PDGFRβ within the CL. NG2 strongly stains the mural cells in the CL, but the staining intensity for NG2 is weak in the theca (Figure 2A). PDGFRβ was strongly expressed by luteal and theca mural cells, which was expected because it functions in pericytes and VSMCs (Figure 2B). The mural cells in the theca layer express higher levels of desmin than the CL mural cells suggesting desmin may mark a

more mature mural cell population (Figure 2C). αSMA expression was restricted to the mural cell population of the theca layer (Figure 2D). The observed expression pattern of mural cell markers in the ovary demonstrated that CL vessels are lined by pericytes, whereas the theca vessels are lined by both pericytes and VSMCs. Differences observed in mural cell populations of the CL is likely due to different requirements for mural cell function in the CL versus the ovarian theca. The theca layer contains larger and more established blood vessels that require support from more mature and contractile αSMA-positive VSMCs. The transient capillary plexus of the CL may instead require a mural cell population that is more versatile and active in angiogenesis, such as the pericyte.

Luteal pericytes express Notch1 and Jagged1

To determine if Notch signaling could contribute to pericyte function in the CL we analyzed Notch receptor and ligand expression in luteal pericytes. Previous work by our group showed that Notch1 is expressed by a subset of luteal and theca endothelial cells, as well as a subset of αSMA-positive mural cells in the theca layer[103]. Jagged1 displayed a similar localization. *In situ* hybridization on ovarian sections showed that *Notch2*, *Notch3*, and *Jagged2* are expressed by granulosa cells of the developing follicle and that *Jagged2* is not expressed by the ovarian vasculature[104]. Since we demonstrated that NG2 is a specific and consistent marker of luteal pericytes we co-stained ovary sections for NG2 and either Notch1, Notch3 or Jagged1 to determine the Notch expression profile of luteal pericytes. Co-staining for NG2 and Notch1 showed that a small subset of pericytes express Notch1 in the CL (Figure 3A). Co-staining for NG2 and Jagged1 showed that luteal pericytes express high levels of the Notch ligand Jagged1 (Figure 3B). Notch3 is not expressed by luteal pericytes, instead Notch3 expression is restricted to the mural cells of the theca layer (Figure 3C). Thus, luteal pericytes express

Notch1 and Jagged1. This data suggests that luteal angiogenesis could be compromised pharmacologically by specifically targeting the Jagged activation of Notch signaling.

$N1_{10-24}$ decoy, a Jagged inhibitor, does not affect ovulation

Given that luteal pericytes express Notch1 and Jagged1, we hypothesized that disrupting Jagged/Notch interactions could alter pericyte coverage and function of the CL capillary plexus. To inhibit Jagged-specific activation of Notch we have employed a Notch decoy construct developed in our lab that contains EGF-like repeats 10-24 of the human NOTCH1 extracellular domain, deemed $N1_{10-24}$ decoy (Figure 4). We refer to this construct as a decoy because the Notch extracellular domain does not have signaling capability, but functions to bind ligand and thus inhibits Notch signaling. $N1_{10-24}$ decoy has been shown to specifically block Jagged ligands (both Jagged1 and Jagged2) and bind to Jagged1. $N1_{10-24}$ decoy is thus a Jagged-specific inhibitor of Notch signaling, whereas full-length human Notch1 extracellular domain (EGF-like repeats 1-36) binds both delta-like ligands and Jagged ligands to inhibit Notch signaling (Kangsamaksin, T., *et al.*, unpublished data)[105]. During pathological angiogenesis, we previously showed that $N1_{10-24}$ decoy disrupts pericyte/endothelial cell interactions in tumor vasculature and causes decreased vascular density, therefore we were interested in analyzing the affects of $N1_{10-24}$ decoy on physiological angiogenesis in the CL (Kangsamaksin, T., *et al.*, unpublished data).

To analyze the effects of $N1_{10-24}$ decoy on luteal angiogenesis, we induced ovulation in pre-pubertal female mice that had been infected with an adenovirus expressing human Fc (control group) or an adenovirus expressing $N1_{10-24}$ decoy (experimental group). These human adenovirus vectors infect the murine liver causing hepatocytes to produce and secrete protein into systemic circulation (data not shown). Thus, adenoviral vectors are used to express secreted proteins of interest to allow for their systemic delivery into the bloodstream and

evaluation as therapeutic entities in the mouse. In a pilot study, we analyzed serum Fc levels following injection of adenovirus expressing Fc during hormonal induction of ovulation. Serum Fc can be detected the day immediately following adenovirus injection with increasing levels observed up until the time of ovary collection at day 4 (Figure 5A). To allow folliculogenesis to proceed normally while still affecting luteinization we injected female mice with adenovirus on the day between PMSG and hCG treatment (Figure 5B).

In experiments to assess $N1_{10-24}$ decoy function, mice injected with adenovirus expressing $N1_{10-24}$ decoy or human Fc expressed high serum levels of their respective decoys at time of ovary collection (Figure 5C). Ovaries isolated from $N1_{10-24}$ decoy treated mice with controlled hormonal stimulation were smaller by weight, as compared to control (Figure 5E). H&E staining of sections of ovaries showed that copora lutea were present in $N1_{10-24}$ decoy treated ovaries (Figure 5D). Quantification of CL number showed no significant difference between groups, suggesting that $N1_{10-24}$ decoy does not affect ovulation or CL formation (Figure 5, F and G).

$N1_{10-24}$ decoy inhibits luteal angiogenesis

Angiogenesis is required for luteinization and maintenance of pregnancy. Previous studies have shown that inhibiting luteal angiogenesis by blocking VEGF signaling results in decreased ovarian weight[99]. We hypothesized that the decreased ovarian weight observed in the $N1_{10-24}$ decoy treatment group may be caused by reduced luteal angiogenesis. To analyze CL vessel content we stained ovaries for the endothelial cell marker CD31. As hypothesized, ovaries isolated from mice treated with $N1_{10-24}$ decoy displayed decreased CL endothelial content, as compared to controls (Figure 6A). The corpora lutea of $N1_{10-24}$ decoy treated mice displayed a 30% reduction in vessel density (Figure 6B). This data suggests that Notch activation through Jagged is pro-angiogenic in the CL

Pericytes have been shown to promote angiogenesis in the ovarian corpus luteum[10]. Furthermore, data from our lab showed that Jagged-specific activation of Notch signaling regulates pericyte/endothelial cell interactions. To determine whether $N1_{10-24}$ decoy affects pericyte recruitment to the CL vasculature we stained ovarian sections for the pericyte marker NG2. We observed that there was a significant reduction in NG2 positive cells in the corpora lutea of $Notch1_{10-24}$ decoy treated mice, as compared to control (Figure 7A). This difference was statistically significant; the $N1_{10-24}$ decoy group showed a 30% reduction in pericyte cell content in the CL compared to control (Figure 7B). However, a significant difference was not observed between the two groups when we assessed pericyte coverage per vessel of the CL capillary plexus by normalizing NG2 staining to CD31 (Figure 7C). Thus, $N1_{10-24}$ decoy inhibited CL pericyte content to the same extent as it inhibits endothelial content following controlled ovarian stimulation.

$N1_{10-24}$ decoy causes luteal hemorrhaging in hyperstimulated ovaries

Our experiments demonstrated that inhibition of Jagged-specific Notch activation causes decreased luteal angiogenesis in a model of ovulation induction while pericyte coverage of the luteal vasculature is unaffected. Pericyte coverage is essential to maintain vessel stability and reduce vascular permeability. In human diseases, lack of adequate pericyte coverage can lead to aneurysm and hemorrhaging when vascular function is stressed. Gonadotropin induced hyperstimulation of ovaries induces a greater number of follicles to ovulate and thus an increase in CL number, as compared to induction of ovulation with controlled ovarian stimulation. In addition, superovulation is accompanied by a more robust angiogenic response and more active endothelium as defined by increased sprouting. We sought to determine whether Notch signaling could affect pericyte function in the CL of hormonally hyperstimulated ovaries with increased angiogenesis, compared to controlled stimulation. To induce superovulation we used

the same experimental design as previously described, but increased the dose of gonadotropins to 20 i.u PMSG and 20 i.u. hCG (Figure 8A). Adenovirus infection with human Fc or $N1_{10-24}$ decoy resulted in high serum expression levels by experimental day 4 (Figure 8B).

Ovarian hyperstimulation with $N1_{10-24}$ decoy treatment caused severe hemorrhaging in the ovary. Hyperstimulated ovaries isolated from mice treated with $N1_{10-24}$ decoy displayed numerous blood-filled corpuscles, which were rarely observed in control (Figure 8C). We also observed an increase in ovarian weight in the $N1_{10-24}$ decoy treated group, as compared to controls (Figure 8D). Closer analysis of H&E stained sections showed that ovaries from $N1_{10-24}$ decoy treated mice contained multiple blood-filled corpora lutea (Figure 8E). On average, the $N1_{10-24}$ decoy treated group had significantly more hemorrhaging corpora lutea per ovary, as compared to controls treated with human Fc (Figure 8F). Yet, no significant difference was observed in normal CL content between the two groups. This was surprising, as we expected to see a reduction in normal CL number in the $N1_{10-24}$ decoy group due to hemorrhaging. This data instead suggests that the $N1_{10-24}$ decoy group may have a higher number of ovulated follicles, as compared to control.

Inhibition of Jagged-specific Notch activation causes vessel dilation without affecting luteal pericyte recruitment.

The luteal hemorrhaging observed with $N1_{10-24}$ decoy treatment suggested that $N1_{10-24}$ decoy caused luteal vascular instability in hyperstimulated ovaries. $N1_{10-24}$ decoy did not alter vascular density under conditions of superovulation (Figure 9I). However, when analyzing the vascular plexus of non-hemorrhaged corpora lutea we noticed that the vessels in the $N1_{10-24}$ decoy treated ovaries appeared enlarged and dilated, as compared to ovaries treated with human Fc (Figure 9, A and B). Vessel dilation is a common phenotype associated with vasculature that lacks adequate mural cell coverage, as displayed by mice with impaired

endothelial Jagged1 expression[36]. Thus, we hypothesized that pericyte coverage may be reduced in the CL when Jagged-specific Notch signaling was inhibited. We stained superovulated ovaries for NG2 to analyze CL pericyte content, but did not see a reduction in pericyte recruitment to the CL in the $N1_{10\text{-}24}$ decoy treated group (Figure 9J). We also stained hyperstimulated ovaries for αSMA to analyze theca VSMC content. We saw that $N1_{10\text{-}24}$ decoy treatment caused decreased αSMA expression in the VSMC of the ovarian theca (Figure 10). Decreased αSMA staining intensity suggests that $N1_{10\text{-}24}$ decoy has an inhibitory affect on mural cell maturation. Inhibition of VSMC maturation could cause altered vascular tone in the ovary and may contribute to the ovarian hemorrhaging phenotype observed in the $N1_{10\text{-}24}$ decoy treatment group. However, as shown in Chapter 4, Figure 2, pericytes in the CL do not express αSMA, so lack of VSMC maturation may contribute to theca vessel dysfunction, but cannot explain the luteal hemorrhaging and luteal vessel dilation caused by $N1_{10\text{-}24}$ decoy treatment.

Inhibition of Jagged-specific Notch activation disrupts pericyte association with luteal blood vessels

Since inhibition of Jagged-specific activation of Notch does not affect luteal pericyte recruitment, we hypothesized that $N1_{10\text{-}24}$ decoy may inhibit pericyte association with luteal vessels to cause the observed vascular phenotypes. When analyzing luteal pericyte content of non-hemorrhaged corpora lutea by staining for NG2. We observed that luteal pericytes in $N1_{10\text{-}24}$ decoy hyperstimulated ovaries had a more intense NG2 signal than those in the control group. *In vitro* data from our lab showed that Notch does not regulate NG2 protein levels in cultured pericytes (Chapter 5, Figure 4). Instead, bright NG2 staining suggested that pericytes could be dissociating from the vasculature, as we have observed similar changes in NG2 staining intensity in the retina of mouse mutants that display altered pericyte/endothelial cell association. Since NG2 is a cell surface marker, we believe that brighter NG2 staining is due to

an increase in cell surface availability to the antibody when pericytes detach from the endothelium. To more thoroughly analyze pericyte/endothelial cell association we took high magnification confocal stacks of copora lutea stained for CD31 (endothelium) and NG2 (pericytes). In the control CL we observed pericytes tightly lining the capillary vessels (Figure 11C). However, in the $N1_{10-24}$ decoy group luteal pericyte morphology was dramatically altered where pericytes appeared to be coming up and off of the endothelium with numerous cellular processes that failed to make contact with the endothelium (Figure 11D).

A similar phenotype of pericyte dissociation and vessel dilation was observed in the remaining capillary plexus of hemorrhaging corpora lutea of $N1_{10-24}$ decoy treated mice. Analysis of the peripheral vasculature of hemorrhaging corpora lutea showed severe vessel dilation in the $N1_{10-24}$ decoy group, as denoted by arrows where large vessel lumens lined by CD31-positive endothelial cells can be observed (Figure 12D). Capillary vessel wall structure also appears to be altered in the capillary plexus of hemorrhaging corpora lutea of the $N1_{10-24}$ decoy group where the endothelial lining of the capillary lumen is discontinuous and at points NG2-positive pericytes can be seen lining the capillary lumen (asterisk). This phenotype was not observed in the rare hemorrhaging CLs of the control super-ovulated ovaries (Figure 12C). This data suggests that the CL hemorrhaging observed in the $N1_{10-24}$ decoy treated group may be due to altered pericyte association leading to vessel abnormalities and thus vascular rupture and hemorrhaging.

DISCUSSION

Luteal angiogenesis is a tightly regulated process that is critical for mammalian reproduction. Following ovulation luteal cells proliferate and differentiate to secrete steroid hormones. The capillary plexus of the corpus luteum ensures systemic delivery of luteal hormones without which successful implantation cannot occur and pregnancy is not maintained.

To ensure its function, the corpus luteum must have adequate vessel perfusion, which is regulated by angiogenic sprouting, remodeling, and vessel stabilization by pericyte coverage. By employing $N1_{10\text{-}24}$ decoy we showed that Jagged-specific activation of Notch regulates luteal angiogenesis by promoting vessel density and pericyte association with luteal endothelium. Specifically, we showed that following controlled ovarian stimulation, which models physiological angiogenesis, treatment with $N1_{10\text{-}24}$ decoy inhibits luteal angiogenesis. Furthermore, in a setting more similar to pathological angiogenesis, $N1_{10\text{-}24}$ decoy caused luteal hemorrhaging and inhibited luteal vascular pericyte coverage following ovarian hyperstimulation.

Through endothelial cell autonomous signaling, Jagged1 promotes sprouting angiogenesis by muting Dll4-activation of Notch signaling[37]. In addition, Jagged1 expressed by endothelial cells and mural cells activates Notch signaling in mural cells to regulate their maturation and coverage of the vasculature[32,36,106]. Our lab has previously analyzed ligand-specific Notch decoys in tumor angiogenesis. This work demonstrated that Jagged ligands act as positive regulators of angiogenesis in the tumor environment. Inhibition of Jagged-specific activation of Notch using $N1_{10\text{-}24}$ decoy inhibits tumor vascular density (Kangsamaksin, T., *et al.*, unpublished data). We also observed that $N1_{10\text{-}24}$ decoy treatment impairs pericyte association with the tumor vasculature. Here we show that $N1_{10\text{-}24}$ decoy also inhibits physiological angiogenesis in the adult mouse corpus luteum following controlled ovarian stimulation. This data demonstrates that Jagged ligands function to promote angiogenesis in a variety of vascular beds. $N1_{10\text{-}24}$ decoy inhibits Jagged1 and Jagged2 activation of Notch (Kangsamaksin, T., *et al.*, unpublished data). We believe that $N1_{10\text{-}24}$ decoy effectively inhibits luteal angiogenesis by preventing Jagged1 from signaling to Notch within the endothelium. In addition, we believe that $N1_{10\text{-}24}$ decoy inhibits Jagged-induced Notch activation in mural cells to prevent proper pericyte function during angiogenesis. During luteal angiogenesis, pericytes are often observed ahead of the vascular front. Based on their location, pericytes may be a source of angiogenic factors,

such as VEGF-A and inhibition of Notch signaling by $N1_{10-24}$ decoy may impair this process. Since $N1_{10-24}$ decoy is secreted systemically it inhibits ligand presentation by every Jagged-expressing cell. Thus, we cannot determine whether the observed phenotypes result from inhibition of Jagged induced Notch activation by endothelial cells, mural cells, or non-vascular cell types in the CL. Granulosa cells of the CL have been shown to express *Notch2*, *Notch3*, and *Jagged2* and effects of $N1_{10-24}$ decoy treatment on granulosa cell function was not assessed. To determine mechanistically why inhibition of Jagged-specific activation of Notch causes reduced angiogenesis, mouse models with tissue specific manipulation of Jagged should be employed.

Our data provides a new role for Notch signaling in female reproduction. Inhibition of luteal angiogenesis by blocking Jagged-specific activation of Notch could prevent uterine implantation of fertilized oocytes, and thus pregnancy. Analysis of the effects of $N1_{10-24}$ decoy on female reproduction was beyond the scope of this chapter. However, future experiments should include analysis of circulating luteal hormone levels following $N1_{10-24}$ decoy treatment. We predict that reduced luteal angiogenesis would correlate with reduced levels of circulating progesterone in mice treated with $N1_{10-24}$ decoy. In humans, implantation occurs 7 to 9 days after ovulation and requires a functional corpus luteum. If the anti-angiogenic effects of $N1_{10-24}$ decoy cause reduced luteal function then $N1_{10-24}$ decoy treatment may prevent successful implantation, and thus inhibit pregnancy. Use of $N1_{10-24}$ decoy as an emergency contraceptive could expand its therapeutic potential. Future experiments should investigate the effects of $N1_{10-24}$ decoy during implantation and pregnancy. Furthermore, we strongly believe that the effects of $N1_{10-24}$ decoy on female fertility must be assessed prior to its use in clinic as a cancer therapeutic.

In the hyperstimulated ovary we showed that Jagged activation of Notch signaling is required for pericytes to properly associate with luteal endothelial cells. It is well established

that endothelial Jagged1 is required during embryonic development to promote VSMC coverage of large vessels. Mice mutant for endothelial Jagged1 display vessel dilation presumably due to impaired arterial VSMC maturation resulting from reduced Notch signaling[28,36]. The role of Notch signaling in pericyte/endothelial cell interactions is less clear. Postnatal analysis of mice mutant for endothelial Jagged1 demonstrated that pericyte recruitment occurs normally in this mouse model[37]. Here we demonstrate that Jagged-specific activation of Notch does not alter the quantity of pericyte coverage of luteal vessels, but instead affects the ability of pericytes to properly associate with the endothelium during luteal angiogenesis.

We observed severe luteal hemorrhaging and pericyte dysfunction in hyperstimulated ovaries with $N1_{10\text{-}24}$ decoy treatment. Ovarian hemorrhaging and pericyte dissociation was not observed with $N1_{10\text{-}24}$ decoy treatment following controlled ovarian stimulation. We believe that hyperstimulation of ovulation using high doses of gonadotropins models pathological angiogenesis. The increased number of ovulated follicles and the robust angiogenic response following superovulation suggests that the luteal endothelium is hyperactive in hyperstimulated ovaries. In the clinic, ovarian hyperstimulation is induced by gonadotropin administration during *in vitro* fertilization therapy to increase ovulation. Ovarian hyperstimulation syndrome (OHSS) occurs for unknown reasons in a subset of patients undergoing *in vitro* fertilization. The luteal vasculature of patients with OHSS is characterized by vessel leakiness due to increased levels of VEGF-A[107]. The relative luteal VEGF-A levels of mice hyperstimulated with high doses of gonadotropins have not been assessed. However, we would predict that similar to human, in the mouse, ovarian hyperstimulation causes increased VEGF-A levels and thus a hyperactive luteal endothelium. Only under conditions of hyperstimulation did we observe overt pericyte dissociation and vascular dysfunction. In the retina and *in vitro* we have shown that Notch signaling regulates pericyte function. We believe that during physiological angiogenesis, as occurs in the CL following controlled ovarian stimulation, compensation for altered pericyte

function can achieve a functional, despite sparser, luteal capillary network. However, when activation of the endothelium is enhanced for example via hormonal ovarian hyperstimulation the effects of altered pericyte function cannot be overcome and results in a dysfunctional luteal capillary plexus. We believe that this is why we observed luteal hemorrhaging only in hyperstimulated ovaries treated with Notch1$_{10\text{-}24}$ decoy, and not under conditions of controlled ovarian stimulation.

It has previously been reported that inhibition of pericyte recruitment to the CL causes luteal hemorrhaging and reduced vascular density[10]. Kuhnert et al. demonstrated that luteal pericytes function to regulate endothelial sprouting and vessel stability in the CL. Our data expands upon this work by showing that Jagged-induced Notch signaling is critical for pericyte function during luteal angiogenesis. The exact mechanism by which Notch signaling regulates pericyte function during luteal angiogenesis remains to be determined. However, we have demonstrated that Notch signaling is essential for pericyte function and the role of Notch in pericyte/endothelial cell interactions deserves closer attention in order to expand our understanding of physiological and pathological angiogenesis.

CHAPTER 4

Figures

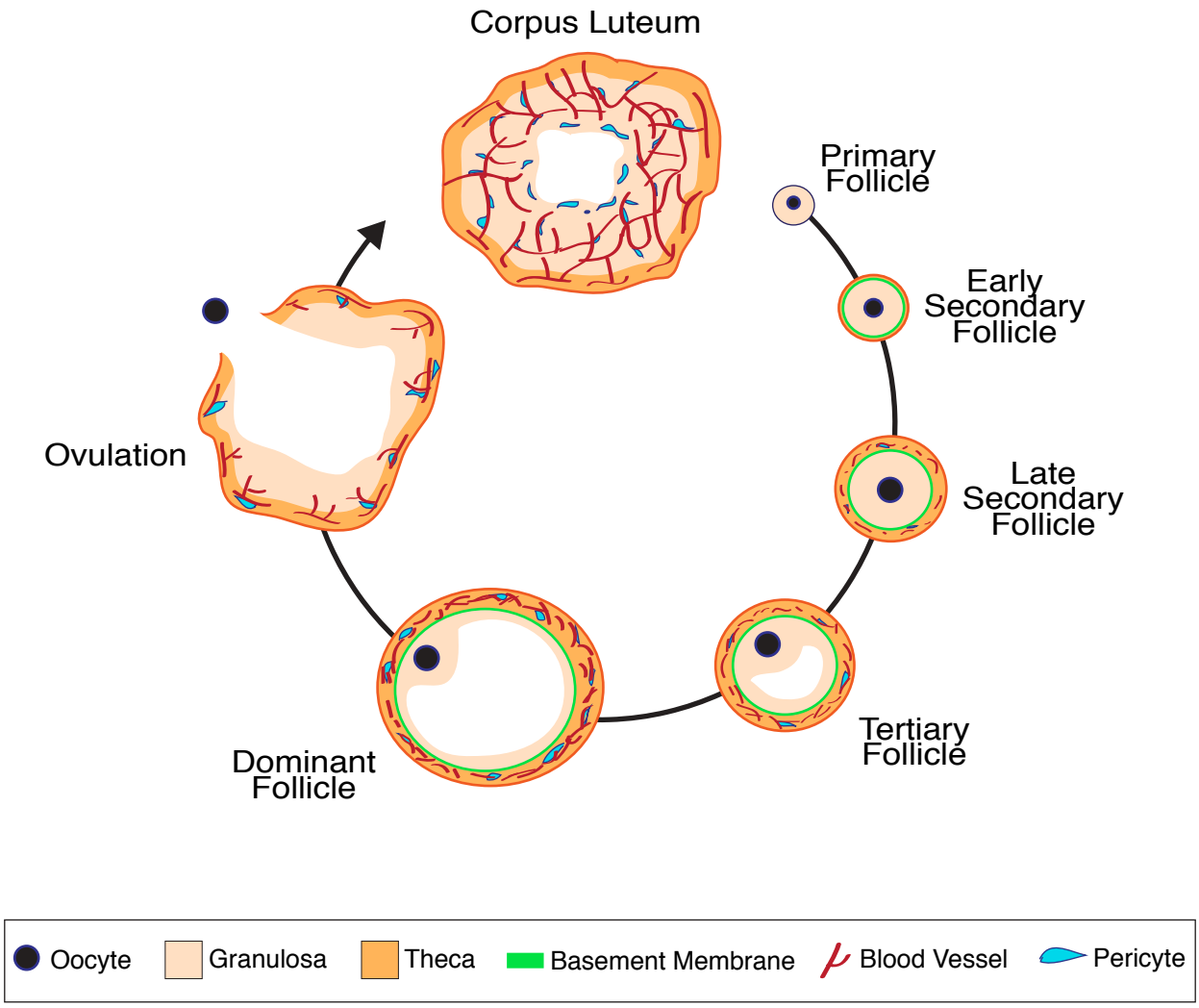

Figure 1. Folliculogenesis, ovulation and corpus luteum formation.

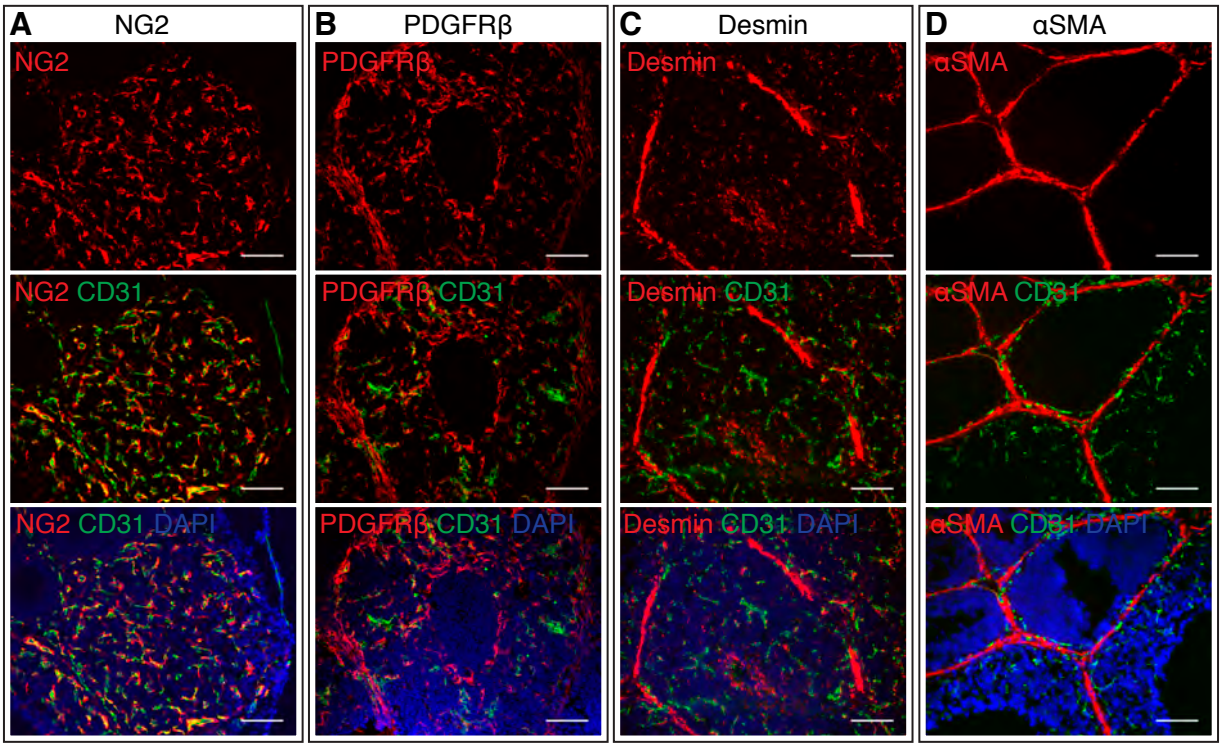

Figure 2. Analysis of expression of mural cell markers in the corpus luteum. Pericytes lining the CD31-positive capillaries (green) of the corpus luteum are positive for NG2 (A), PDGFR-β (B) and desmin (C). αSMA expression is restricted to the mural cells lining the theca blood vessels (D). DAPI in blue. Scale bars; 100 μm.

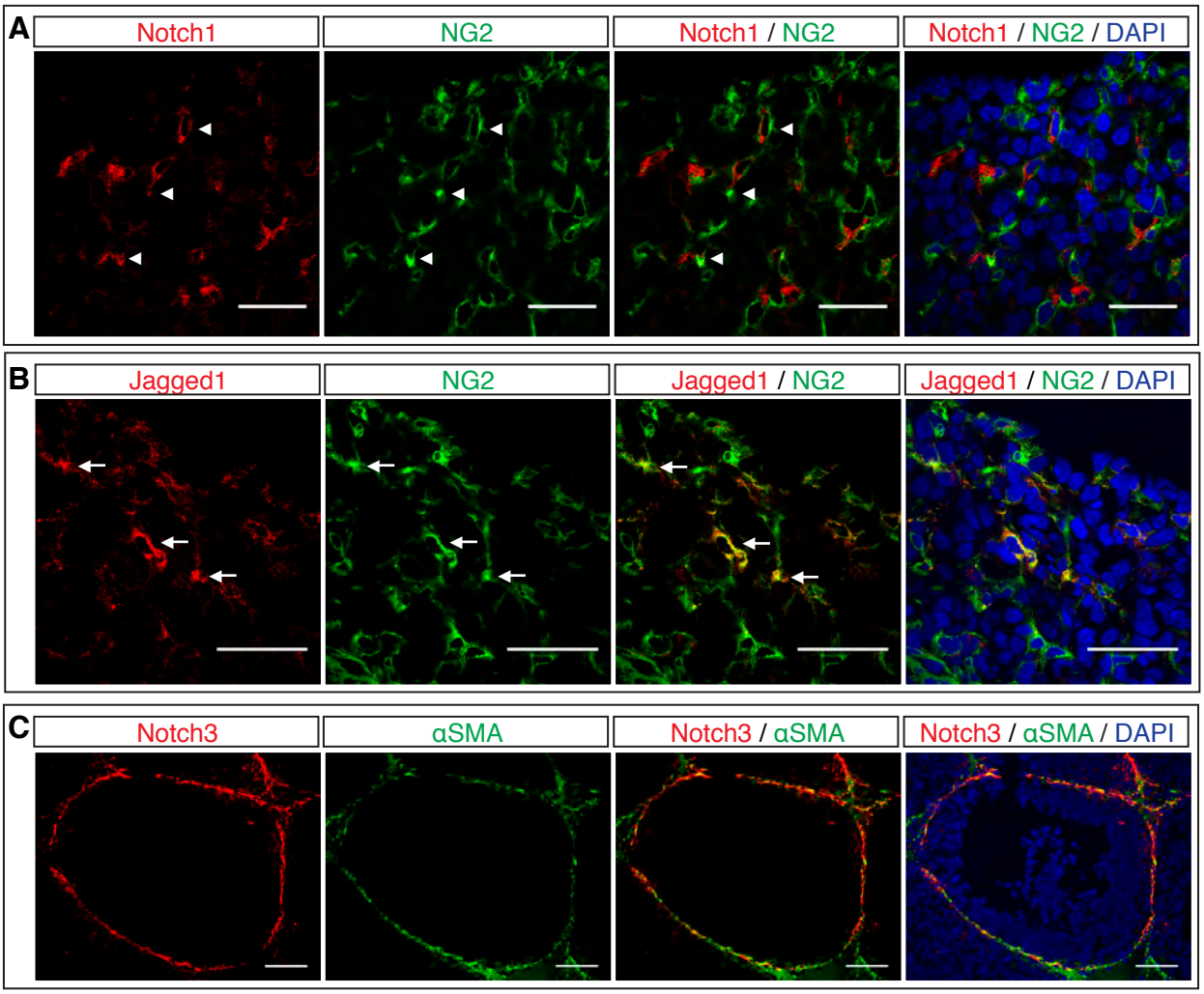

Figure 3. Luteal pericytes express Notch1 and Jagged1, but not Notch3. Sections of ovaries isolated from pre-pubescent female mice stimulated with gonadotropins to induce ovulation were stained for NG2 (green) and Notch1 (A) or NG2 (green) and Jagged1 (B) or αSMA (green) and Notch3 (C). A subset of NG2-positive pericytes in the CL express Notch1 (arrowheads). Jagged1 expression is observed in NG2-positive pericytes in the CL (arrows). Notch3 is not expressed at detectable levels by luteal pericytes. DAPI staining shows nuclei in blue. Scale bars; 50 μm (A and B), 100 μm (C).

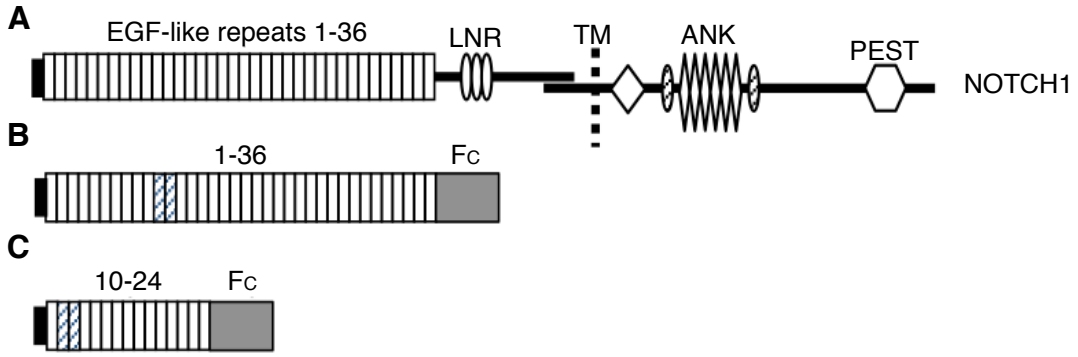

Figure 4. Structure of the jagged inhibitor, $N1_{10-24}$ decoy. The extracellular domain of human NOTCH1 is composed of 36 EGF-like repeats (A). Full-length Notch decoy expresses the entire extracellular domain of human NOTCH1 and binds delta-like and jagged ligands to inhibit all Notch signaling (B). The $N1_{10-24}$ decoy is composed of EGF-like repeats 10-24 and specifically binds jagged ligands (C). Notch decoy variants are fused to human IgG Fc. EGF: epidermal growth factor, LNR: LIN-12/Notch repeats, TM: transmembrane domain, ANK: ankyrin repeats, PEST: proline [P], glutamic acid [E], serine [S], and threonine [T] degradation domain. Figure adapted from Kangsamaksin T., *et al*., unpublished data.

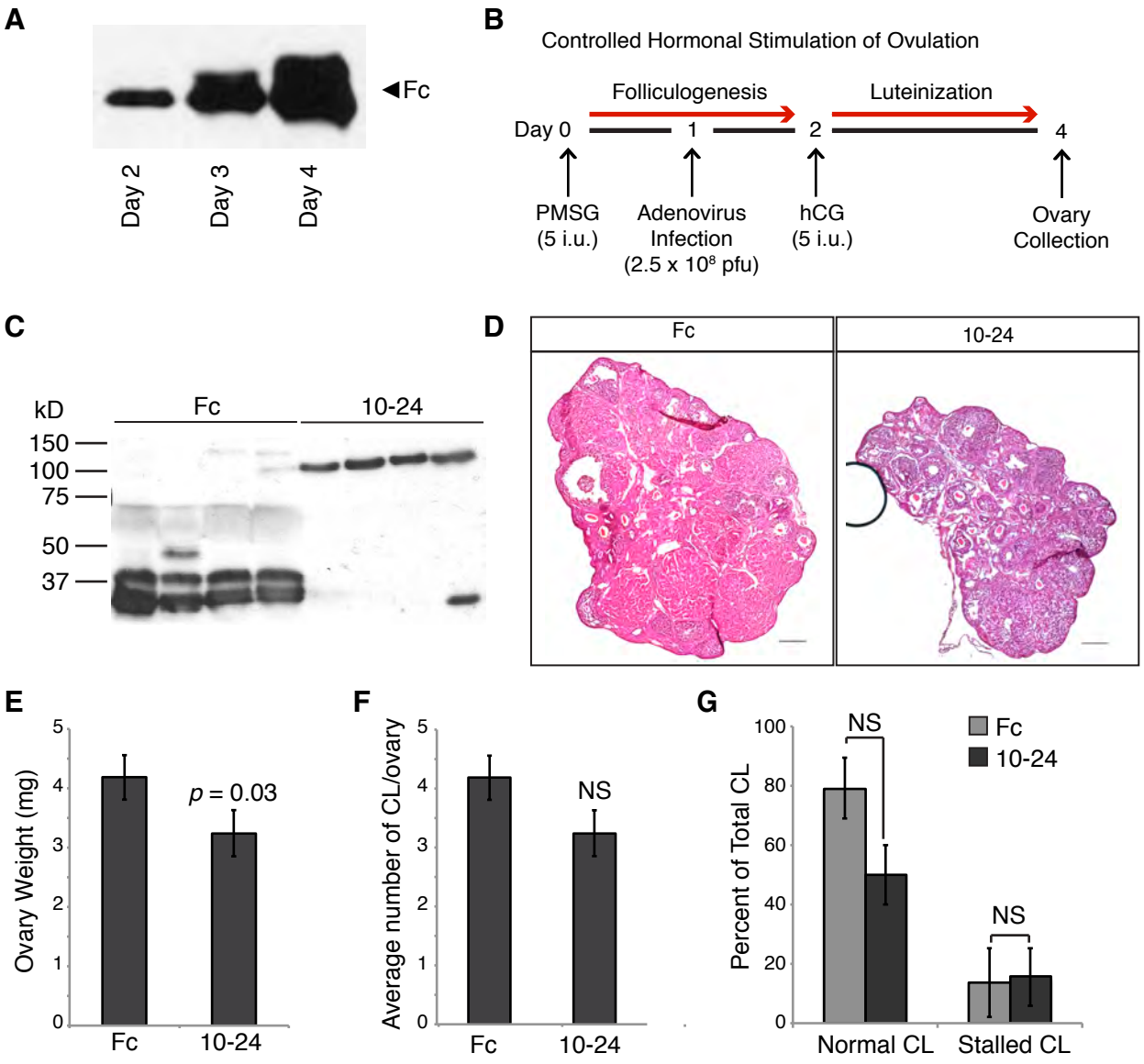

Figure 5. Assessment of $N1_{10-24}$ decoy treatment following controlled hormonal stimulation of ovulation. Western blot for human Fc following injection of adenovirus expressing human Fc (A). Sexually immature female mice were injected with 5 i.u. PMSG and 5 i.u. hCG to induce controlled ovulation, adenovirus is injected on day 1 (B). At day 4, western blot for human Fc shows high levels of serum Fc (approximately 30 kD) in the control group and high serum levels of $N1_{10-24}$ decoy (approximately 140 kD) in the experimental group (C). H&E staining of ovary sections shows that ovulation occurs normally in the $N1_{10-24}$ decoy treated group (D). Ovaries isolated from $N1_{10-24}$ decoy treated mice are smaller in weight following controlled hormonal stimulation (E). Quantification of CL number (F) and CL development (G) shows no significant difference between treatment groups. n=4, 2 ovaries/mouse. Error bars represent SD of the mean. Scale bars; 200 µm. 10-24 = $N1_{10-24}$ decoy.

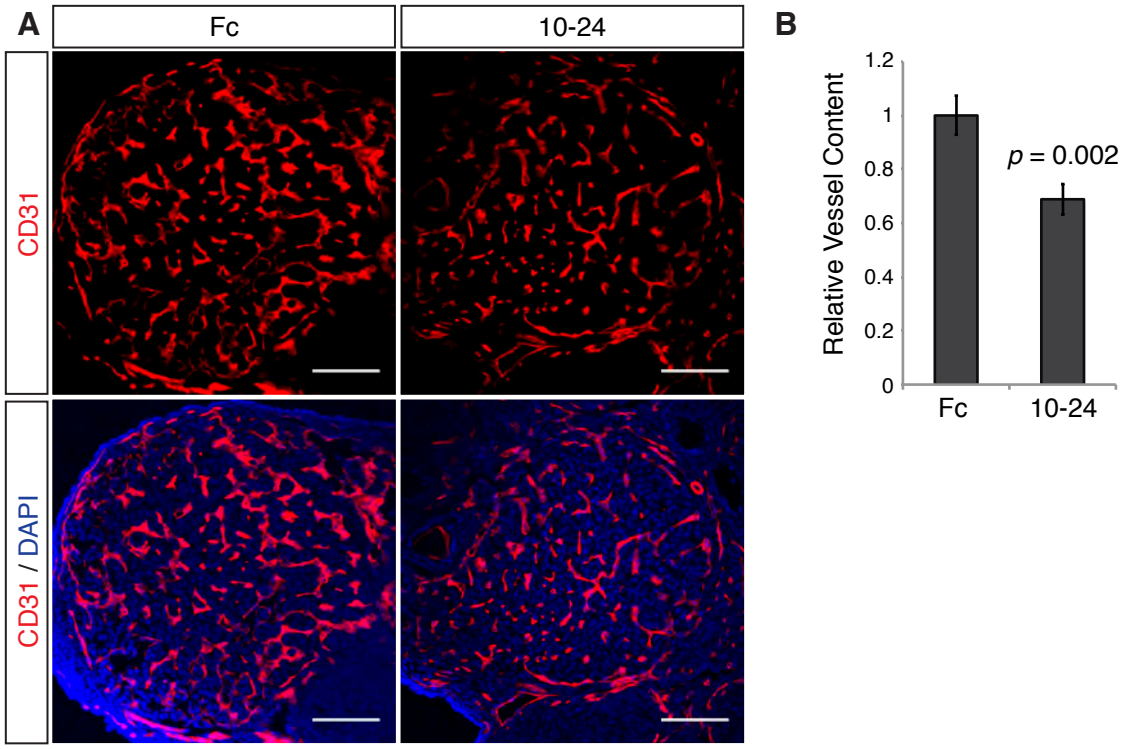

Figure 6. Analysis of luteal vascularization with $N1_{10-24}$ decoy treatment following controlled stimulation of ovulation. Sections of ovaries from human Fc and $N1_{10-24}$ decoy treated mice stained for the endothelial marker CD31 (red) and DAPI (blue) to show total cell content of the CL (A). Quantification of CL vessel content as measured by CD31 staining normalized to DAPI to control for differences in CL progression (B). n=4, 2 ovaries/mouse, 2 sections/ovary. Error bars represent SD of the mean. Scale bars; 100 µm.

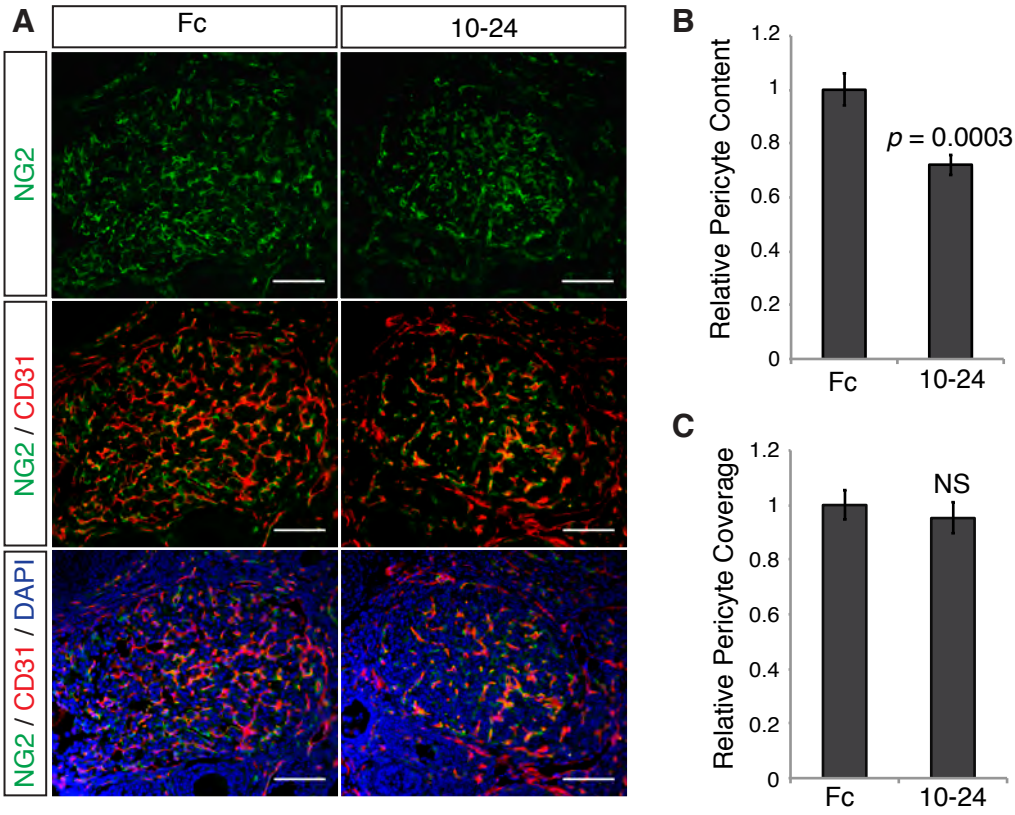

Figure 7. Analysis of luteal pericyte content with $N1_{10-24}$ decoy treatment following controlled stimulation of ovulation. Ovary sections fluorescently stained for CD31 (red), the pericyte marker NG2 (green) and DAPI (blue) (A). Quantification of luteal NG2 staining normalized to DAPI shows that $N1_{10-24}$ decoy inhibits pericyte recruitment to the CL (B), but luteal vessels have normal pericyte coverage (C). n=4, 2 ovaries/mouse, 2 sections/ovary. Error bars represent SD of the mean. Scale bars; 100 µm.

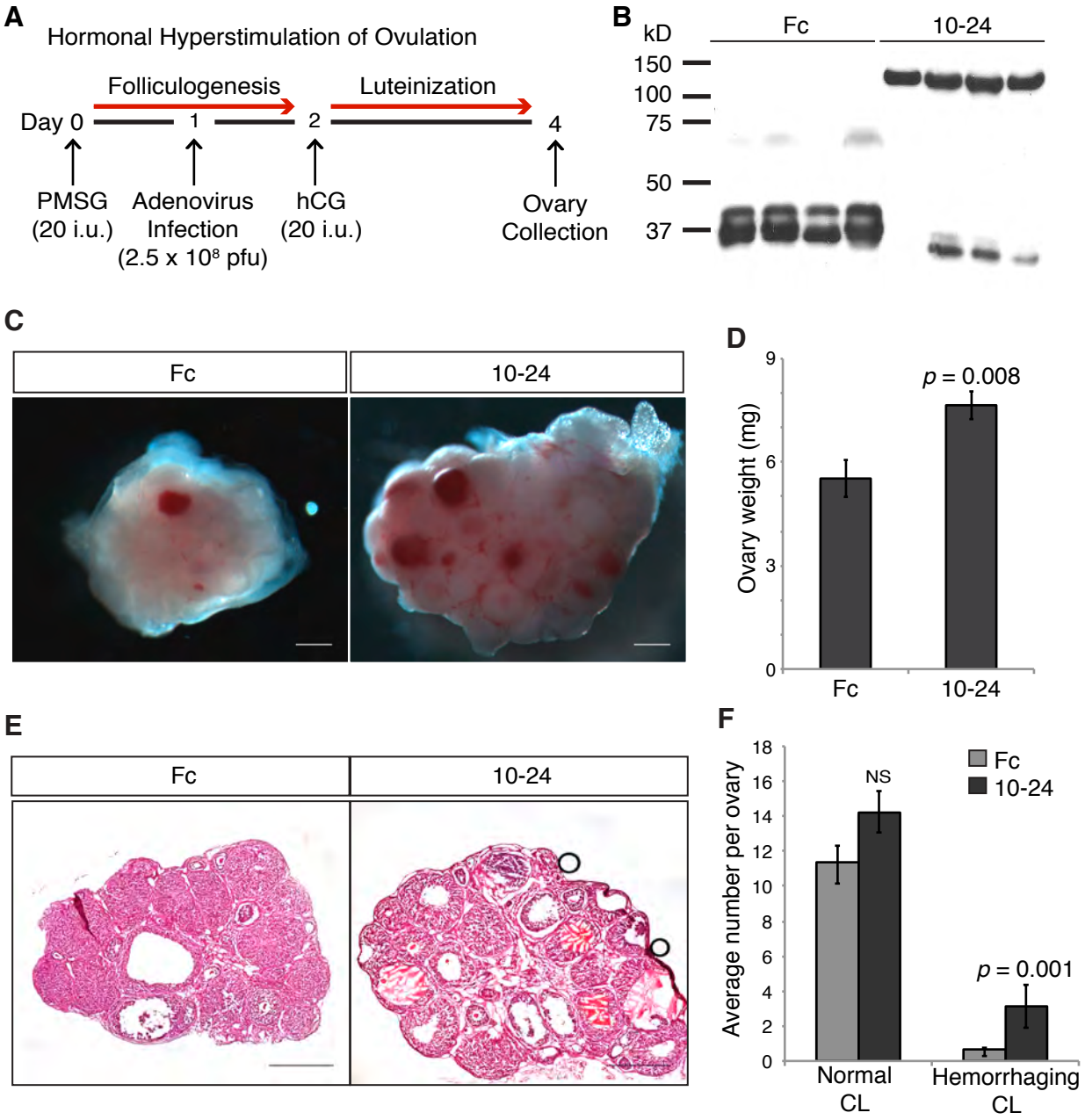

Figure 8. Assessment of hyperstimulated ovaries isolated from mice treated with $N1_{10-24}$ decoy. 20 i.u. PMSG and 20 i.u. hCG injected i.p. causes ovarian hyperstimulation (A). Western blot for human Fc shows high serum levels of Fc in the control group and high serum levels of $N1_{10-24}$ decoy in the experimental group at time of ovary collection (B). Gross pictures show hemorrhaging in hyperstimulated ovaries isolated from Ad-$N1_{10-24}$ decoy treated female mice (C). Quantification of ovarian weight at time of collection (D). H&E staining of ovaries show hemorrhaging of corpora lutea with $N1_{10-24}$ decoy treatment (E). Quantification of normal and hemorrhaging corpora lutea (F). n=4, 2 ovaries/mouse. Error bars represent SD of the mean. Scale bars; 100 µm (C), 200 µm (E).

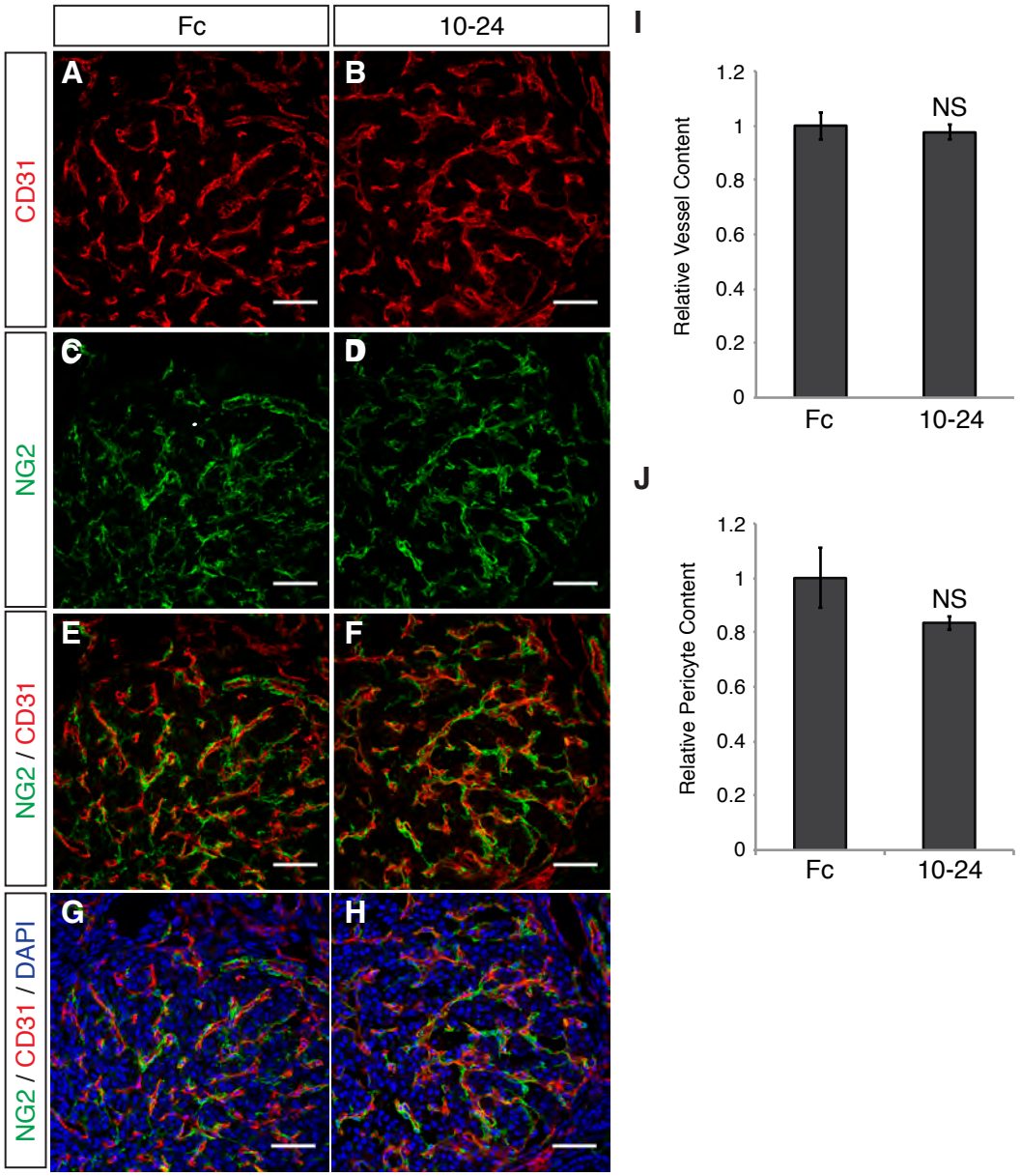

Figure 9. Vascular analysis of corpora lutea following ovarian hyperstimulation and $N1_{10-24}$ decoy treatment. Ovary sections fluorescently stained for CD31 (red), NG2 (green) and DAPI (blue) to visualize endothelial cells, pericytes, and cell nuclei, respectively (A-G). Quantification of luteal vascular content normalized to total luteal cell content (H). Quantification of luteal pericyte content normalized to total luteal cell content (I). n=4, 1 ovary/mouse, 2 sections/ovary. Error bars represent SD of the mean. Scale bars; 50 µm.

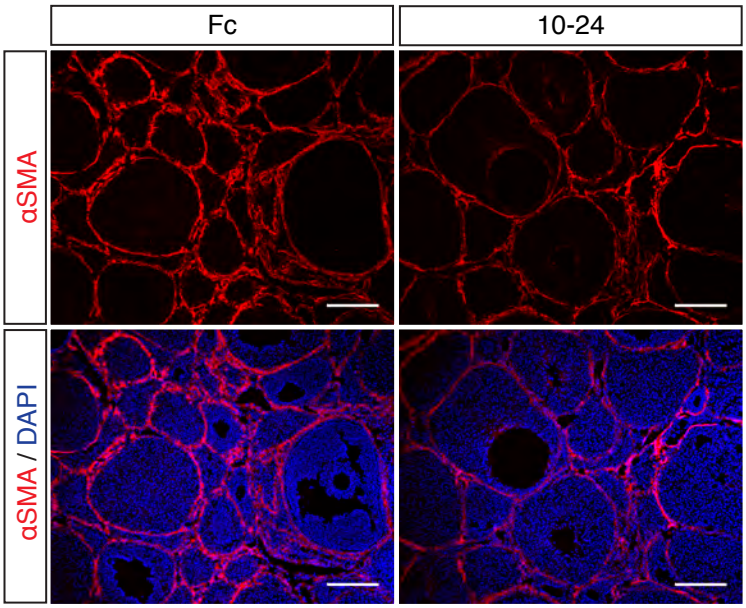

Figure 10. αSMA expression is reduced in $N1_{10-24}$ decoy-treated, hyperstimulated ovaries. Ovary sections fluorescently stained for αSMA (red) show reduced αSMA expression in the ovarian theca of $N1_{10-24}$ decoy treated female mice, as compared to control. DAPI staining shown in blue. Scale bars; 200 μm.

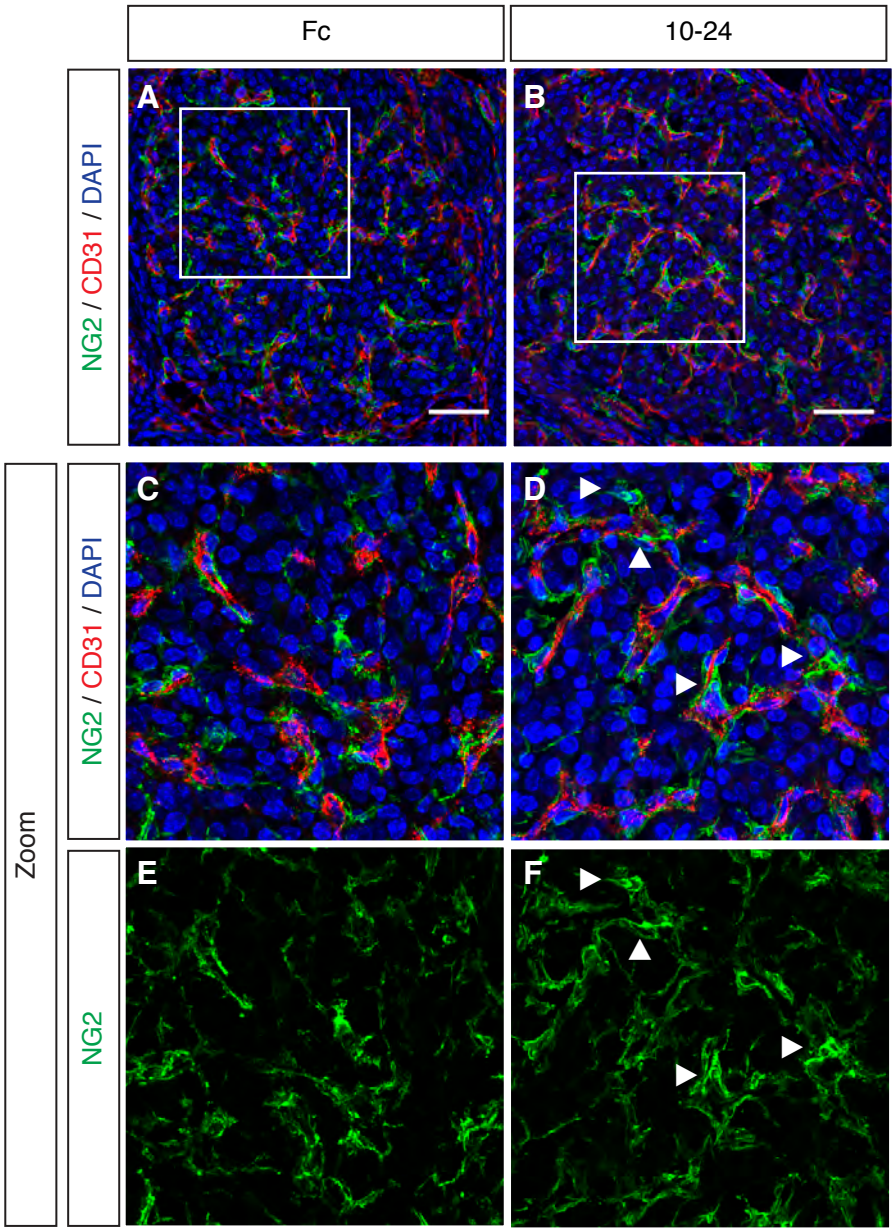

Figure 11. Pericyte association with luteal vessels is compromised in N1$_{10-24}$ decoy treated mice with ovarian hyperstimulation. High magnification confocal stacks of non-hemorrhaged corpora lutea of Fc-treated (A) and N1$_{10-24}$ decoy treated (B) mice. Ovaries fluorescently stained for CD31 (red) to visualize the endothelium, NG2 (green) to mark pericytes, and DAPI (blue) for visualization of cell nuclei. Zoomed images of areas marked by white boxes in A and B allow for closer assessment of pericyte association with the vasculature (C-F). Arrowheads show pericytes that are poorly associated with endothelial cells in the Notch1$_{10-24}$ decoy treated corpus luteum. Scale bars; 50 µm.

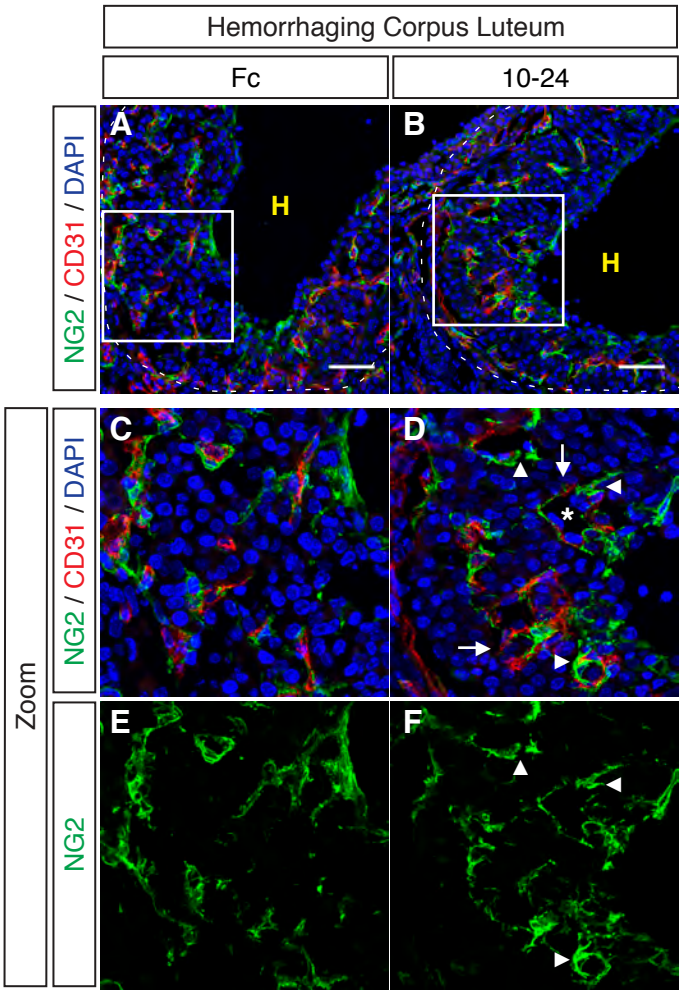

Figure 12. Analysis of vessel structure in hemorrhaging corpora lutea of mice treated with N1$_{10-24}$ decoy. High magnification confocal stacks of hemorrhaging corpora lutea stained for CD31 (red), NG2 (green), and DAPI (blue) of control (A) and N1$_{10-24}$ decoy treated (B) female mice with hormonal hyperstimulation of ovulation. A yellow "H" marks the hemorrhagic core of the CL and a dotted white line shows the periphery of the CL. Zoomed pictures of areas marked by white boxes (C-F). Arrows mark dilated capillaries, arrowheads mark dissociating pericytes, and asterisk shows vessel with discontinuous endothelial cell lining in the hemorrhaging CL of the Notch1$_{10-24}$ decoy treated ovary. Scale bars; 50µm.

CHAPTER 5

Notch regulates the PDGF-B/PDGFR-β signaling pathway

INTRODUCTION

To date, the study of Notch signaling in mural cells has primarily focused on the role of Notch in vascular smooth muscle cell (VSMC) differentiation and function. In part this derives from the fact that human NOTCH3 mutations are associated with a disease state involving VSMCs. Mutations in Notch3 cause cerebral autosomal dominant arteriopathy with subcortical infarcts and leukoencephalopathy (CADASIL)[18]. CADASIL is the most commonly inherited stroke disease in humans and is characterized by degeneration of the VSMC lining of small and medium-sized blood vessels leading to cerebral vessel dysfunction, ischemic stroke, and premature death. The pathology of CADASIL underlines the important role Notch3 plays in VSMC function, and thus has spurred extensive research in understanding Notch in VSMCs. However, Notch is also expressed by pericytes, the mural cells lining capillaries and small arterioles and venules. Whereas VSMCs regulate vascular contractility, pericytes fulfill a more active role in angiogenesis because of their association with sprouting and remodeling capillary endothelial cells. Since pericytes and VSMCs have distinct functions in the vasculature, the role of Notch signaling may also be different in these two mural cell types.

Of the four Notch receptors found in mammals, VSMCs express Notch1, Notch2, and Notch3[108]. Endothelial cells and vascular smooth muscle cells express the Notch ligand Jagged1 allowing for cell autonomous and cell non-autonomous activation of VSMC Notch signaling. Notch promotes VSMC differentiation to a contractile mature cell phenotype by inducing expression of contractile proteins, such as α-smooth muscle cell actin (αSMA), smoothelin and myosin light chain kinase (MLCK)[23,32,35].

In VSMCs Notch induces expression of the receptor tyrosine kinase PDGFR-β[22]. PDGFR-β is expressed by pericytes and VSMCs. PDGF-B, the ligand for PDGFR-β, is expressed and secreted as a homodimer (PDGF-BB) by endothelial tip cells during angiogenesis to attract pericytes to the nascent sprout[13]. When activated by ligand binding,

PDGFR-β promotes cellular proliferation, survival and migration[4,109]. Mice mutant for PDGF-B or PDGFR-β die perinatally due to severe hemorrhaging caused by a lack of mural cell coverage in a variety of vascular beds[4,7,67]. Interestingly, when Notch is activated in VSMCs, migration toward PDGF-BB is inhibited despite increased PDGFR-β expression[22]. This suggests that Notch promotion of VSMC differentiation for contractile function overrides the chemotactic response provided by increased PDGFR-β in these mature VSMCs.

It has been proposed that mural cells associated with different types of vessels fall along a continuum of cellular differentiation[5]. This theory posits that pericytes are undifferentiated and "plastic" vascular cells as compared to the contractile mature VSMCs that make up the tunica media of large arteries (See Chapter 1 for detailed review). Notch has been shown to promote contractile VSMC differentiation, however Notch inhibits fibroblast differentiation to a vascular smooth muscle cell fate[110]. Since Notch signaling fulfills different functions during different stages of mural cell differentiation and as it is not clear how Notch functions in pericytes, we investigated the role of Notch in pericytes. We found that Notch promoted PDGFR-β expression in pericytes, similar to VSMCs. Unlike VSMCs, Notch signaling promotes cell migration toward PDGF-BB in pericytes.

RESULTS

Analysis of Notch signaling in cultured pericytes

We analyzed Notch signaling in primary human brain vascular pericytes (HBVP) isolated from the brain microvasculature. This pericyte line has successfully been used in endothelial cell/pericyte network formation assays developed by the Davis lab[65]. Using a similar co-culture assay, the Davis lab reports that VSMCs fail to support endothelial tube formation, as is seen when using HBVP, demonstrating that pericytes and VSMCs have distinct phenotypes when grown in association with isolated endothelial cells (Davis lab, unpublished data).

VSMCs express Notch1, Notch2, Notch3, and the Notch ligand Jagged1[108]. We analyzed Notch receptor and ligand gene expression in HBVP and compared expression levels to human umbilical venous endothelial cells (HUVEC). HBVP express *NOTCH1*, *NOTCH2*, and *NOTCH3*, whereas HUVEC express *NOTCH1*, *NOTCH2*, and *NOTCH4* (Figure 1). Both HUVEC and HBVP also express high levels of *JAGGED1*, whereas *DLL4* is expressed at a significantly higher level in HUVEC. *JAGGED2* is not expressed by HUVEC or HBVP (data not shown). Thus, cultured pericytes have a similar Notch receptor and ligand gene expression profile to VSMCs and do not express high levels of endothelial specific genes, Dll4 and Notch4.

We next determined if Notch signal activation in pericytes increased expression of Notch target gents by analyzing expression of HES/HEY genes in HBVP expressing activated forms of Notch. The Notch intracellular domain-containing transcriptional complex promotes transcription of a variety of gene targets including the HES and HEY transcriptional repressors (see Chapter 1 for detailed review). Co-culture of VSMCs with endothelial cells has been shown to induce VSMC Notch signaling and subsequent expression of HEYL and HES1[106]. To activate Notch in pericytes, we infected HBVP with adenovirus expressing the intracellular domain of Notch1 (Ad-N1IC). Notch signal activation in pericytes induced expression of *HEY1*, *HEYL*, *HES1*, and *HES5* (Figure 2). *HEYL* was the most strongly induced gene analyzed, suggesting that HEYL may be an important downstream target of Notch in pericytes. This data demonstrated that Notch activation induces the expression of canonical Notch targets in cultured pericytes.

Notch inhibits endothelial PDGF-B expression and promotes PDGFR-β expression in pericytes

PDGFR-β is a direct gene target of Notch1 and Notch3 in cultured vascular smooth muscle cells[22]. Since we showed that Notch signals in pericytes, we wanted to see if Notch signaling also regulates PDGFR-β expression in pericytes. We analyzed pericytes with

activated Notch1 and activated Notch3 and found that both Notch1 and Notch3 induced PDGFR-β expression in pericytes (Figure 3A). When analyzing human umbilical venous endothelial cells (HUVEC) with active Notch signaling we observed that activated Notch1 (N1IC) and activated Notch4 (Notch4/int3) repressed expression of PDGF-B, the ligand for PDGFR-β (Figure 3C). This data fits with current models where Notch functions during sprouting angiogenesis by being active in stalk endothelial cells while Notch signaling is low in endothelial tip cells. In addition, in endothelial tip versus stalk cell differentiation PDGF-B has been shown to be strongly expressed by endothelial tip cells during sprouting angiogenesis[111]. Thus, our findings are consistent with increased PDGF-B levels being associated with tip cells where Notch activity is low. We propose that Notch regulates the PDGFR-β signaling pathway by repressing endothelial PDGF-B expression and inducing PDGFR-β expression in pericytes.

Notch signaling in pericytes is necessary for PDGFR-β expression and reduced Notch signaling impairs PDGF-BB directed pericyte migration

To further characterize the role of Notch in PDGFR-β signaling, we inhibited Notch signaling in pericytes and analyzed PDGFR-β protein expression. HBVP were treated with increasing concentrations of the γ-secretase inhibitor, compound E, which blocks proteolytic cleavage of the Notch proteins and thus inhibit nuclear translocation of the Notch intracellular domain. Consequently, compound E inhibits all canonical Notch signaling. We observed a dose dependent inhibition of PDGFR-β protein expression with exposure to increasing concentrations of compound E (Figure 4A). This data demonstrates that Notch signaling is required in pericytes to maintain PDGFR-β expression.

To determine if reduced PDGFR-β expression caused by compound E treatment alters pericyte function we analyzed the effects of compound E on PDGF-BB directed pericyte invasion and migration (Figure 4B). We used compound E at a concentration of 200 μM where

we observed the greatest inhibition of PDGFR-β expression, without significant effects on pericyte viability. In untreated pericytes, PDGF-BB increased pericyte migration through Matrigel, as compared to serum free media (SFM). Inhibition of Notch signaling by compound E treatment completely inhibited pericyte migration in SFM and dramatically reduced their migration through Matrigel toward PDGF-BB. Thus, Notch signaling in pericytes promotes pericyte migration and invasion through Matrigel towards PDGF-BB. Furthermore, this data suggests that Notch regulates pericyte function by promoting PDGFR-β expression.

Combined inhibition of Notch1 and Notch3 alters pericyte morphology and reduces PDGFR-β expression

In VSMCs, both Notch1 and Notch3 have been shown to promote PDGFR-β expression[22]. To specifically analyze the role of Notch1 and Notch3 in regulating pericyte PDGFR-β expression we made HBVP cell lines with Notch1 knockdown, Notch3 knockdown, or combined knockdown of Notch1 and Notch3 using shRNA. HBVP cell lines with Notch1 knockdown appeared morphologically similar to control (Figure 5B) and had a similar rate of growth as control HBVP (data not shown). HBVP cell lines with Notch3 knockdown displayed altered cell morphology characterized by cellular elongation and an increased number of cellular processes (Figure 5C). Knockdown of Notch3 modestly reduced cell proliferation (data not shown). Knockdown of both Notch1 and Notch3 dramatically affected pericyte morphology and viability (Figure 5D). Combined reduction of Notch1 and Notch3 caused cellular enlargement, decreased cell attachment, and inhibited proliferation, suggesting that both Notch1 and Notch3 are required for normal pericyte function and that some Notch expression is required for pericyte viability.

We hypothesized that the observed defects in pericyte proliferation and viability observed when both Notch1 and Notch3 were inhibited may be due to reduced PDGFR-β

expression. We compared PDGFR-β protein expression in HBVP cell lines with NOTCH1 knockdown, NOTCH3 knockdown, and combined knockdown of NOTCH1 and NOTCH3 (Figure 5E). We observed that HBVP with reduced NOTCH1 or NOTCH3 displayed decreased PDGFR-β protein levels, as compared to control. However, combined knockdown of NOTCH1 and NOTCH3 resulted in a dramatic reduction of PDGFR-β protein expression, as compared to control or either NOTCH1 knockdown or NOTCH3 knockdown alone. This data suggests that Notch1 and Notch3 both contribute to PDGFR-β expression in cultured pericytes to promote proper cell function and viability.

Pericyte expression of $N1_{1-36}$ decoy inhibits endothelial network formation

Inhibition of Notch signaling dramatically affected cellular function of pericytes cultured alone in a monolayer. However, culturing pericytes alone does not adequately recapitulate physiological conditions since *in vivo* pericytes are found in close association with endothelial cells. Endothelial cell/pericyte co-culture experiments have demonstrated that endothelial Jagged1 initiates a positive feedback loop in pericytes where Notch3 activation induces Jagged1 and Notch3 expression in VSMCs[106]. Since pericytes are critical regulators of angiogenesis and endothelial cells have been shown to induce Notch signaling in VSMCs, we wanted to analyze endothelial network formation in the presence of pericytes when Notch signaling is inhibited. To inhibit Notch signaling we made HBVP cell lines that express the pan Notch ligand inhibitor Notch1 decoy ($N1_{1-36}$ decoy) developed in our lab from the extracellular domain of rat Notch1[105]. We previously established that the $N1_{1-36}$ decoy blocks Jagged and Delta-like ligands from activating Notch signaling[105]. Endothelial cells (HUVEC) expressing RFP (red) were embedded in a collagen gel with control HBVP or HBVP expressing $N1_{1-36}$ decoy. After 7 days, robust endothelial networks can be observed when HUVEC are co-cultured with control HBVP (Figure 6A). However, endothelial network formation is dramatically reduced

when HUVEC are co-cultured with pericytes expressing $N1_{1-36}$ decoy (Figure 6B). Furthermore, network formation over time is reduced in the presence of HBVP expressing $N1_{1-36}$ decoy (Figure 6C). This data fits *in vivo* findings from our lab that demonstrated that treatment with full length N1 decoy inhibits tumor angiogenesis and developmental retinal angiogenesis (Kangsamaksin, T., *et al.*, unpublished data). This is the first evidence to show that $N1_{1-36}$ decoy expression by pericytes can inhibit endothelial cell network formation.

DISCUSSION

We demonstrated that Notch signaling regulates the PDGF-B/PDGFR-β signaling pathway *in vitro*. Inhibition of Notch signaling using compound E or shRNA-targeted reduction of Notch1 and Notch3 transcripts caused reduced PDGFR-β expression in pericytes. In cultured endothelial cells, Notch activation inhibited PDGF-B expression, the ligand for PDGFR-β. In addition, we observed reduced PDGF-BB directed migration in pericytes with reduced canonical Notch signaling. The functional consequence of Notch inhibition was evaluated where endothelial network formation was impaired when HUVEC were cultured with pericytes expressing Notch1 decoy to inhibit Notch signaling.

Notch has primarily been studied in more mature vascular smooth muscle cells. Our data expands the role of Notch in regulating mural cell function to the pericyte. In line with the VSMC Notch expression profile, cultured pericytes express Notch1 and Notch3 and the Notch ligand, Jagged1. Notch induces PDGFR-β expression in vascular smooth muscle cells[22]. We showed that Notch induces PDGFR-β expression in pericytes. Our work demonstrated that Notch signaling promotes PDGF-BB directed pericyte migration, whereas Notch inhibits PDGF-BB directed migration in VSMCs, despite increased levels of PDGFR-β. This difference in cellular function in response to Notch may reflect the different functional requirements for VSMC and pericytes. By inducing expression of contractile proteins in VSMCs, Notch regulates VSMC

differentiation to a contractile and more mature mural cell phenotype[72,108]. Differentiation and maturation of VSMCs requires that cells cease to proliferate and migrate. Thus, to promote cellular differentiation, Notch may inhibit VSMC migration despite increased PDGFR-β expression. Our data suggests that Notch has a unique role in pericytes where instead of regulating cell differentiation, we believe Notch functions to promote PDGFR-β induced cell migration in pericytes.

In VSMCs, PDGFR-β has been shown to be a direct target of Notch1 and Notch3. However, it has been demonstrated that Notch1 and Notch3 bind distinct *cis*-elements in the PDGFR-β promoter showing that they independently regulate PDGFR-β[11,22]. We showed that combined deficiency of Notch1 and Notch3 reduced PDGFR-β protein levels in cultured pericytes to a greater extent than inhibition of Notch1 or Notch3 alone. This data suggests that both Notch1 and Notch3 are required in pericytes for proper PDGFR-β expression and normal pericyte function. We showed that inhibition of Notch1 in pericytes is sufficient to cause decreased PDGFR-β expression providing additional evidence for a role for Notch1 in regulating mural cell function. Notch1 and Notch3 may have distinct functions in mural cells. In fact, it is possible that the balance of Notch1 and Notch3 may contribute to differing mural cell phenotypes and cell differentiation. Future experiments focusing on the distinct roles of Notch1 and Notch3 signaling in VSMCs versus pericytes will help define unique mural cell phenotypes and functions.

We conclude that Notch has different functions in pericytes and VSMCs. It is well established that pericytes and VSMCs fulfill unique roles in the vasculature. Unlike VSMCs, pericytes line small blood vessels and capillaries where they share a basement membrane with the endothelium. Thus, pericytes have an intimate relationship with endothelial cells during angiogenesis and in the quiescent vasculature. Our data shows that despite similarities in VSMC and pericyte Notch expression, Notch signaling results in different functional outcomes in

pericytes than it does in VSMCs. These findings help to define pericytes and VSMCs as unique cell types with distinct modes of cell signaling regulation.

CHAPTER 5

Figures

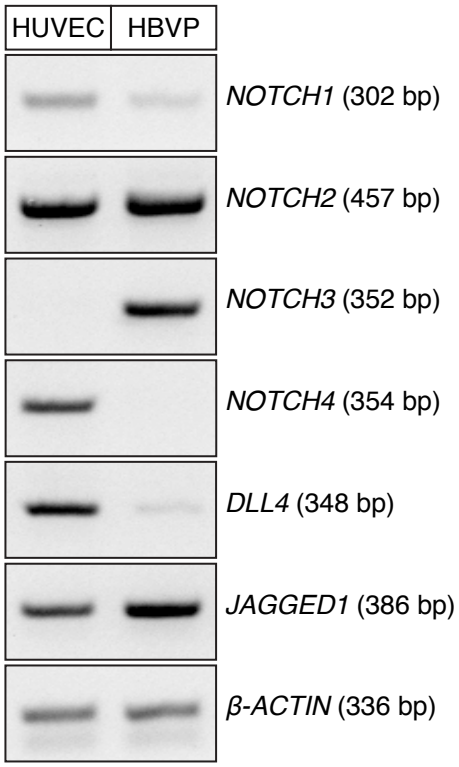

Figure 1. Notch receptor and ligand expression in human brain vascular pericytes. mRNA expression of Notch receptors and ligands in human umbilical venous endothelial cells (HUVEC) and human brain vascular pericytes (HBVP). Size of amplicon in base pairs (bp) shown in parentheses. Relative gene expression is shown with *β-ACTIN*.

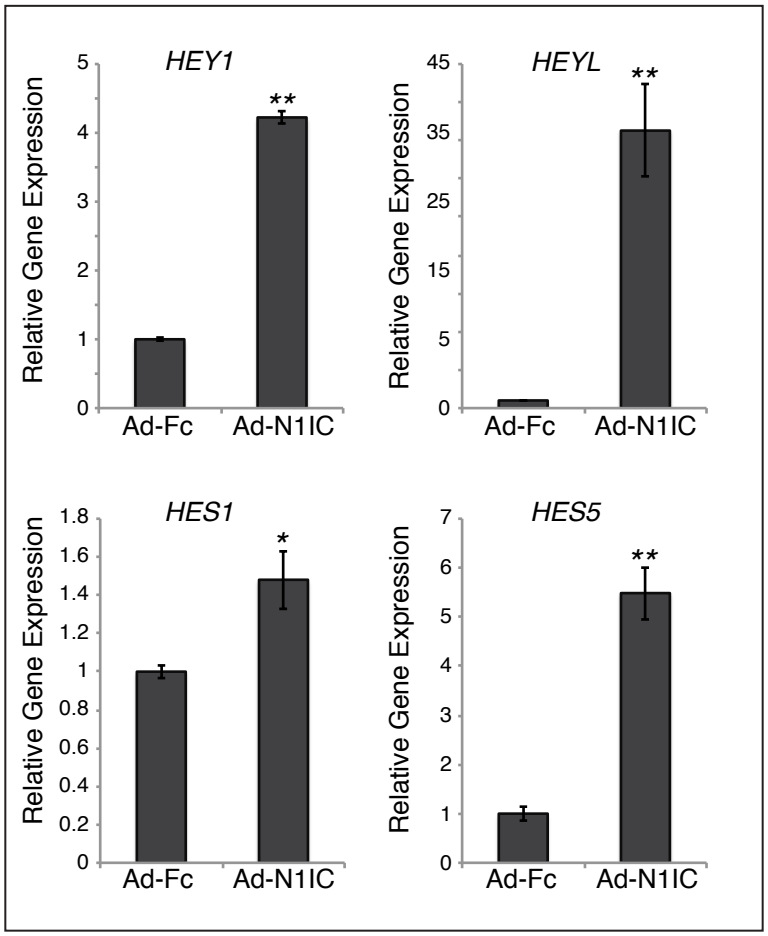

Figure 2. Notch activation induces *HEY1*, *HEYL*, *HES1*, and *HES5* expression in HBVP. HBVP were infected with adenovirus expressing the intracellular domain of Notch1 (Ad-N1IC) or Fc (Ad-Fc) as control. Quantitative RT-PCR on HBVP cDNA. Error bars represent standard deviation. * $p<0.05$, ** $p<0.005$.

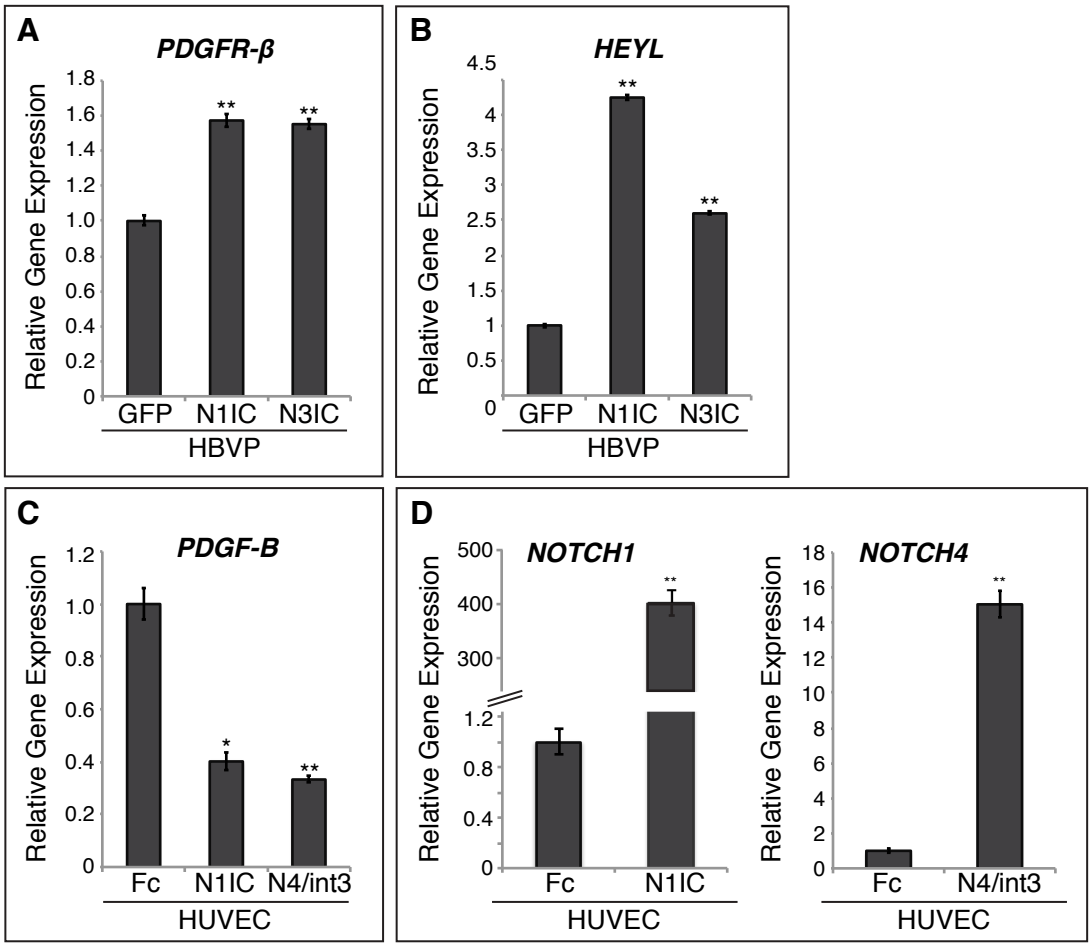

Figure 3. Notch inhibits *PDGF-B* in HUVEC and induces *PDGFR-β* in pericytes. Quantitative RT-PCR to analyze relative gene expression. Analysis of *PDGFR-β* gene expression in HBVP cell lines expressing activated Notch1 (N1IC), activated Notch3 (N3IC) or GFP as control (A). Increased levels of the downstream Notch target *HEYL* validates Notch activation in HBVP cell lines (B). HUVEC cell lines expressing N1IC, activated Notch4 (N4/int3) or Fc as control. HUVEC with activated Notch display reduced *PDGF-B* transcript levels (C). Validation of activation of Notch; HUVEC-N1IC have increased *NOTCH1* transcript levels and HUVEC N4/int3 have increased *NOTCH4* transcript levels (D). Error bars represent standard deviation. *p<0.01, **p<0.001.

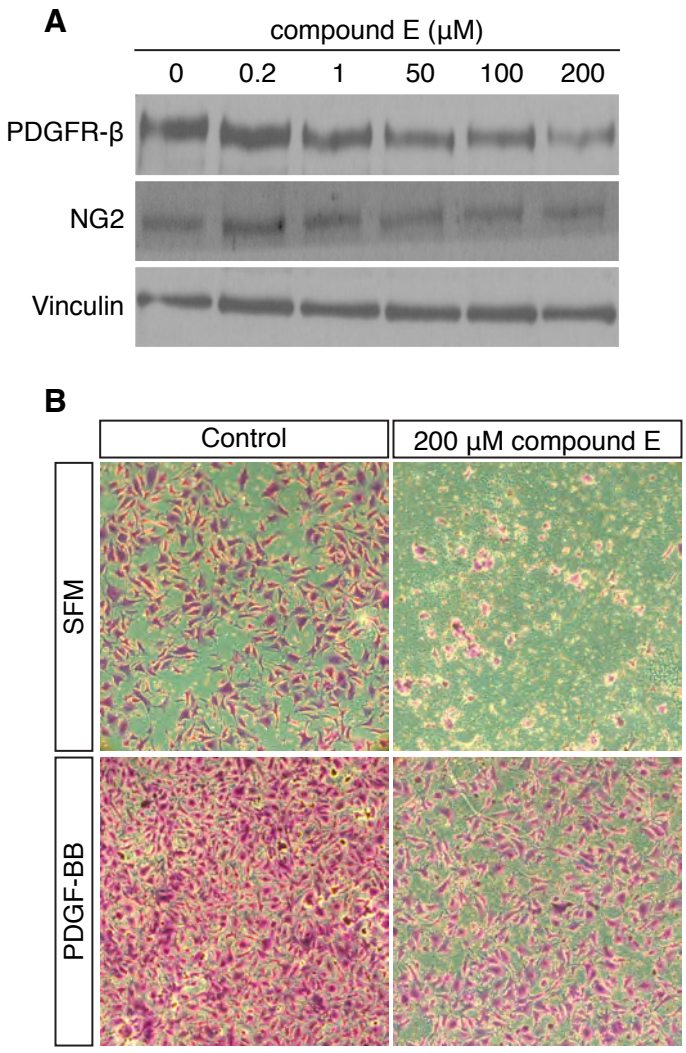

Figure 4. Inhibition of Notch signaling in pericytes inhibits PDGF-BB directed migration. Western blot for PDGFR-β and NG2 in pericytes treated with increasing concentrations of compound E (A). Vinculin is used as a loading control. Pericytes treated with compound E display reduced Matrigel invasion in serum free media (SFM) and in media containing 20 ng/μl human recombinant PDGF-BB (B).

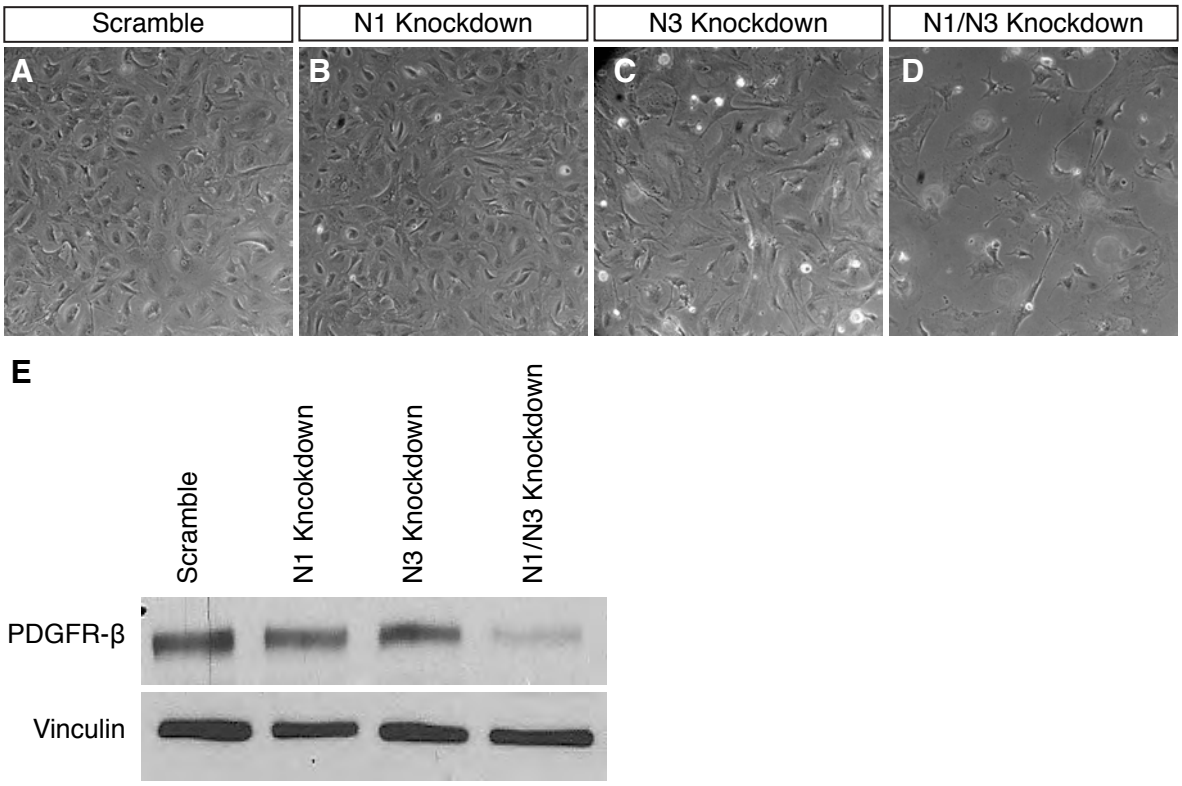

Figure 5. Analysis of pericyte cell lines with combined knockdown of NOTCH1 and NOTCH3. Analysis of cell morphology of HBVP cell lines made using lentiviral constructs expressing scrambled shRNA (control), human NOTCH1-shRNA (N1 knockdown), human NOTCH3-shRNA (N3 knockdown), and both NOTCH1-shRNA and NOTCH3-shRNA (N1/N3 knockdown) (A-D). Corresponding western blot for PDGFR-β on cell lysates isolated from Notch knockdown cell lines (E). Vinculin is used as a loading control.

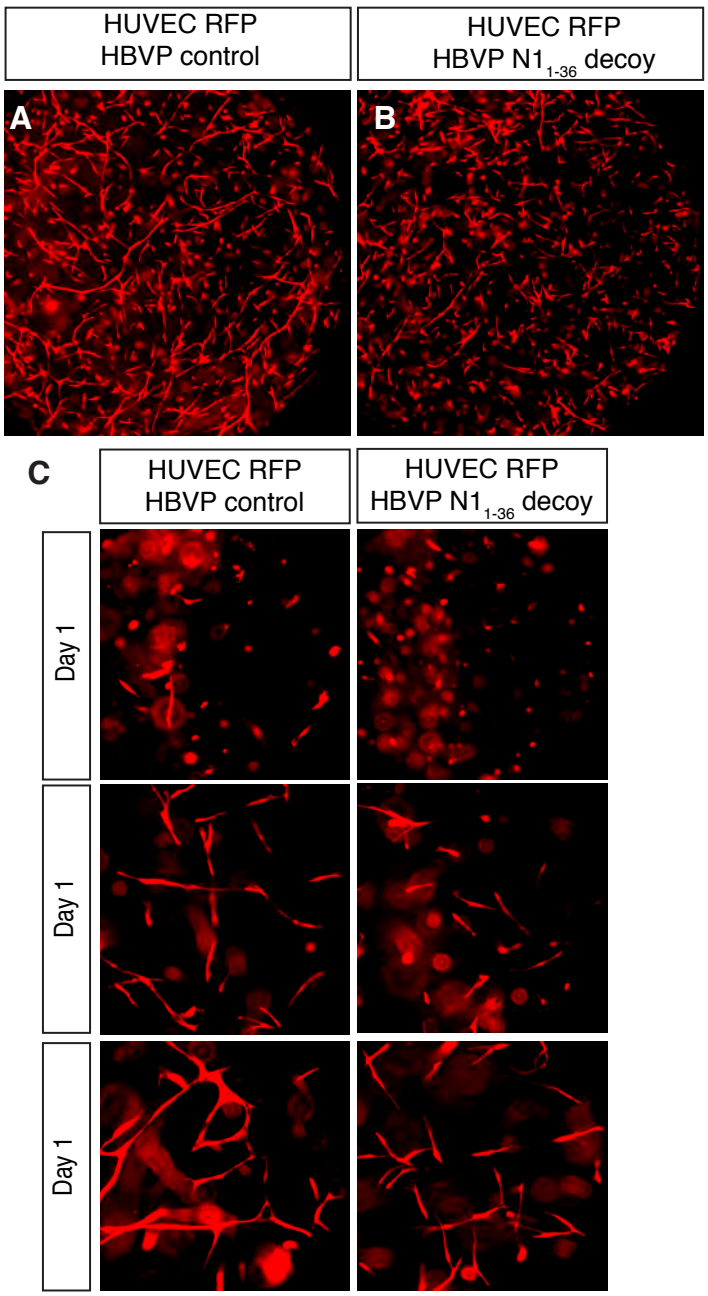

Figure 6. The pan Notch ligand inhibitor, $N1_{1-36}$ decoy inhibits network formation in a pericyte/endothelial cell co-culture assay. Endothelial cells expressing RFP were embedded in a 2.5 mg/ml collagen gel with HBVP lentivirally infected with full-length rat Notch1 extracellular domain ($N1_{1-36}$ decoy) or HBVP expressing GFP, as control. Endothelial network formation is shown in red. After 7 days, inhibition of Notch signaling with $N1_{1-36}$ decoy inhibits endothelial network formation, as compared to control (A and B). An equivalent number of endothelial cells are present at Day 1 in both experimental groups, however network formation is inhibited over time, as shown at Day 5 and Day 7 when endothelial cells are co-cultured with HBVP expressing $N1_{1-36}$ decoy (C).

CHAPTER 6

Discussion

Here we demonstrate a novel role for Notch in angiogenesis where it signals in pericytes to regulate endothelial cell sprouting, vessel maturation and vascular function. We showed that both Notch1 and Notch3 are required to promote pericyte recruitment and association with the endothelium during angiogenesis and that these processes depend upon Jagged activation of Notch. We also showed that loss of proper pericyte/endothelial cell association due to Notch deficiency results in dramatic vascular anomalies including increased vessel density, vessel enlargement, increased vascular permeability, and arteriovenous malformations. We also demonstrated that Notch signaling has unique functional outcomes in pericytes, as compared to previous reports of Notch function in vascular smooth muscle cells. Our work expands the role of Notch signaling in angiogenesis while demonstrating the critical role pericytes play in regulating endothelial function.

Notch regulates pericyte recruitment during angiogenesis

We showed that *Notch1*$^{+/-}$, *Notch3*$^{-/-}$, *Notch1*$^{+/-}$*;Notch3*$^{+/-}$, and *Notch1*$^{+/-}$*;Notch3*$^{-/-}$ mice displayed reduced pericyte coverage during retinal angiogenesis. We postulated that there were two possible causes for decreased pericyte coverage of the vasculature: 1) Notch deficiency impairs pericyte recruitment to new blood vessels, 2) Notch deficiency causes reduced pericyte viability. Analysis, of cleaved-caspase 3 staining in the retina to assess for apoptosis showed no difference in pericyte apoptosis in the mouse mutants analyzed (data not shown). Thus, we concluded that Notch does not affect pericyte viability in the retina.

During angiogenesis, endothelial cells recruit pericytes by secreting PDGF-B, which signals through PDGFR-β expressed by pericytes to induce their proliferation and migration to new blood vessels. Ablation of PDGF-B/PDGFR-β signaling in the mouse reduced brain pericyte content by approximately 95% demonstrating that this signaling pathway is critical for pericyte recruitment in the central nervous system[4,112]. We established that Notch signaling

regulates PDGFR-β expression in cultured human brain pericytes. We also showed that Notch signaling inhibits PDGF-B expression in endothelial cells. In the nascent angiogenic sprout, it has been established that Notch1 regulates endothelial tip versus stalk cell identity. This model centers on the fact that Notch1 inhibits VEGFR-2 expression where endothelial tip cells express low levels of Notch1 and high Dll4 to allow for high VEGFR-2 expression and thus induction of a migratory and highly VEGF-responsive cellular phenotype[71]. High Dll4 in the tip cell can then activate Notch1 signaling in the neighboring endothelial stalk cell to inhibit sprouting of the stalk cell through downregulation of VEGFR-2. PDGF-B is also expressed at high levels by endothelial tip cells where it is secreted to induce pericyte recruitment to nascent angiogenic sprouts[13]. We demonstrated that Notch1 inhibits PDGF-B expression in endothelial cells. This new data can be used to refine the model describing the role of Notch in sprouting angiogenesis to include its function in regulating the PDGF-B/PDGR- β signaling pathway (Figure 1). Our model proposes that low Notch1 levels in the endothelial tip cell of an angiogenic sprout allows for increased PDGF-B expression, whereas Dll4-induced Notch signaling in the neighboring stalk cell represses PDGF-B expression by the stalk cell. Notch-mediated repression of PDGF-B sets that stage for Notch1 signaling to establish an extracellular gradient of high PDGF-BB surrounding the tip cell and lower PDGF-BB along the stalk cell to guide pericyte migration along the endothelial sprout. To expand the role of Notch in pericyte recruitment, we also demonstrated that Notch induces PDGFR-β expression in pericytes and that Notch signaling is required for PDGF-BB directed pericyte migration *in vitro*. Thus, we propose that Notch regulates pericyte recruitment in two ways; by establishing a PDGF-BB gradient for migrating pericytes to follow and by enhancing pericyte response to PDGF-BB through induction of PDGFR-β expression.

The validity of our proposed model for Notch regulation of PDGF-B/PDGFR-β during angiogenesis remains to be assessed *in vivo*. We have stained Notch1/Notch3 mutant P5

retinas for PDGFR-β protein expression. Careful assessment of different vascular areas of wholemount retinas stained for PDGFR-β did not show a significant difference in PDGFR-β expression levels across genotypes (data not shown). However, it is possible that antibody staining of wholemount retinas is not sensitive enough to detect mild decreases in PDGFR-β protein levels, which could still result in impaired pericyte recruitment. Assessment of retinal PDGFR-β mRNA levels could provide for greater sensitivity. Assessment of PDGF-BB expression by the endothelium in Notch mutant mice would also be of value. Our model suggests that mice with Notch1 haploinsufficiency would display increased endothelial PDGF-B expression. One would expect that increased PDGF-BB levels would cause increased pericyte recruitment, however we observed decreased pericyte recruitment in mice with Notch1 heterozygosity. Despite increased PDGF-BB levels, we believe that reduced PDGFR-β expression due to Notch deficiency in the pericyte could cause a defect in pericyte recruitment in Notch1 heterozygous mice. Furthermore, from our model Notch1 deficiency would also disrupt PDGF-BB gradient formation, which could hinder pericyte recruitment despite increased PDGF-BB levels in *Notch1*$^{+/-}$ mice.

A role for Notch in pericyte maturation

Pericytes and vascular smooth muscle cells are collectively referred to as mural cells because they both contribute to the vessel wall. However, pericytes and VSMCs perform very different functions in the vasculature. VSMCs are contractile cells that line larger vessels to regulate vessel tone through modulation of vasodilation and vasoconstriction. In contrast, pericytes function to promote vessel stability and inhibit vascular permeability of small vessels and capillary networks. A current theory proposes that pericytes and vascular smooth muscle cells fall along a continuum of mural cell differentiation where pericytes are considered immature, undifferentiated mural cells that are capable of maturing into contractile terminally

differentiated VSMCs[5]. Identification of mural cells lining medium sized vessels that display an intermediate cellular phonotype with characteristics of both pericytes and VSMCs supports this theory. An opposing theory could postulate that pericytes and VSMCs are distinct cell types with distinct origins that undergo distinct maturation events.

Mural cell maturation can be defined as the phenotypic changes that allow for different types of mural cells to fulfill their specific function in the fully developed vasculature. Accordingly, maturation allows for VSMCs to be contractile and pericytes to appropriately support and associate with the microvascular endothelium. Notch regulates VSMC maturation by inducing expression of contractile proteins[113]. Mouse models with altered Notch signaling in vascular smooth muscle cells display phenotypes associated with impaired VSMC function, such as vessel dilation and decreased vascular tone[32,34,36]. We propose that pericyte maturation involves cellular events that transform the migratory and proliferative pericyte into a cell that ceases migration and instead associates with the endothelium to promote vessel stability and quiescence. We observed loss of pericyte association with the retinal endothelium in *Notch1*$^{+/-}$*;Notch3*$^{-/-}$ mice, and thus concluded that pericyte maturation was impaired in this mouse model. Impaired pericyte maturation in mice deficient for Notch caused alterations in basement membrane deposition and a destabilized capillary network. Our work supports a role for Notch in regulating pericyte maturation that is independent from its role in promoting VSMC differentiation and suggests that Notch has distinct roles in distinct mural cell populations. Furthermore, our findings suggest that pericytes and VSMCs are distinct cell types that undergo independent maturation events to fulfill their functional role in the vasculature.

In the CNS, pericytes are a critical component of the blood-brain barrier, which regulates molecular transport across and between endothelial cells. Loss of pericyte coverage in the CNS leads to increased vascular permeability and vessel dysfunction due to impaired blood-brain barrier function[69,70]. Loss of pericyte coverage is also associated with several vascular

diseases, such as stroke and diabetic retinopathy[5]. In diabetic retinopathy, pericyte dissociation precedes vascular abnormalities and retinal neuronal death[114]. In mouse models of ischemic stroke, blood-brain barrier function is impaired and ischemia can induce pericyte dissociation and migration away from the cerebral vaculature[115]. The vascular dysfunction that accompanies pathologies associated with pericyte loss demonstrates the critical role mature pericytes play in maintaining vessel barrier function and vascular stability. The vascular phenotypes we observed in *Notch1*$^{+/-}$*;Notch3*$^{-/-}$ mice, such as increased vessel permeability and altered basement membrane deposition suggest that a functional blood-retinal barrier is not established in this mouse model. Our data suggests that Notch signaling in the pericytes may be altered in the aforementioned vasculopathies. Future experiments that investigate the role of Notch signaling in pericyte function in the blood-brain barrier and retina-blood barrier could provide novel therapeutic targets for cerebral and retinal vasculopathies.

Notch signaling produces divergent phenotypes in the pericyte

We showed that Notch promotes both pericyte recruitment and pericyte maturation. These findings suggest that Notch signaling regulates two distinct pathways in pericyte function leading one to question how Notch functions in the same cell to regulate divergent phenotypes. The nature of Notch signaling allows for it to be temporally regulated in a highly dose dependent manner[20]. Jagged1 activation of Notch3 in VSMCs has been shown to induce a positive feedback loop that induces Jagged1 and Notch3 expression in the VSMC, thus amplifying Notch signaling in the mural cell compartment[106]. In the pericyte, Notch signaling can be activated by multiple ligands expressed by the vasculature including Dll1, Dll4, and Jagged1. Activation of Notch through different Notch ligands has been shown to induce different functional outcomes in endothelial cells where Dll4 activation of Notch promotes endothelial cell sprouting and instead Jagged1 inhibits endothelial cell sprouting (Kangsamaksin T., at al., unpublished data)[37].

Activation of Notch signaling by different ligands may similarly result in different pericyte phenotypes. One can postulate that Notch signaling levels may differ in pericytes that are migrating versus those associated with the endothelium. A migratory pericyte may be exposed to high levels of Jagged1 and Dll4 expressed by endothelial cells that are actively sprouting and expanding. In contrast, endothelial cells undergoing lumenization and maturation may present the pericyte with a different ligand profile and thus induce a level of Notch signaling required for pericyte maturation. Furthermore, pericytes that are associated with the endothelium have less contact with endothelial cells due to the basement membrane, again altering ligand exposure and changing the potential for Notch signaling in the pericyte. Pericyte exposure to varying types and levels of Notch ligands may govern the different cellular phenotypes associated with Notch signaling and requires further investigation.

Mural cell dysfunction contributes to AVMs

We demonstrated that *Notch1*$^{+/-}$*;Notch3*$^{-/-}$ mice develop arteriovenous malformations in the retina. AVMs are vascular anomalies, which are characterized by unstable vessels that are prone to rupture, thus increasing the patients risk for stroke and death[77,43]. Endothelial dysfunction has been implicated in the development of AVMs, however the pathogenesis of AVMs remains unclear[86,116,117]. Since Notch3 is restricted to the mural cell compartment and *Notch3*$^{-/-}$ mice, as well as *Notch1*$^{+/-}$*;Notch3*$^{-/-}$ mice display AVMs, our work supports a role for mural cells in AVM pathogenesis. It has previously been shown that a subset of brain AVMs display decreased mural cell coverage[79]. In *Alk1* deficient mice that display impaired TGF-β signaling, AVMs developed following stimulation of angiogenesis through ectopic VEGF-A expression[46]. The dysplastic vessels of these AVMs displayed loss of mural cell coverage with decreased PDGFR-β expression, providing additional evidence for mural cell dysfunction in the development of AVMs.

Before the appearance of AVMs in *Notch1*$^{+/-}$*;Notch3*$^{-/-}$ mice we observed enlarged venules and increased vascular density as a result of pericyte dysfunction. Improper pericyte association with the endothelium due to Notch deficiency resulted in impaired vascular differentiation into segregated arteriolar, venular, and capillary vascular structures. Thus, we believe that arteriovenous shunts and AVMs arise as de novo vascular abnormalities in *Notch1*$^{+/-}$*;Notch3*$^{-/-}$ mice due to alterations in the capillary network caused by pericyte dysfunction. In humans, most brain AVMs are commonly believed to be congenital vascular abnormalities. Our findings support a congenital origin for AVMs. Furthermore, our data suggests that impaired pericyte function during the development of the circulatory system contributes to AVMs. To determine if our findings in the mouse translate to the clinic, future studies should investigate pericyte coverage and pericyte Notch expression in human brain AVMs.

A two-hit hypothesis for vessel dysfunction

In humans, the inherited vascular disease hereditary hemorrhagic telangiectasia (HHT) is characterized by AVMs and caused by mutations in either ALK1 or ENG (the gene that encodes for endoglin) leading to impaired TGF-β signaling[43]. Mouse models mutant for Alk1 do not develop congenital AVMs, but instead develop AVMs when exposed to ectopic VEGF-A or following wounding[46]. From these findings, the authors proposed a two-hit hypothesis model for AVM development in HHT where both endothelial dysfunction and endothelial activation are required for AVMs to form.

Notch1 inhibits VEGFR-2 expression in endothelial cells, therefore Notch1 heterozygosity allows for increased endothelial VEGFR-2 expression and thus, endothelial activation. Our data demonstrated that *Notch3*$^{-/-}$ mice displayed mural cell dysfunction and abnormal capillary beds. However, additional loss of Notch1 in *Notch1*$^{+/-}$*;Notch3*$^{-/-}$ mice caused

bona fide AVMs characterized by vascular tangles and arteriovenous shunts. We believe that *Notch1*$^{+/-}$;*Notch3*$^{-/-}$ mice develop AVMs due to pericyte dysfunction caused by Notch deficiency combined with endothelial activation caused by *Notch1* heterozygosity. Thus, we propose an alternative two-hit hypothesis model for AVM development where pericyte dysfunction and endothelial activation are both required for AVMs (Figure 2). Analysis of AVMs in mice mutant for Notch3 with endothelial-specific deletion of Notch1 could address this hypothesis.

In the ovary, pericyte dysfunction combined with endothelial activation also led to impaired vascular function. Ovarian hyperstimulation is characterized by increased VEGF-A levels leading to an activated endothelium due to increased VEGFR-2 signaling[107]. Jagged-specific inhibition of Notch signaling with $N1_{10\text{-}24}$ decoy inhibited pericyte association with luteal vessels in the ovarian corpus luteum. However, $N1_{10\text{-}24}$ decoy only caused luteal hemorrhaging in hyperstimulated ovaries, but not in ovaries that had undergone controlled stimulation of ovulation. We believe that when endothelial cell function is properly regulated during angiogenesis, compensatory mechanisms enable a functional vascular network to form despite altered pericyte function. However, when pericyte association with the endothelium is impaired and endothelial cells are excessively activated through increased VEGFR-2 signaling, severe vascular dysfunction ensues. Accordingly, proper pericyte association with the endothelium is especially required during times of endothelial activation, such as inflammation and in tumor angiogenesis. Thus, regulation of Notch function in pericytes could provide a novel target for diseases characterized by pathological angiogenesis.

Conclusion

Pericytes provide a unique function in angiogenesis by regulating endothelial cell sprouting and vessel maturation. In quiescent vasculature, pericytes contribute to vessel permeability and stability. We demonstrated that Notch signaling regulates pericyte recruitment

to nascent blood vessels. We also showed that Notch is required for pericyte maturation to enable their association with the endothelium and that this process is critical for basement membrane deposition to promote vessel stabilization. Pericyte dysfunction has been reported in vasculopathies such as diabetic retinopathy and stroke. Our work demonstrates that altered pericyte function due to Notch deficiency also contributes to the development of arteriovenous malformations and loss of retina-blood barrier integrity. Our works suggest that the role of Notch in pericyte/endothelial cell interactions is a previously unappreciated component of several vascular diseases including stroke, arteriovenous malformations, and retinopathies.

DISCUSSION

Figures

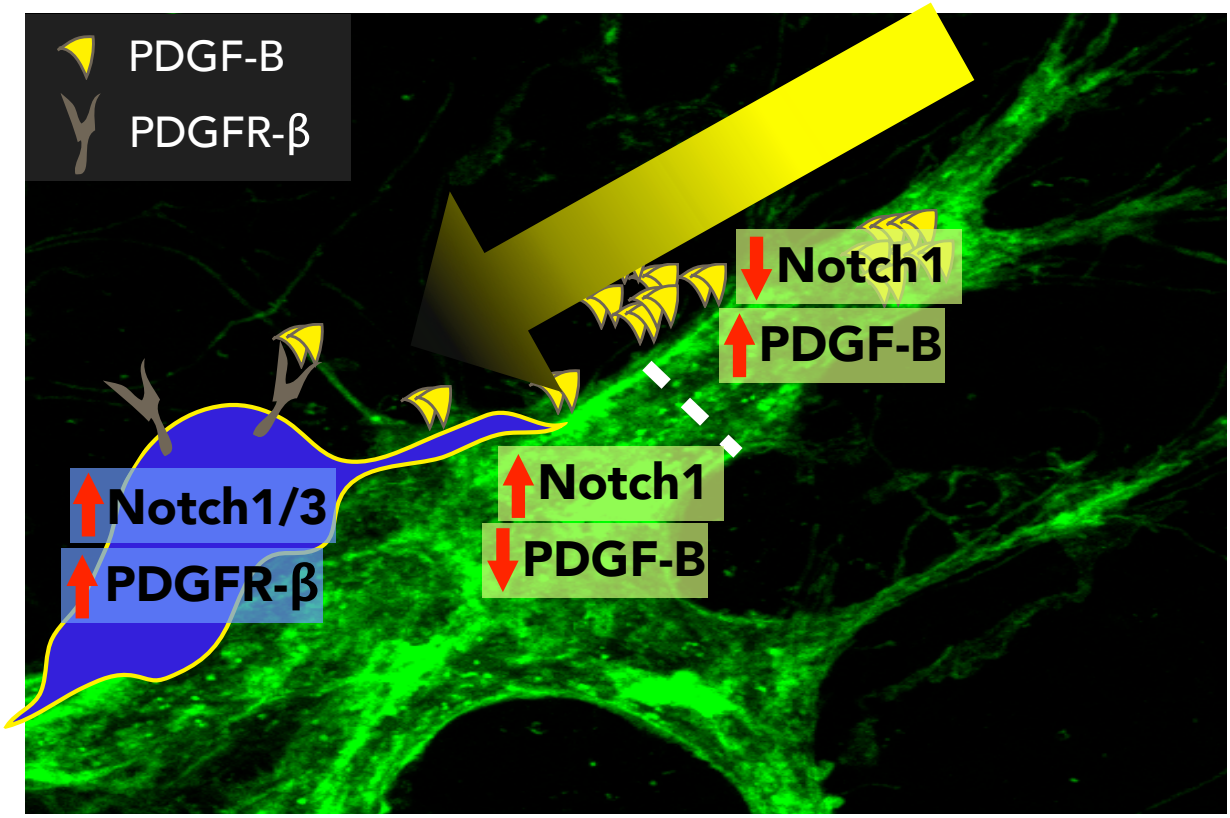

Figure 1. Notch regulation of PDGF-B/PDGFR-β signaling during angiogenesis. Notch1 inhibits PDGF-B expression in HUVEC. Low levesl of Notch1 in the endothelial tip cell of an angiogenic sprout allows for high PDGF-B expression, whereas high Notch1 in the stalk cell inhibits PDGF-B expression in the stalk cell. Differential Notch1 expression in tip versus stalk cells establishes a PDGF-BB gradiant to guide pericyte recruitment to nascent angiogenic sprouts. In pericytes, Notch1 and Notch3 induce PDGFR-β expression to promote their migration during angiogenesis. Endothelium shown in green, dotted white line is predicted border between endothelial tip and stalk cell. Pericyte shown in blue.

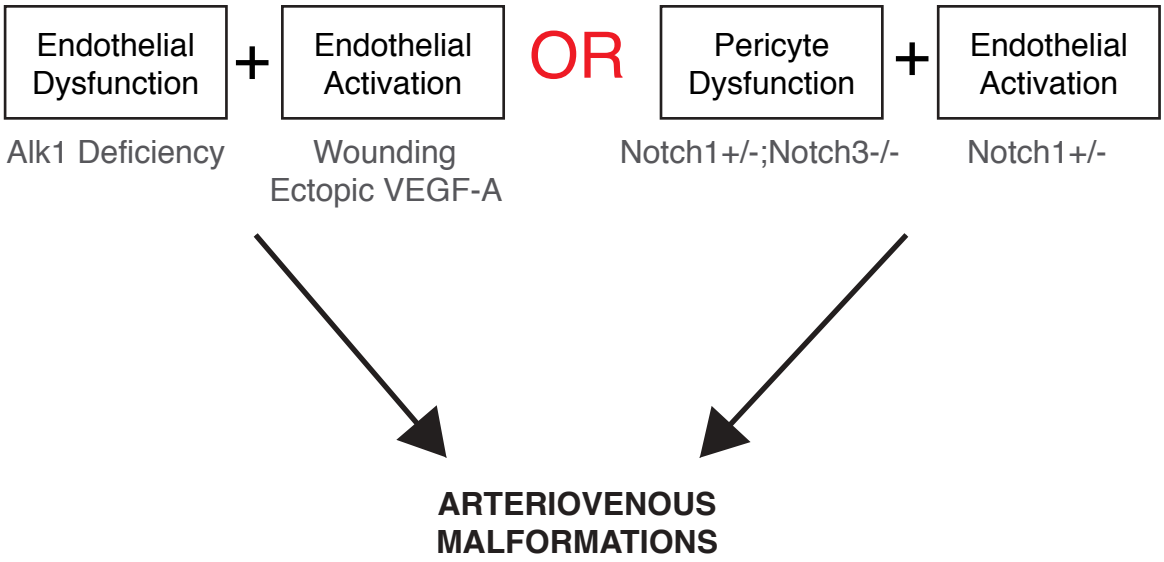

Figure 2. Pericyte dysfunction contributes to arteriovenous malformations. A two-hit hypothesis for the formation of AVMs has been previously proposed where endothelial dysfunction (for example through Alk1 deficiency) combined with endothelial activation (by wounding or delivery of ectopic VEGF-A) are both required for the development of AVMS. We propose an additional model where AVMs develop when pericyte dysfunction (by Notch deficiency) is combined with endothelial activation (by Notch1 heterozygosity).

REFERENCES

1. Noden DM. Embryonic origins and assembly of blood vessels. *Am. Rev. Respir. Dis.* 1989;140(4):1097–1103.

2. Potente M, Gerhardt H, Carmeliet P. Basic and therapeutic aspects of angiogenesis. *Cell*. 2011;146(6):873–887.

3. Lindblom P, Gerhardt H, Liebner S, et al. Endothelial PDGF-B retention is required for proper investment of pericytes in the microvessel wall. *Genes Dev*. 2003;17(15):1835–1840.

4. Hellström M, Kalén M, Lindahl P, Abramsson A, Betsholtz C. Role of PDGF-B and PDGFR-beta in recruitment of vascular smooth muscle cells and pericytes during embryonic blood vessel formation in the mouse. *Development*. 1999;126(14):3047–3055.

5. Armulik A, Genové G, Betsholtz C. Pericytes: developmental, physiological, and pathological perspectives, problems, and promises. *Dev. Cell*. 2011;21(2):193–215.

6. Stratman AN, Malotte KM, Mahan RD, Davis MJ, Davis GE. Pericyte recruitment during vasculogenic tube assembly stimulates endothelial basement membrane matrix formation. *Blood*. 2009;114(24):5091–5101.

7. Levéen P, Pekny M, Gebre-Medhin S, et al. Mice deficient for PDGF B show renal, cardiovascular, and hematological abnormalities. *Genes Dev*. 1994;8(16):1875–1887.

8. Soriano P. Abnormal kidney development and hematological disorders in PDGF beta-receptor mutant mice. *Genes Dev*. 1994;8(16):1888–1896.

9. Hellström M, Gerhardt H, Kalén M, et al. Lack of pericytes leads to endothelial hyperplasia and abnormal vascular morphogenesis. *J Cell Biol*. 2001;153(3):543–553.

10. Kuhnert F, Tam BYY, Sennino B, et al. Soluble receptor-mediated selective inhibition of VEGFR and PDGFRbeta signaling during physiologic and tumor angiogenesis. *Proc Natl Acad Sci USA*. 2008;105(29):10185–10190.

11. Uemura A. Recombinant angiopoietin-1 restores higher-order architecture of growing blood vessels in mice in the absence of mural cells. *Journal of Clinical Investigation*. 2002;110(11):1619–1628.

12. Etchevers HC, Vincent C, Le Douarin NM, Couly GF. The cephalic neural crest provides pericytes and smooth muscle cells to all blood vessels of the face and forebrain. *Development*. 2001;128(7):1059–1068.

13. Armulik A, Abramsson A, Betsholtz C. Endothelial/pericyte interactions. *Circ Res*. 2005;97(6):512–523.

14. Majesky MW. Developmental basis of vascular smooth muscle diversity. *Arterioscler Thromb Vasc Biol*. 2007;27(6):1248–1258.

15. Gerhardt H, Betsholtz C. Endothelial-pericyte interactions in angiogenesis. *Cell Tissue Res.* 2003;314(1):15–23.

16. Greenwald I. LIN-12/Notch signaling: lessons from worms and flies. *Genes Dev*. 1998;12(12):1751–1762.

17. Gridley T. Notch signaling in vascular development and physiology. *Development*. 2007;134(15):2709–2718.

18. Joutel A, Corpechot C, Ducros A, et al. Notch3 mutations in CADASIL, a hereditary adult-onset condition causing stroke and dementia. *Nature*. 1996;383(6602):707–710.

19. Ranganathan P, Weaver KL, Capobianco AJ. Notch signalling in solid tumours: a little bit of everything but not all the time. *Nat. Rev. Cancer*. 2011;11(5):338–351.

20. Andersson ER, Sandberg R, Lendahl U. Notch signaling: simplicity in design, versatility in function. *Development*. 2011;138(17):3593–3612.

21. Kopan R, Ilagan MXG. The canonical Notch signaling pathway: unfolding the activation mechanism. *Cell*. 2009;137(2):216–233.

22. Jin S, Hansson EM, Tikka S, et al. Notch signaling regulates platelet-derived growth factor receptor-beta expression in vascular smooth muscle cells. *Circ Res*. 2008;102(12):1483–1491.

23. Noseda M, Fu Y, Niessen K, et al. Smooth Muscle alpha-actin is a direct target of Notch/CSL. *Circ Res*. 2006;98(12):1468–1470.

24. Iso T, Kedes L, Hamamori Y. HES and HERP families: multiple effectors of the Notch signaling pathway. *J. Cell. Physiol.* 2003;194(3):237–255.

25. Taylor KL, Henderson AM, Hughes CCW. Notch activation during endothelial cell network formation in vitro targets the basic HLH transcription factor HESR-1 and downregulates VEGFR-2/KDR expression. *Microvasc Res*. 2002;64(3):372–383.

26. Roca C, Adams RH. Regulation of vascular morphogenesis by Notch signaling. *Genes Dev*. 2007;21(20):2511–2524.

27. Krebs LT, Xue Y, Norton CR, et al. Notch signaling is essential for vascular morphogenesis in mice. *Genes Dev*. 2000;14(11):1343–1352.

28. Xue Y, Gao X, Lindsell CE, et al. Embryonic lethality and vascular defects in mice lacking the Notch ligand Jagged1. *Hum. Mol. Genet.* 1999;8(5):723–730.

29. Hrabe De Angelis M, McIntyre J, Gossler A. Maintenance of somite borders in mice requires the Delta homologue DII1. *Nature*. 1997;386(6626):717–721.

30. Gale NW, Dominguez MG, Noguera I, et al. Haploinsufficiency of delta-like 4 ligand results in embryonic lethality due to major defects in arterial and vascular development. *Proc Natl Acad Sci USA*. 2004;101(45):15949–15954.

31. Ruchoux MM, Domenga V, Brulin P, et al. Transgenic mice expressing mutant Notch3 develop vascular alterations characteristic of cerebral autosomal dominant arteriopathy with subcortical infarcts and leukoencephalopathy. *Am. J. Pathol.* 2003;162(1):329–342.

32. Domenga V, Fardoux P, Lacombe P, et al. Notch3 is required for arterial identity and maturation of vascular smooth muscle cells. *Genes Dev*. 2004;18(22):2730–2735.

33. Kofler NM, Shawber CJ, Kangsamaksin T, et al. Notch signaling in developmental and tumor angiogenesis. *Genes Cancer*. 2011;2(12):1106–1116.

34. Belin de Chantemèle EJ, Retailleau K, Pinaud F, et al. Notch3 is a major regulator of vascular tone in cerebral and tail resistance arteries. *Arterioscler Thromb Vasc Biol*. 2008;28(12):2216–2224.

35. Basu S, Srinivasan DK, Yang K, et al. Notch Transcriptional Control of Vascular Smooth Muscle Regulatory Gene Expression and Function. *J Biol Chem*. 2013.

36. High FA, Lu MM, Pear WS, et al. Endothelial expression of the Notch ligand Jagged1 is required for vascular smooth muscle development. *Proc Natl Acad Sci USA*. 2008;105(6):1955–1959.

37. Benedito R, Roca C, Sörensen I, et al. The notch ligands Dll4 and Jagged1 have opposing effects on angiogenesis. *Cell*. 2009;137(6):1124–1135.

38. Liu H, Zhang W, Kennard S, Caldwell RB, Lilly B. Notch3 is critical for proper angiogenesis and mural cell investment. *Circ Res*. 2010;107(7):860–870.

39. Monet M, Domenga V, Lemaire B, et al. The archetypal R90C CADASIL-NOTCH3 mutation retains NOTCH3 function in vivo. *Hum. Mol. Genet.* 2007;16(8):982–992.

40. Joutel A, Andreux F, Gaulis S, et al. The ectodomain of the Notch3 receptor accumulates within the cerebrovasculature of CADASIL patients. *J Clin Invest*. 2000;105(5):597–605.

41. Fouillade C, Baron-Menguy C, Domenga-Denier V, et al. Transcriptome analysis for Notch3 target genes identifies Grip2 as a novel regulator of myogenic response in the cerebrovasculature. *Arterioscler Thromb Vasc Biol*. 2013;33(1):76–86.

42. Murphy PA, Lu G, Shiah S, Bollen AW, Wang RA. Endothelial Notch signaling is upregulated in human brain arteriovenous malformations and a mouse model of the disease. *Lab. Invest.* 2009;89(9):971–982.

43. Whitehead KJ, Smith MCP, Li DY. Arteriovenous malformations and other vascular malformation syndromes. *Cold Spring Harb Perspect Med*. 2013;3(2):.

44. ZhuGe Q, Zhong M, Zheng W, et al. Notch-1 signalling is activated in brain arteriovenous malformations in humans. *Brain*. 2009;132(Pt 12):3231–3241.

45. Murphy PA, Lam MTY, Wu X, et al. Endothelial Notch4 signaling induces hallmarks of brain arteriovenous malformations in mice. *Proc. Natl. Acad. Sci. U.S.A.* 2008;105(31):10901–10906.

46. Walker EJ, Su H, Shen F, et al. Arteriovenous malformation in the adult mouse brain resembling the human disease. *Ann. Neurol.* 2011;69(6):954–962.

47. Vikkula M, Boon LM, Carraway KL, et al. Vascular dysmorphogenesis caused by an activating mutation in the receptor tyrosine kinase TIE2. *Cell*. 1996;87(7):1181–1190.

48. Chen W, Guo Y, Walker EJ, et al. Reduced Mural Cell Coverage and Impaired Vessel Integrity After Angiogenic Stimulation in the Alk1-deficient Brain. *Arterioscler Thromb Vasc Biol*. 2013;33(2):305–310.

49. Swiatek PJ, Lindsell CE, Del Amo FF, Weinmaster G, Gridley T. Notch1 is essential for postimplantation development in mice. *Genes Dev*. 1994;8(6):707–719.

50. Conlon RA, Reaume AG, Rossant J. Notch1 is required for the coordinate segmentation of somites. *Development*. 1995;121(5):1533–1545.

51. Krebs LT, Starling C, Chervonsky AV, Gridley T. Notch1 activation in mice causes arteriovenous malformations phenocopied by ephrinB2 and EphB4 mutants. *Genesis*. 2010;48(3):146–150.

52. McCright B, Gao X, Shen L, et al. Defects in development of the kidney, heart and eye vasculature in mice homozygous for a hypomorphic Notch2 mutation. *Development*. 2001;128(4):491–502.

53. Varadkar P, Kraman M, Despres D, et al. Notch2 is required for the proliferation of cardiac neural crest-derived smooth muscle cells. *Dev. Dyn.* 2008;237(4):1144–1152.

54. Krebs LT, Xue Y, Norton CR, et al. Characterization of Notch3-deficient mice: normal embryonic development and absence of genetic interactions with a Notch1 mutation. *Genesis*. 2003;37(3):139–143.

55. Wang Q, Zhao N, Kennard S, Lilly B. Notch2 and Notch3 function together to regulate vascular smooth muscle development. *PLoS ONE*. 2012;7(5):e37365.

56. Uyttendaele H, Ho J, Rossant J, Kitajewski J. Vascular patterning defects associated with expression of activated Notch4 in embryonic endothelium. *Proc Natl Acad Sci USA*. 2001;98(10):5643–5648.

57. Limbourg A, Ploom M, Elligsen D, et al. Notch ligand Delta-like 1 is essential for postnatal arteriogenesis. *Circ Res*. 2007;100(3):363–371.

58. Duarte A, Hirashima M, Benedito R, et al. Dosage-sensitive requirement for mouse Dll4 in artery development. *Genes Dev*. 2004;18(20):2474–2478.

59. Hellström M, Phng L-K, Hofmann JJ, et al. Dll4 signalling through Notch1 regulates formation of tip cells during angiogenesis. *Nature*. 2007;445(7129):776–780.

60. Trindade A, Kumar SR, Scehnet JS, et al. Overexpression of delta-like 4 induces arterialization and attenuates vessel formation in developing mouse embryos. *Blood*. 2008;112(5):1720–1729.

61. Saint-Geniez M, D'Amore PA. Development and pathology of the hyaloid, choroidal and retinal vasculature. *Int. J. Dev. Biol.* 2004;48(8-9):1045–1058.

62. Duncan AW, Rattis FM, DiMascio LN, et al. Integration of Notch and Wnt signaling in hematopoietic stem cell maintenance. *Nat. Immunol.* 2005;6(3):314–322.

63. Park SO, Wankhede M, Lee YJ, et al. Real-time imaging of de novo arteriovenous malformation in a mouse model of hereditary hemorrhagic telangiectasia. *J Clin Invest*. 2009;119(11):3487–3496.

64. Jaffe EA, Nachman RL, Becker CG, Minick CR. Culture of human endothelial cells derived from umbilical veins. Identification by morphologic and immunologic criteria. *J Clin Invest*. 1973;52(11):2745–2756.

65. Koh W, Stratman AN, Sacharidou A, Davis GE. In vitro three dimensional collagen matrix models of endothelial lumen formation during vasculogenesis and angiogenesis. *Meth Enzymol*. 2008;443:83–101.

66. Tell von D, Armulik A, Betsholtz C. Pericytes and vascular stability. *Exp Cell Res*. 2006;312(5):623–629.

67. Lindahl P. Pericyte Loss and Microaneurysm Formation in PDGF-B-Deficient Mice. *Science*. 1997;277(5323):242–245.

68. Tallquist MD, French WJ, Soriano P. Additive effects of PDGF receptor beta signaling pathways in vascular smooth muscle cell development. *PLoS Biol.* 2003;1(2):E52.

69. Daneman R, Zhou L, Kebede AA, Barres BA. Pericytes are required for blood-brain barrier integrity during embryogenesis. *Nature*. 2010;468(7323):562–566.

70. Armulik A, Genové G, Mäe M, et al. Pericytes regulate the blood-brain barrier. *Nature*. 2010;468(7323):557–561.

71. Blanco R, Gerhardt H. VEGF and notch in tip and stalk cell selection. *Cold Spring Harb Perspect Med*. 2013;3(1):.

72. Fouillade C, Monet-Leprêtre M, Baron-Menguy C, Joutel A. Notch signalling in smooth muscle cells during development and disease. *Cardiovasc Res*. 2012.

73. Lobov IB, Renard RA, Papadopoulos N, et al. Delta-like ligand 4 (Dll4) is induced by VEGF as a negative regulator of angiogenic sprouting. *Proc. Natl. Acad. Sci. U.S.A.* 2007;104(9):3219–3224.

74. Suchting S, Freitas C, le Noble F, et al. The Notch ligand Delta-like 4 negatively regulates endothelial tip cell formation and vessel branching. *Proc Natl Acad Sci USA*. 2007;104(9):3225–3230.

75. Gariano RF, Gardner TW. Retinal angiogenesis in development and disease. *Nature*. 2005;438(7070):960–966.

76. Fruttiger M. Development of the retinal vasculature. *Angiogenesis*. 2007;10(2):77–88.
77. Fleetwood IG, Steinberg GK. Arteriovenous malformations. *Lancet*. 2002;359(9309):863–873.

78. Fruttiger M. Development of the mouse retinal vasculature: angiogenesis versus vasculogenesis. *Invest Ophthalmol Vis Sci*. 2002;43(2):522–527.

79. Tu J, Stoodley MA, Morgan MK, Storer KP. Ultrastructure of perinidal capillaries in cerebral arteriovenous malformations. *Neurosurgery*. 2006;58(5):961–70– discussion 961–70.

80. Nakagawa S, Deli MA, Nakao S, et al. Pericytes from brain microvessels strengthen the barrier integrity in primary cultures of rat brain endothelial cells. *Cell. Mol. Neurobiol.* 2007;27(6):687–694.

81. Simonavicius N, Ashenden M, van Weverwijk A, et al. Pericytes promote selective vessel regression to regulate vascular patterning. *Blood*. 2012;120(7):1516–1527.

82. Saunders WB, Bohnsack BL, Faske JB, et al. Coregulation of vascular tube stabilization by endothelial cell TIMP-2 and pericyte TIMP-3. *J Cell Biol*. 2006;175(1):179–191.

83. Benjamin LE, Hemo I, Keshet E. A plasticity window for blood vessel remodelling is defined by pericyte coverage of the preformed endothelial network and is regulated by PDGF-B and VEGF. *Development*. 1998;125(9):1591–1598.

84. Bell RD, Winkler EA, Sagare AP, et al. Pericytes control key neurovascular functions and neuronal phenotype in the adult brain and during brain aging. *Neuron*. 2010;68(3):409–427.

85. Knutsson KA, De Benedetto U, Querques G, et al. Primitive retinal vascular abnormalities: tumors and telangiectasias. *Ophthalmologica*. 2012;228(2):67–77.

86. Murphy PA, Kim TN, Lu G, et al. Notch4 Normalization Reduces Blood Vessel Size in Arteriovenous Malformations. *Science Translational Medicine*. 2012;4(117):117ra8–117ra8.

87. Stenzel D, Franco CA, Estrach S, et al. Endothelial basement membrane limits tip cell formation by inducing Dll4/Notch signalling in vivo. *EMBO Rep.* 2011;12(11):1135–1143.

88. Estrach S, Cailleteau L, Franco CA, et al. Laminin-binding integrins induce Dll4 expression and Notch signaling in endothelial cells. *Circ Res*. 2011;109(2):172–182.

89. Hynes RO. Cell-matrix adhesion in vascular development. *J. Thromb. Haemost.* 2007;5 Suppl 1:32–40.

90. Scheppke L, Murphy EA, Zarpellon A, et al. Notch promotes vascular maturation by inducing integrin-mediated smooth muscle cell adhesion to the endothelial basement membrane. *Blood*. 2012;119(9):2149–2158.

91. Robinson RS, Woad KJ, Hammond AJ, et al. Angiogenesis and vascular function in the ovary. *Reproduction*. 2009;138(6):869–881.

92. Fraser HM, Wulff C. Angiogenesis in the corpus luteum. *Reprod. Biol. Endocrinol.* 2003;1:88.

93. Redmer DA, Reynolds LP. Angiogenesis in the ovary. *Rev. Reprod.* 1996;1(3):182–192.

94. Kamat BR, Brown LF, Manseau EJ, Senger DR, Dvorak HF. Expression of vascular permeability factor/vascular endothelial growth factor by human granulosa and theca lutein cells. Role in corpus luteum development. *Am. J. Pathol.* 1995;146(1):157–165.

95. Stocco C, Telleria C, Gibori G. The molecular control of corpus luteum formation, function, and regression. *Endocr. Rev.* 2007;28(1):117–149.

96. Wulff C, Wilson H, Rudge JS, et al. Luteal angiogenesis: prevention and intervention by treatment with vascular endothelial growth factor trap(A40). *J. Clin. Endocrinol. Metab.* 2001;86(7):3377–3386.

97. Zimmermann RC, Xiao E, Husami N, et al. Short-term administration of antivascular endothelial growth factor antibody in the late follicular phase delays follicular development in the rhesus monkey. *J. Clin. Endocrinol. Metab.* 2001;86(2):768–772.

98. Ferrara N, Chen H, Davis-Smyth T, et al. Vascular endothelial growth factor is essential for corpus luteum angiogenesis. *Nat Med*. 1998;4(3):336–340.

99. Zimmermann RC, Hartman T, Bohlen P, Sauer MV, Kitajewski J. Preovulatory treatment of mice with anti-VEGF receptor 2 antibody inhibits angiogenesis in corpora lutea. *Microvasc Res*. 2001;62(1):15–25.

100. Zimmermann RC, Hartman T, Kavic S, et al. Vascular endothelial growth factor receptor 2-mediated angiogenesis is essential for gonadotropin-dependent follicle development. *J Clin Invest*. 2003;112(5):659–669.

101. Redmer DA, Doraiswamy V, Bortnem BJ, et al. Evidence for a role of capillary pericytes in vascular growth of the developing ovine corpus luteum. *Biol. Reprod.* 2001;65(3):879–889.

102. Goede V, Schmidt T, Kimmina S, Kozian D, Augustin HG. Analysis of blood vessel maturation processes during cyclic ovarian angiogenesis. *Lab. Invest.* 1998;78(11):1385–1394.

103. Vorontchikhina MA, Zimmermann RC, Shawber CJ, Tang H, Kitajewski J. Unique patterns of Notch1, Notch4 and Jagged1 expression in ovarian vessels during folliculogenesis and corpus luteum formation. *Gene Expr Patterns*. 2005;5(5):701–709.

104. Johnson J, Espinoza T, McGaughey RW, Rawls A, Wilson-Rawls J. Notch pathway genes are expressed in mammalian ovarian follicles. *Mech Dev*. 2001;109(2):355–361.

105. Funahashi Y, Hernandez SL, Das I, et al. A notch1 ectodomain construct inhibits endothelial notch signaling, tumor growth, and angiogenesis. *Cancer Research*. 2008;68(12):4727–4735.

106. Liu H, Kennard S, Lilly B. NOTCH3 expression is induced in mural cells through an autoregulatory loop that requires endothelial-expressed JAGGED1. *Circ Res*. 2009;104(4):466–475.

107. Wang T-H, Horng S-G, Chang C-L, et al. Human chorionic gonadotropin-induced ovarian hyperstimulation syndrome is associated with up-regulation of vascular endothelial growth factor. *J. Clin. Endocrinol. Metab.* 2002;87(7):3300–3308.

108. Boucher J, Gridley T, Liaw L. Molecular pathways of notch signaling in vascular smooth muscle cells. *Front Physiol*. 2012;3:81.

109. Hirschi KK, Rohovsky SA, Beck LH, Smith SR, D'Amore PA. Endothelial cells modulate the proliferation of mural cell precursors via platelet-derived growth factor-BB and heterotypic cell contact. *Circ Res*. 1999;84(3):298–305.

110. Proweller A, Pear WS, Parmacek MS. Notch signaling represses myocardin-induced smooth muscle cell differentiation. *J Biol Chem*. 2005;280(10):8994–9004.

111. Gerhardt H, Golding M, Fruttiger M, et al. VEGF guides angiogenic sprouting utilizing endothelial tip cell filopodia. *J Cell Biol*. 2003;161(6):1163–1177.

112. Enge M, Bjarnegård M, Gerhardt H, et al. Endothelium-specific platelet-derived growth factor-B ablation mimics diabetic retinopathy. *EMBO J*. 2002;21(16):4307–4316.

113. Wang T, Baron M, Trump D. An overview of Notch3 function in vascular smooth muscle cells. *Prog Biophys Mol Biol*. 2008;96(1-3):499–509.

114. Hammes H-P, Lin J, Renner O, et al. Pericytes and the pathogenesis of diabetic retinopathy. *Diabetes*. 2002;51(10):3107–3112.

115. del Zoppo GJ. Inflammation and the neurovascular unit in the setting of focal cerebral ischemia. *Neuroscience*. 2009;158(3):972–982.

116. Mahmoud M, Allinson KR, Zhai Z, et al. Pathogenesis of arteriovenous malformations in the absence of endoglin. *Circ Res*. 2010;106(8):1425–1433.

117. Larrivée B, Prahst C, Gordon E, et al. ALK1 signaling inhibits angiogenesis by cooperating with the Notch pathway. *Dev. Cell*. 2012;22(3):489–500.